

Measurements of 1st, 2nd and 3rd azimuthal anisotropy in $\sqrt{s_{NN}}=200\text{GeV}$ Cu+Au collisions at RHIC-PHENIX

RHIC-PHENIX実験における $\sqrt{s_{NN}}=200\text{GeV}$

銅・金衝突での1次、2次、3次方位角異方性の測定

Pre-Defense
Oct. 28th 2016
Hiroshi Nakagomi
High Energy Nuclear Physics Group

Outline

✓ Introduction

- Quark Gluon Plasma(QGP)
- Azimuthal anisotropy
- CuAu collisions

✓ Experiment/Analysis

- PHENIX
- centrality, event plane
- Simulation

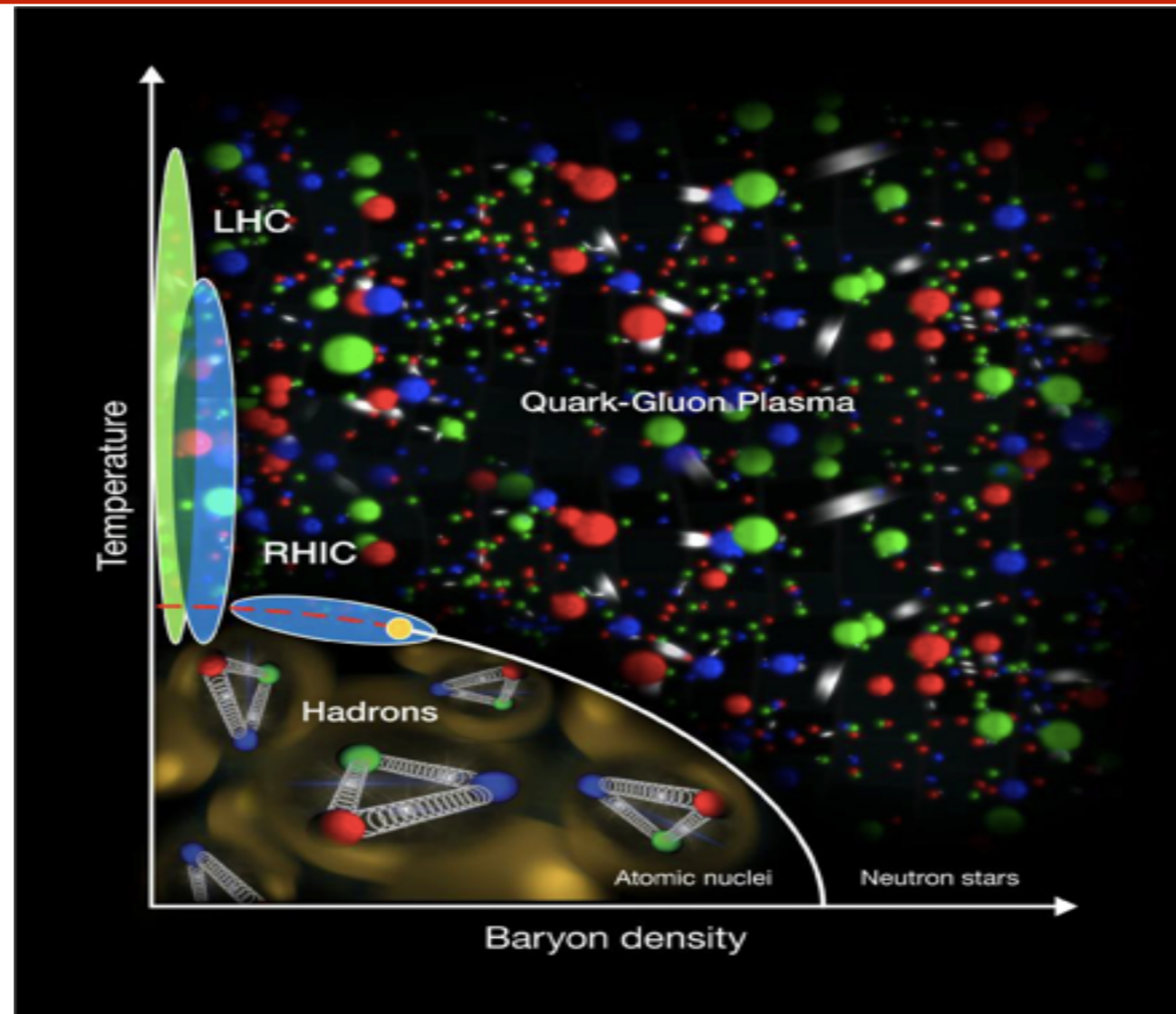
✓ Results/Discussions

- v_n at mid, forward/backward rapidities
- Initial model study
- Theory comparison

✓ Summary

Introduction

Quark Gluon Plasma(QGP)



QGP is a state of nuclear matter

- **extremely high temperature, density**
- **consist of asymptotic free quarks and gluons**
- **Almost perfect liquid**

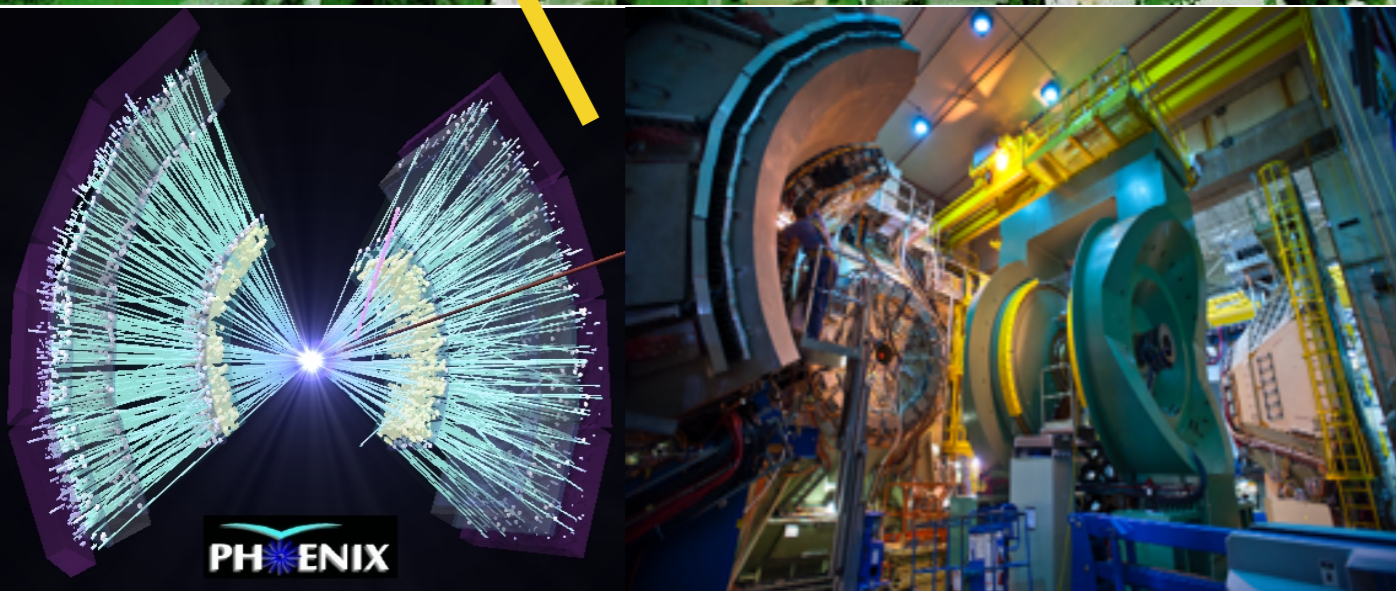
Predicted phase transition ε_c and T_c by Lattice QCD calculation

- **$T_c \sim 170 \text{ MeV}$**
- **$\varepsilon_c \sim 1 \text{ [GeV/fm}^3\text{]}$**

Relativistic Heavy Ion Collider(RHIC)



Species	Energies
Au+Au	200, 130, 62.4GeV 39, 27, 22.4GeV 19.6 14.6, 7.7GeV
Cu+Cu	200, 62.4, 22.4GeV
U+U	193GeV
Cu+Au	200GeV
3He+Au	200GeV
d+Au	200GeV
p+Au	200GeV
p+Al	200GeV
p+p	510, 500, 200GeV 62.4GeV



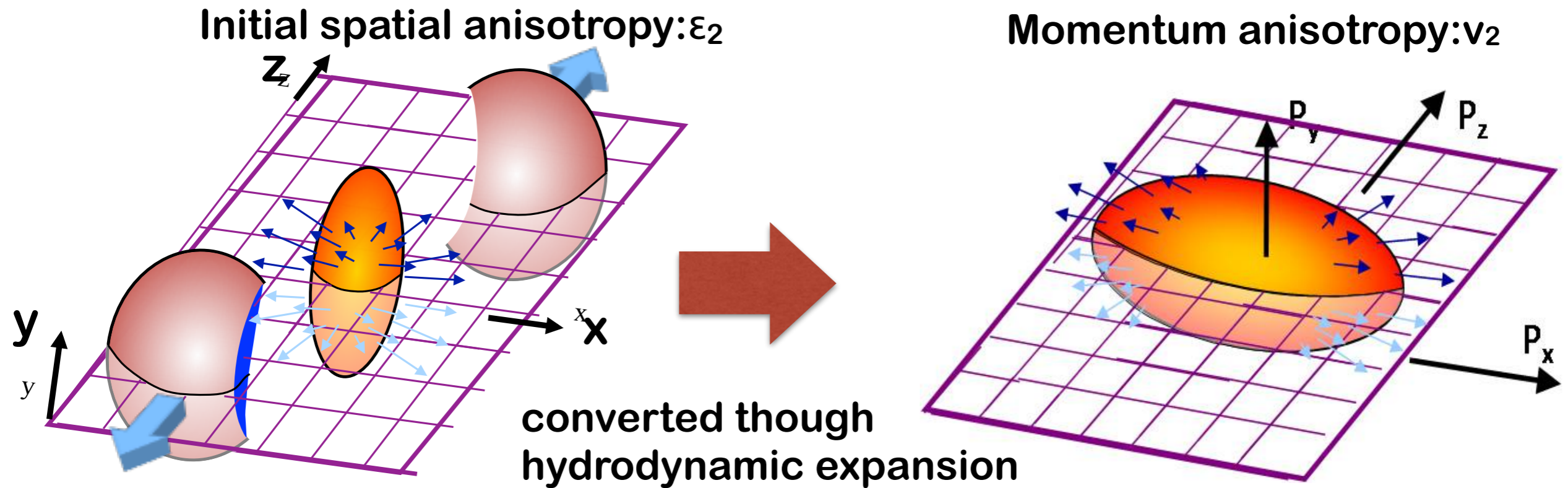
Wide range of species and energies

Relativistic heavy ion collision
is unique tool to form QGP

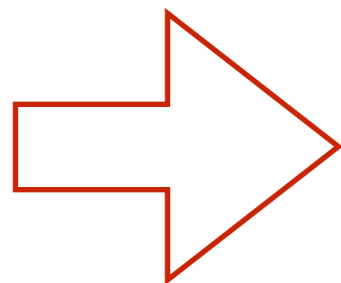
Au+Au 200GeV@RHIC

$-\varepsilon_{Bj} \sim 5 [\text{GeV}/\text{fm}^3] > \varepsilon_c$

Azimuthal anisotropy: Elliptic flow



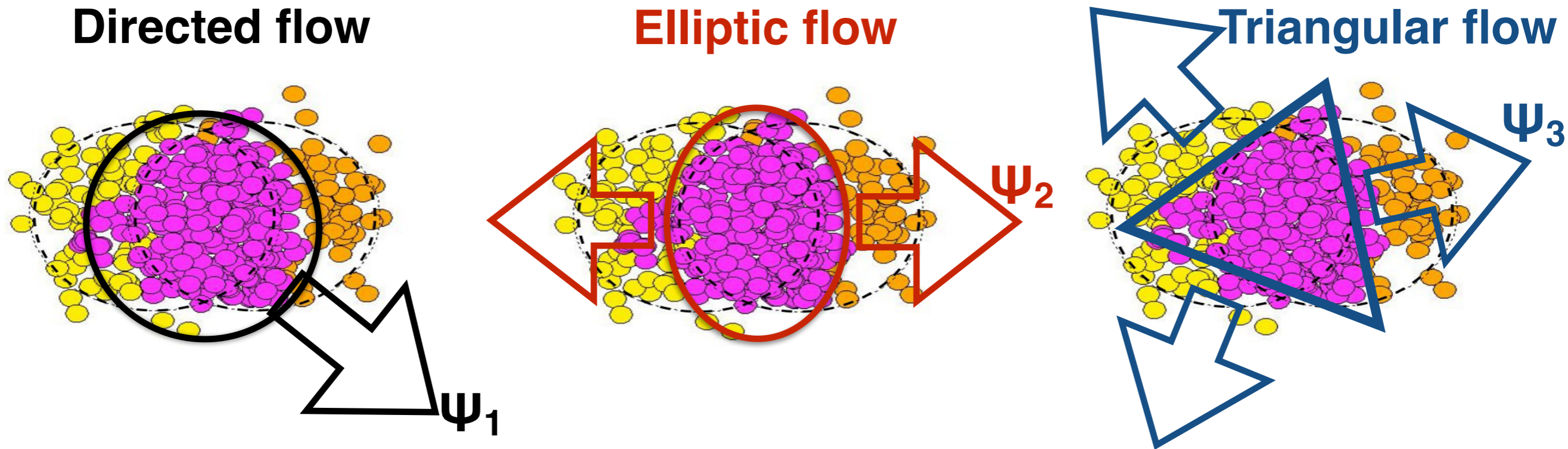
- ✓ Particle production will have an elliptical azimuthal distribution.
- Initial spatial anisotropy ε_2 \rightarrow Momentum anisotropy v_2
 - Non-isotropic pressure gradient



Sensitive to

- initial condition
(Glauber(nucleon),KLN(gluon)..etc.)
- viscosity of QGP (η/s)

Azimuthal anisotropy: Directed, Triangular flow

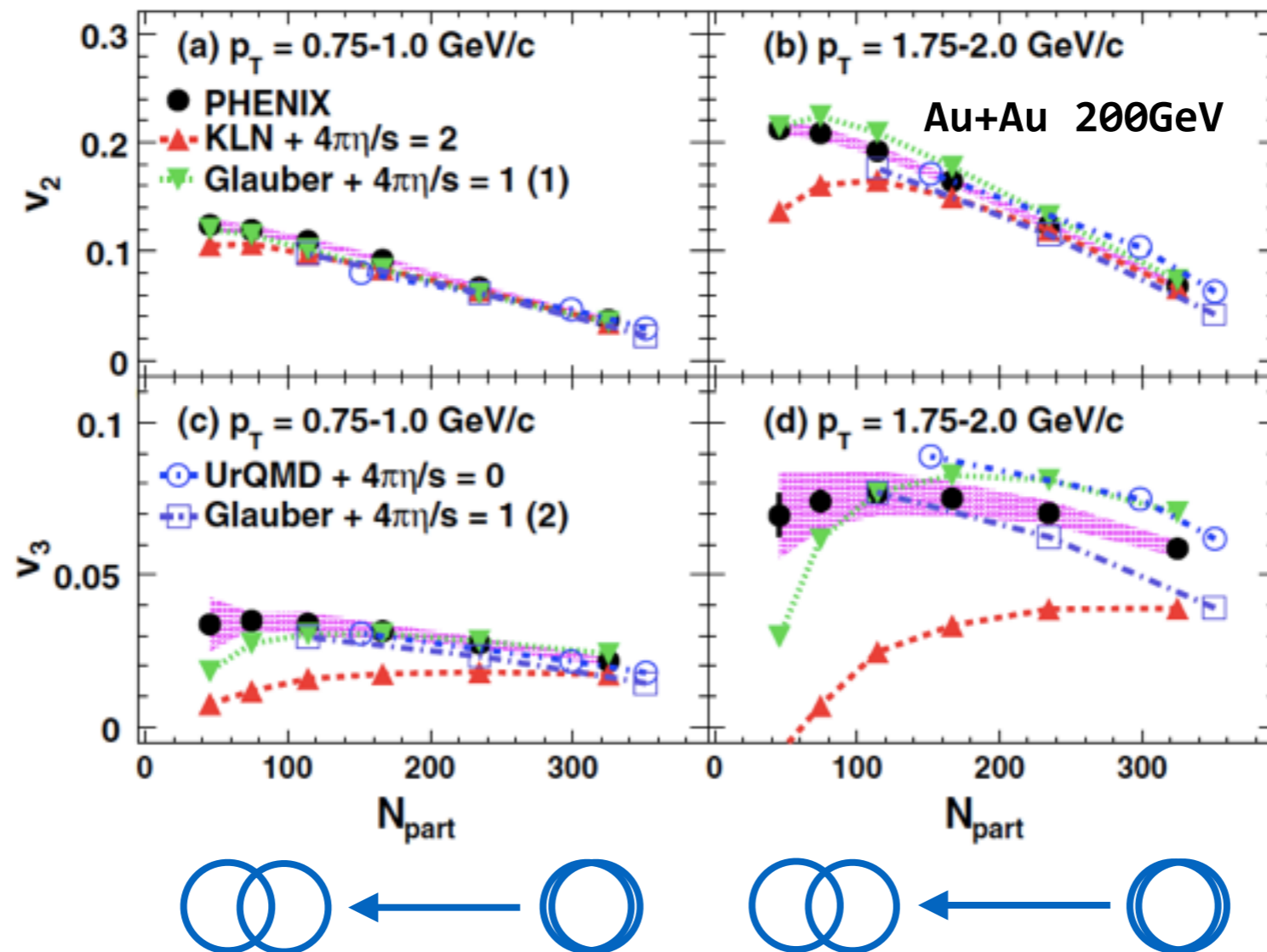


Event by event, initial participant fluctuation can lead to

- Directed particle production anisotropy v_1
- Triangular particle production anisotropy v_3
- v_4, v_5, v_6

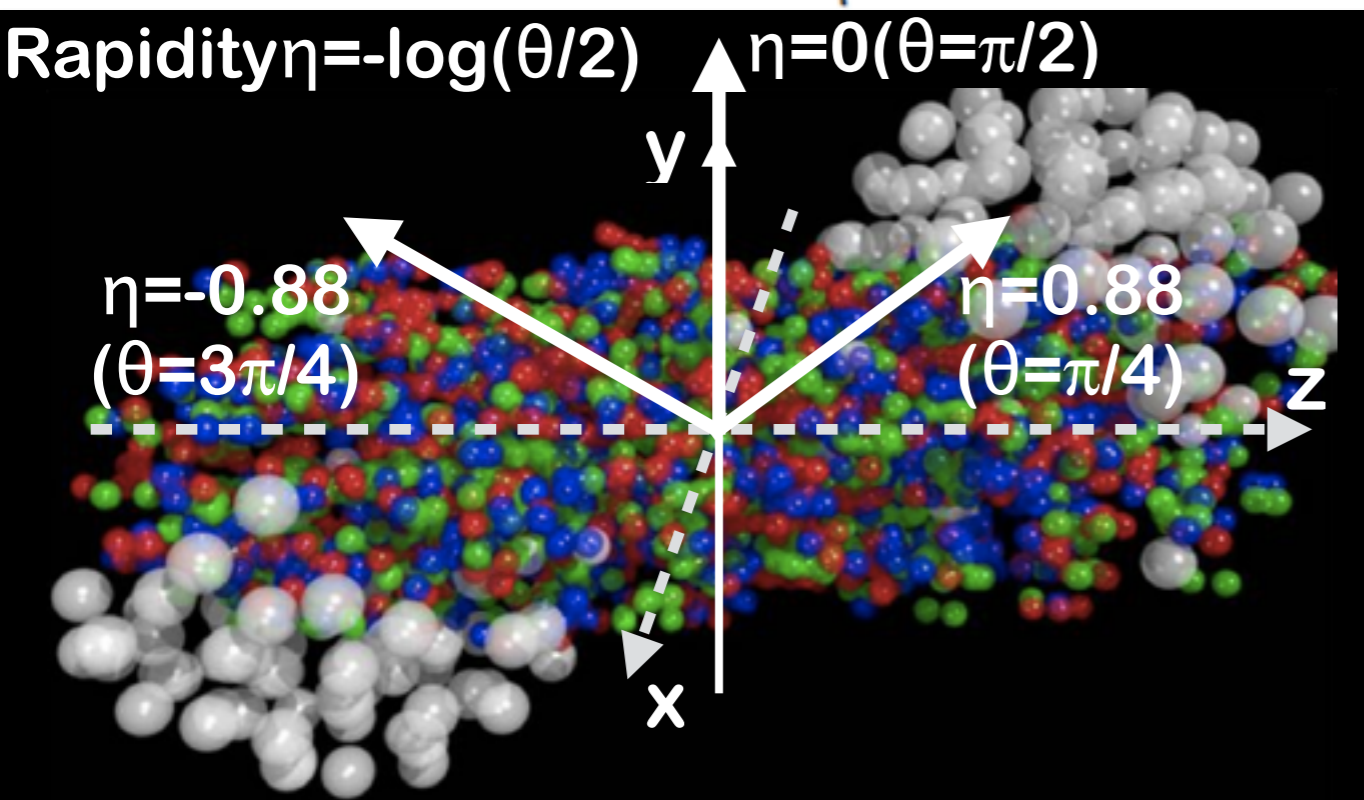
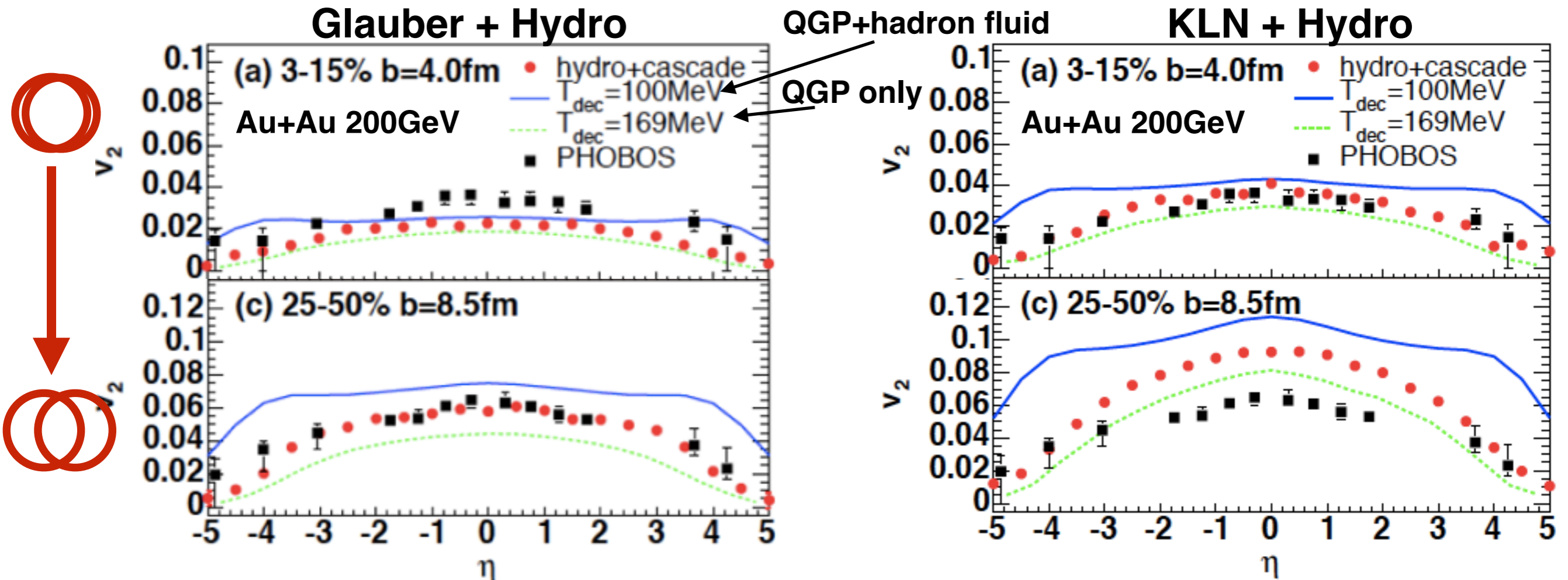
v_n constrain initial condition & viscosity

v_2, v_3 theory comparison



v_2, v_3 are sensitive to initial condition and viscosity of QGP
 - Theoretically, initial condition and viscosity have uncertainty
 -> v_n are good constraint of both of them

η dependence of v_2 with different initial conditions

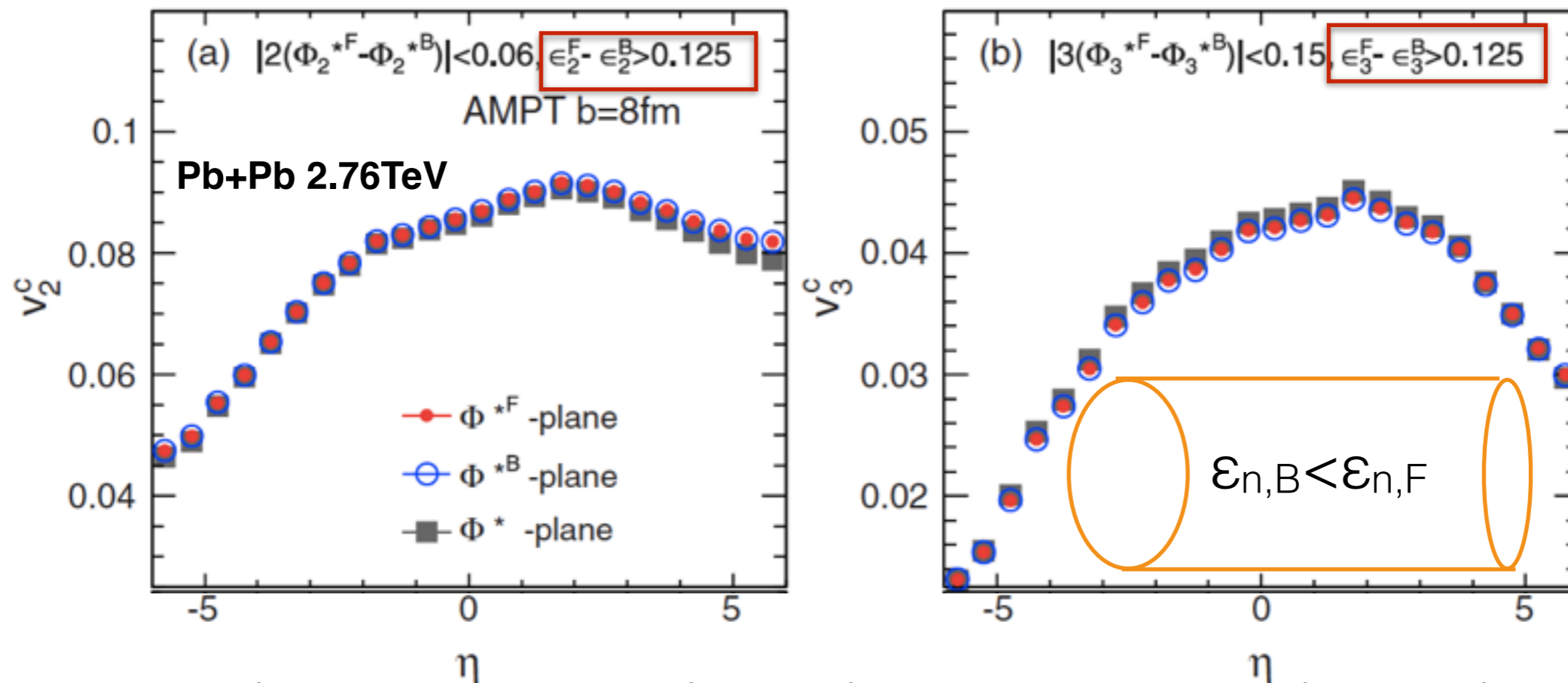


Phys.Lett.B636:299-304

- $\sqrt{v_2(\eta)}$ depends on initial condition
- v_2 with KLN $>$ v_2 with Glauber
- v_2 with Glauber reproduce data in mid-central collision
- v_2 with KLN reproduce data in central collision

Rapidity dependence of initial condition

PhysRevC.90.034915



✓ initial geometry has been considered to be

rapidity independent

✓ Initial conditions on target and projectile nuclei are not same event

$$\epsilon_n(+\eta) > \epsilon_n(-\eta)$$



$$v_n(+\eta) > v_n(-\eta)$$

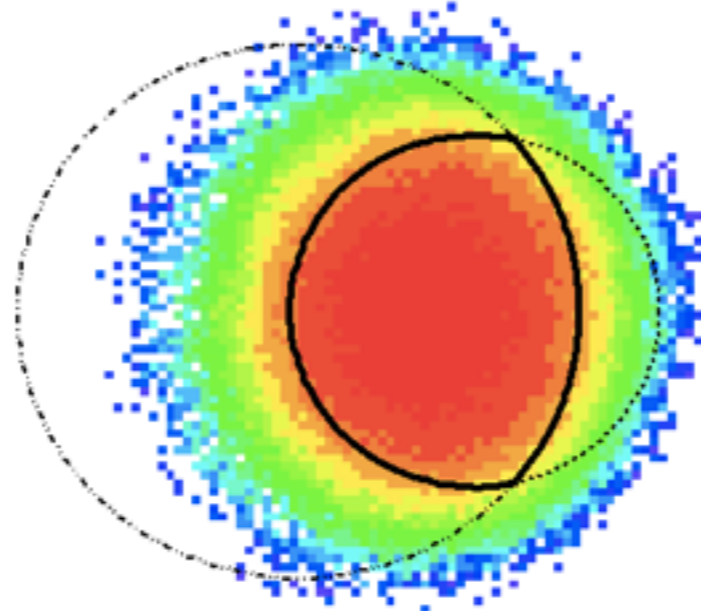
✓ Initial geometry has strong rapidity dependence



$$\epsilon_n(\eta) = \alpha \epsilon_n(+\eta) + \beta \epsilon_n(-\eta)$$

Motivation: Why Cu+Au is analyzed ?

Multiply-interacting
nucleons



**So far, v_n have been studied in symmetric collision systems
First asymmetric Cu+Au collisions were operated in 2012**

Asymmetric initial condition provides

- **Intrinsic triangularity of overlap zone -> larger v_3**
 - **Different left/right pressure gradient -> v_1**
 - **Different Forward/Backward density and geometry
-> Rapidity asymmetric v_n**
- > Measurements of v_n in asymmetric system could be good study of initial condition**

My activity

M1~M2 (2011~2013)

Repair VTX @BNL
 JPS Spring & Fall (Talk)
 QM2012 (poster)
 ATHIC 2012 (Talk)
 Au+Au flow analysis using VTX

D1(2013~2014)

Repair VTX @BNL
 Shift taking & detector expert
 for Run 13, Run14
 Cu+Au flow analysis

D2 (2014~2015)

QM2014(Talk)
 JPS-DNP(Talk)
 Shift taking & detector expert
 for Run 14, Run15

D3(2015~2016)

QM2015(Poster)
 TGSW2015 (Talk)
 WWND2016(Talk)

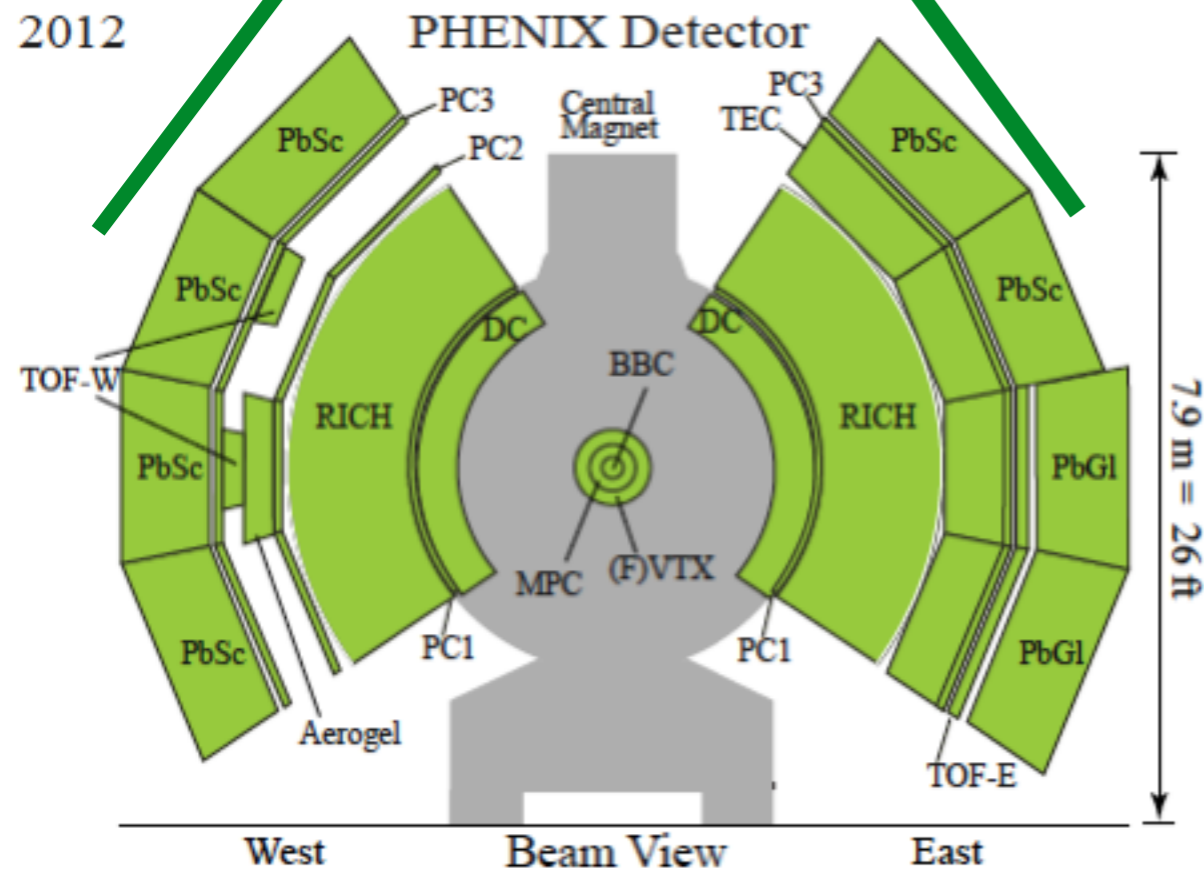
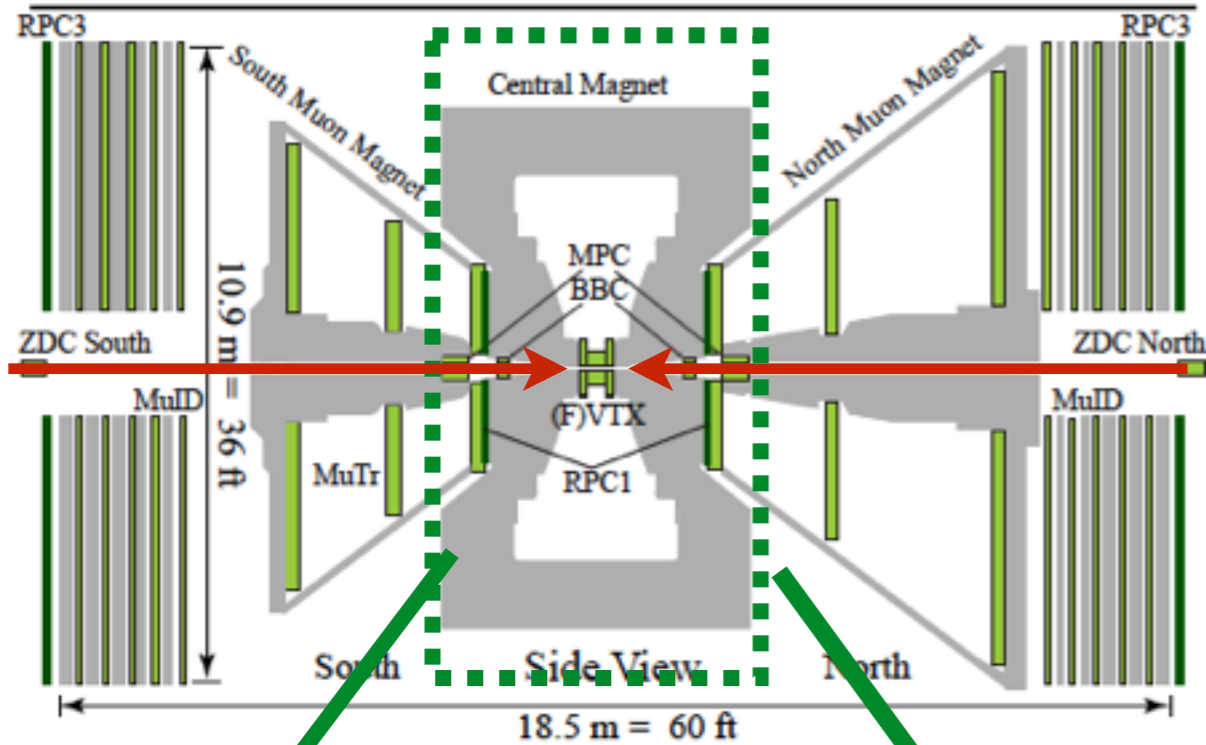
D4 (2016~)

Cu+Au flow paper is
 accepted by PRC

Domestic conference
 International conference
 Hardware and shift
 Analysis

Experiment Analysis

PHENIX detectors



Trigger, centrality, collision vertex
Event plane

-Beam Beam counter(BBC)
($3 < |\eta| < 4$)

Event plane

-Zero degree calorimeter
-Shower max detector

Charged particle Tracking

-Drift Chamber(DC) ($|\eta| < 0.35$)

- Momentum

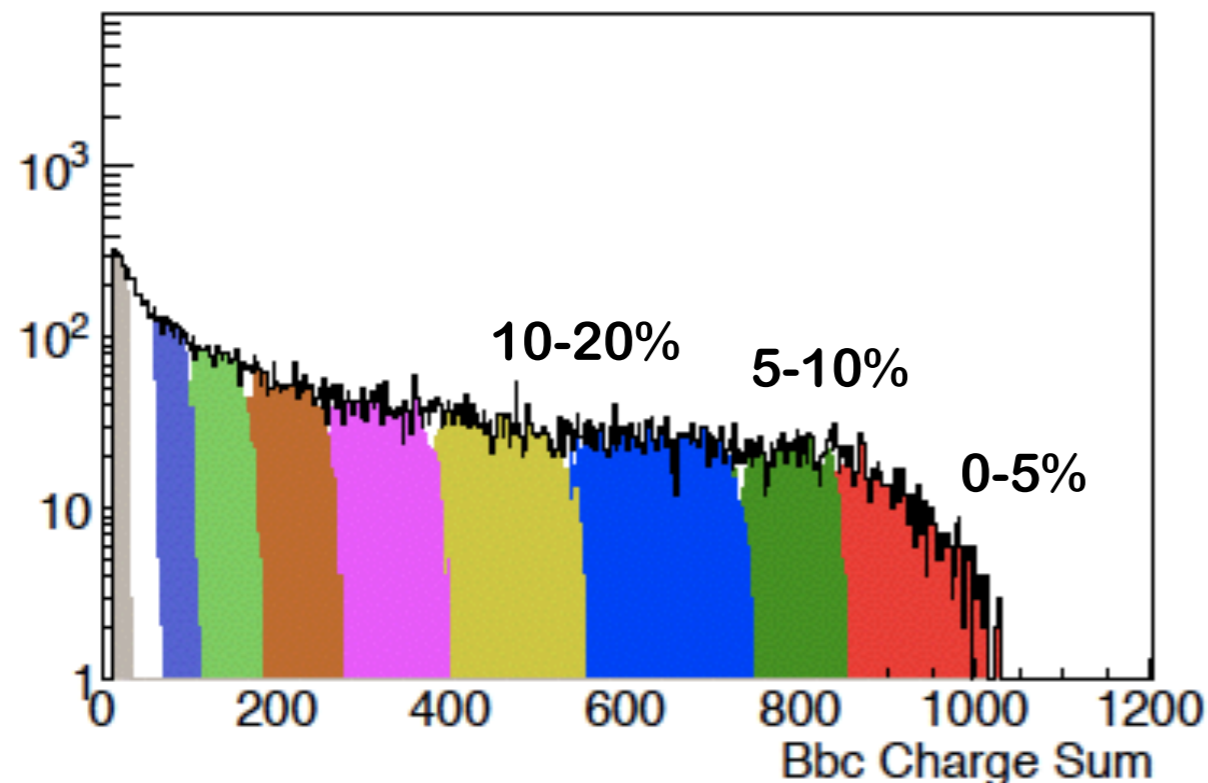
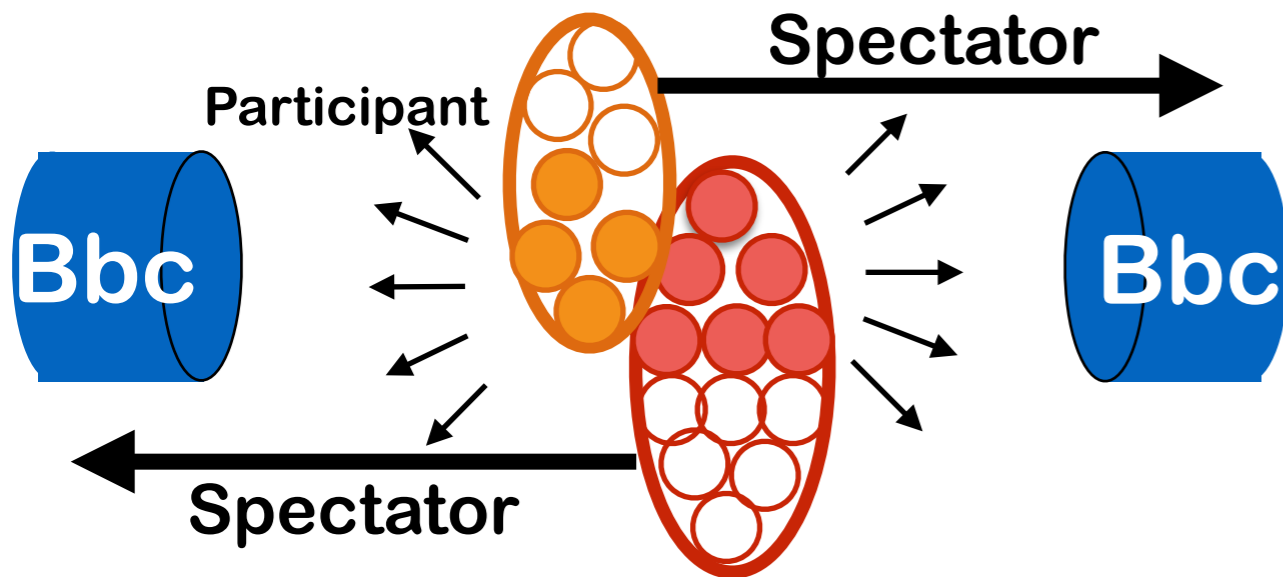
-Pad Chamber(PC) ($|\eta| < 0.35$)

- Hit position

-Electro magnetic
calorimeter(EMC) ($|\eta| < 0.35$)

- Hit position

Collision centrality



✓ Fraction of events in terms of total geometrical cross section
-Overlap zone of two nuclei

$$\propto \text{Multiplicity}$$

✓ Experimentally, overlap zone is classified by multiplicity in Bbc
- Multiplicity in Bbc

$$\propto \text{Overlap zone}$$

✓ Each percentile contains same number of events
- Most central collision 0 %
- Most peripheral collisions 100%

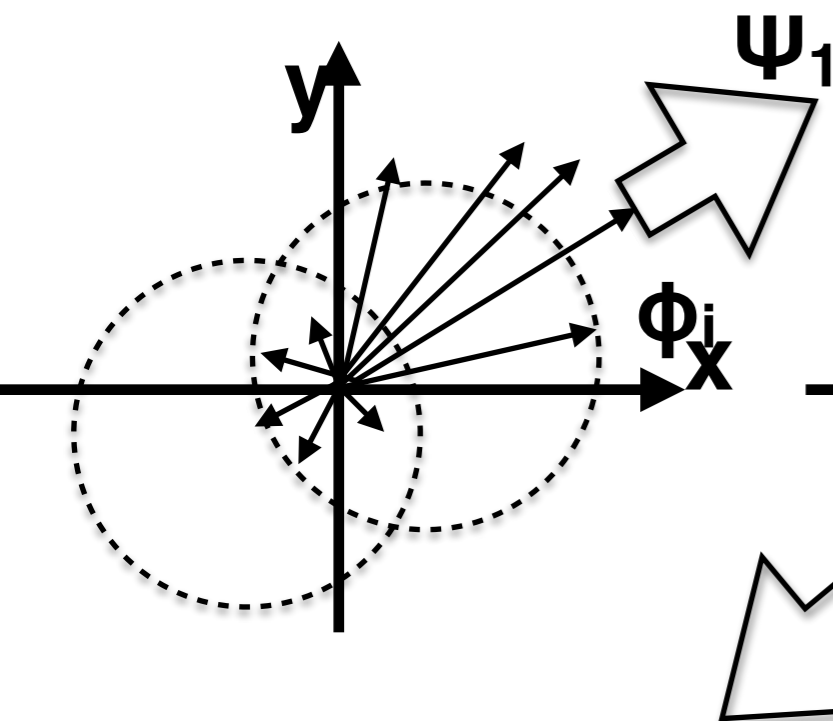
Anisotropy measurement via Event Plane method

Event plane(EP) method

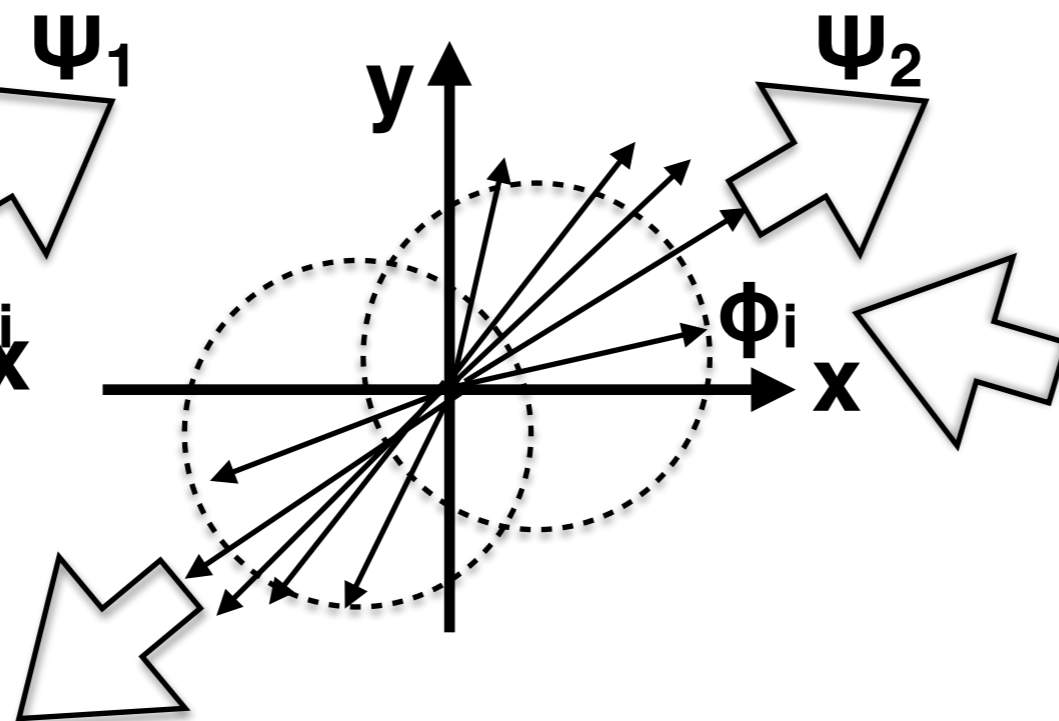
- one of the flow measurement methods
- produced particles are measured with respect to EP
- EP is the azimuthal direction most particles are emitted to
- observed v_n is corrected by EP resolution

$$v_n = \frac{\langle \cos(n[\phi - \Psi_n^{obs}]) \rangle}{\text{Res}\{\Psi_n^{obs}\}}$$

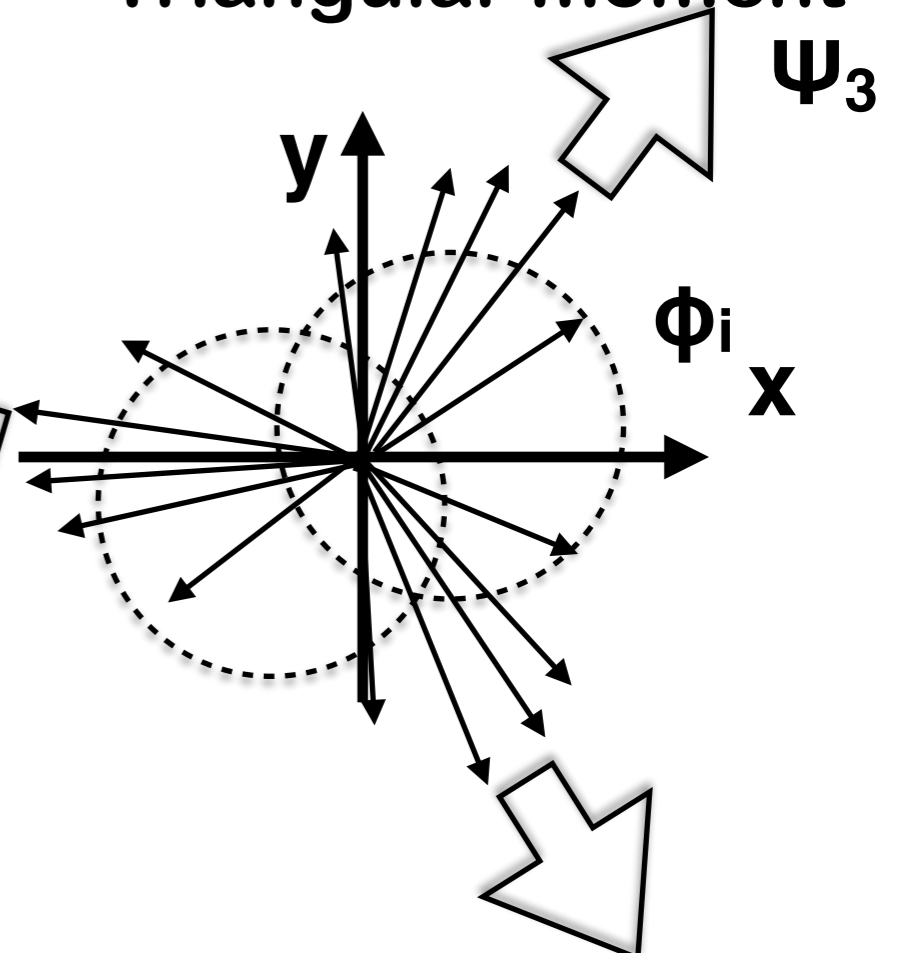
Directed moment



Elliptic moment



Triangular moment Ψ_3



Event plane detectors and resolutions

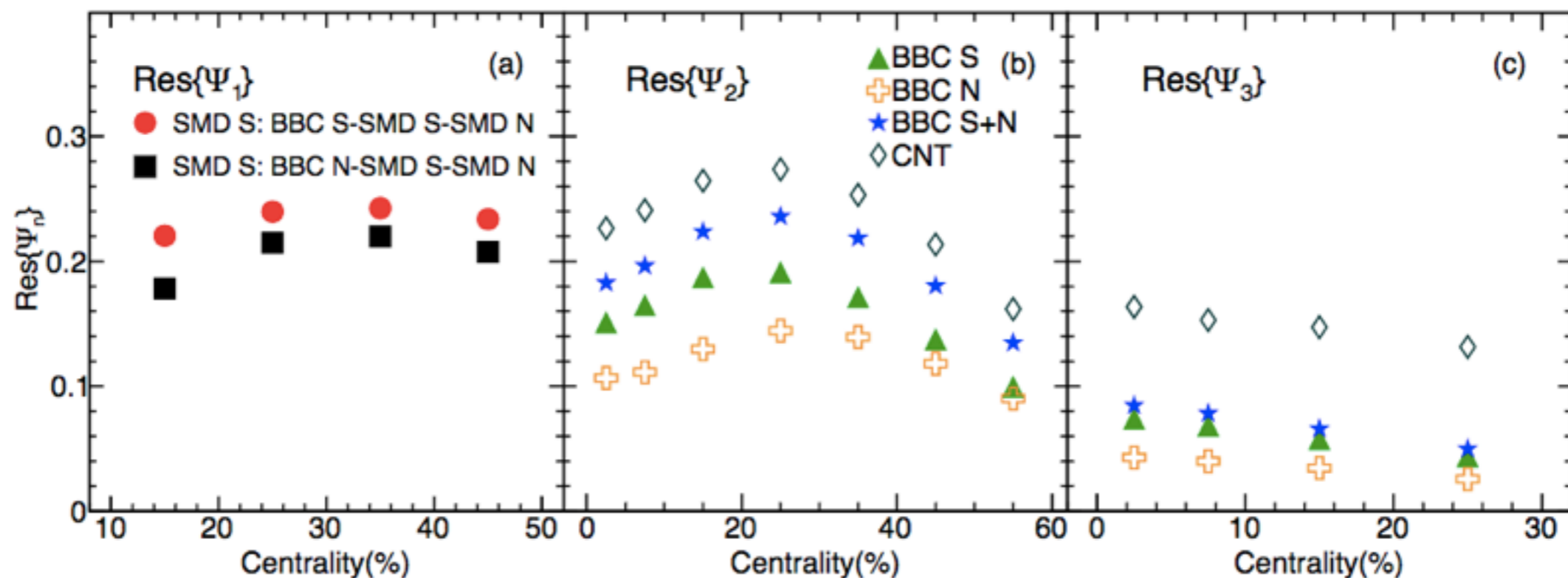
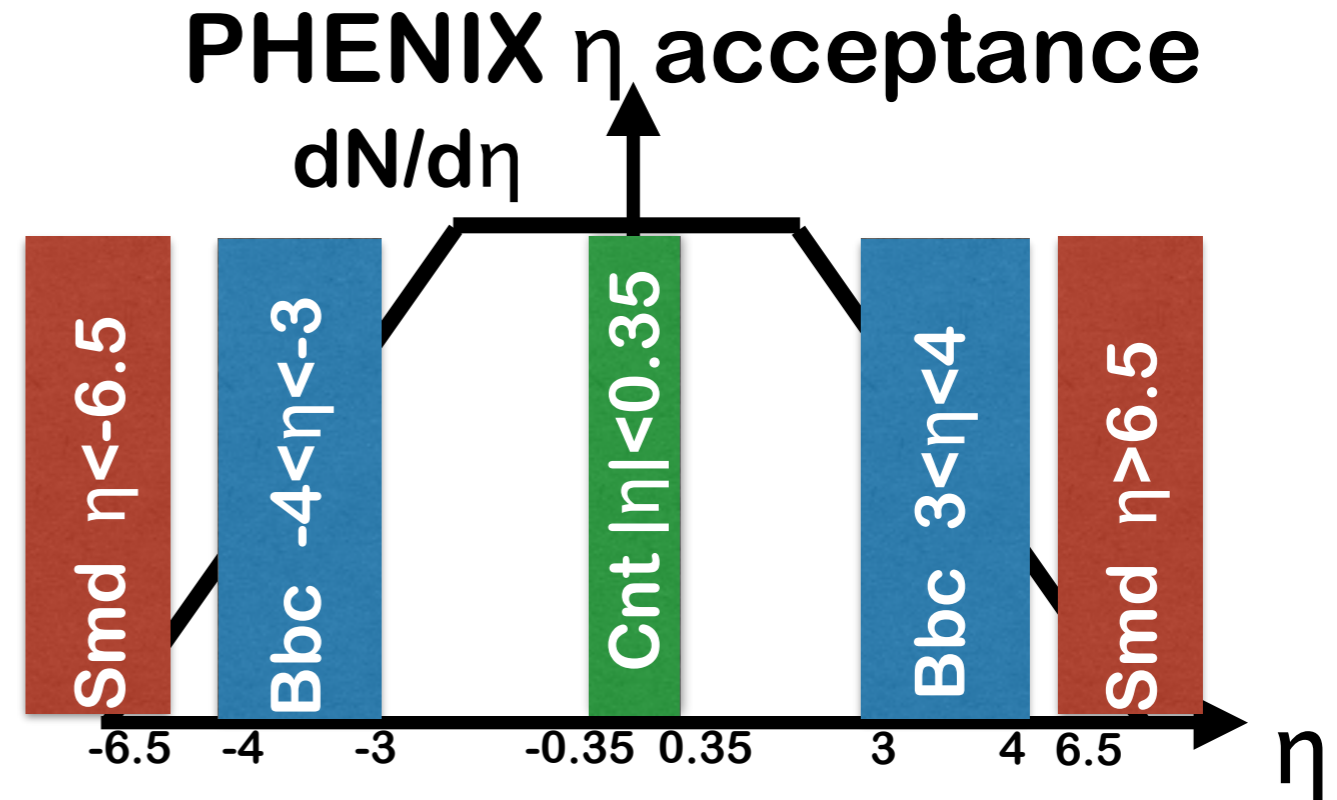
Event Plane detectors

- 2nd, 3rd Event plane
 - Bbc, Cnt
- 1st Event plane
 - Bbc, Smd

Event Plane resolution

- Estimated from EP correlations (3sub method)

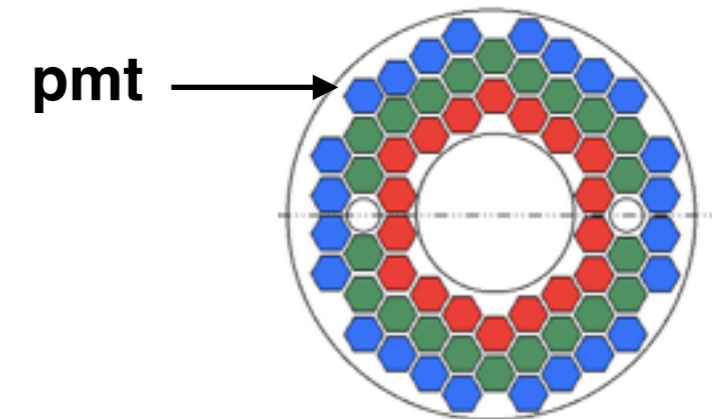
$$\text{Res}\{\Psi_n^{\text{obs}}\} = \langle \cos(n[\Psi_n^{\text{obs}} - \Psi_n^{\text{true}}]) \rangle$$



v_n measurement at Bbc ($3 < |\eta| < 4$)

✓ v_n is measured using 64 Bbc pmts

- Bbc can not reconstruct tracks
- Measured v_n include back ground



✓ Full Geant simulation with PHENIX configuration

- Measured $v_n \rightarrow$ True v_n

$$v_n^{\text{true}} = \frac{v_n^{\text{mes}}}{R_n}$$

$$R_n = \frac{v_{n,\text{output}}^{\text{Sim}}}{v_{n,\text{input}}^{\text{Sim}}}$$

$v_{n,\text{input}}^{\text{Sim}}$
Input v_n from particle simulation

$v_{n,\text{output}}^{\text{Sim}}$
Output v_n from Geant simulation

✓ Correction factor R_n

- R_2 : 0.74
- R_3 : 0.66

✓ Systematic study

- $dN/d\eta$
- p_T spectra
- v_n (pt)
- v_n (eta)

Systematic sources

$\sqrt{v_n}$ at mid- η

- East and West arm difference
- CNT track cut
- Event Plane difference
- Event Plane resolution difference

$\sqrt{v_n}$ at F/B- η

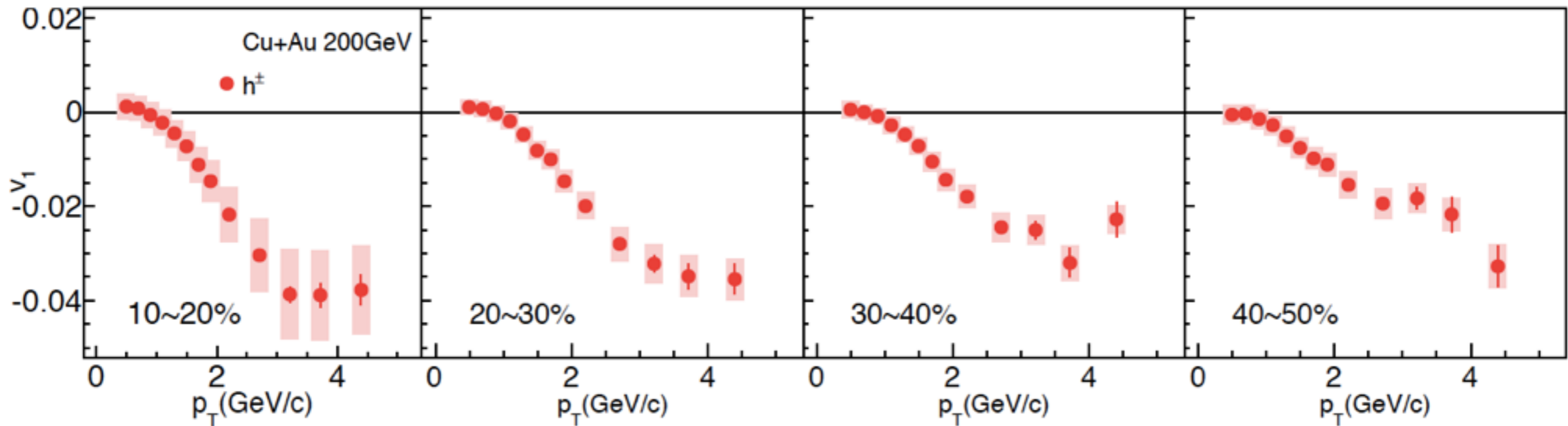
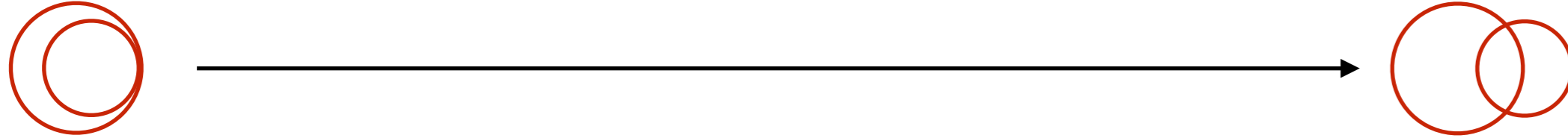
- Event Plane difference
- Geant simulation
 - $dN/d\eta$ distribution
 - p_T distribution
 - p_T dependence of v_n
 - η dependence of v_n

Results

Discussions

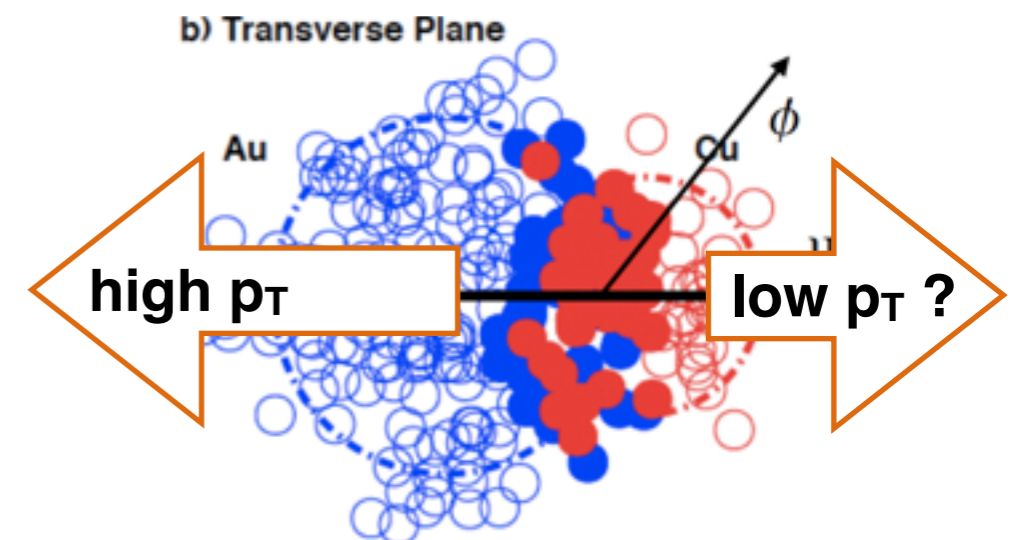
- v_1, v_2, v_3 at mid- η
- v_2, v_3 at F/B - η
- Initial condition study
- v_1, v_2, v_3 theory comparison

Charged hadron $v_1(p_T)$ in Cu+Au collisions

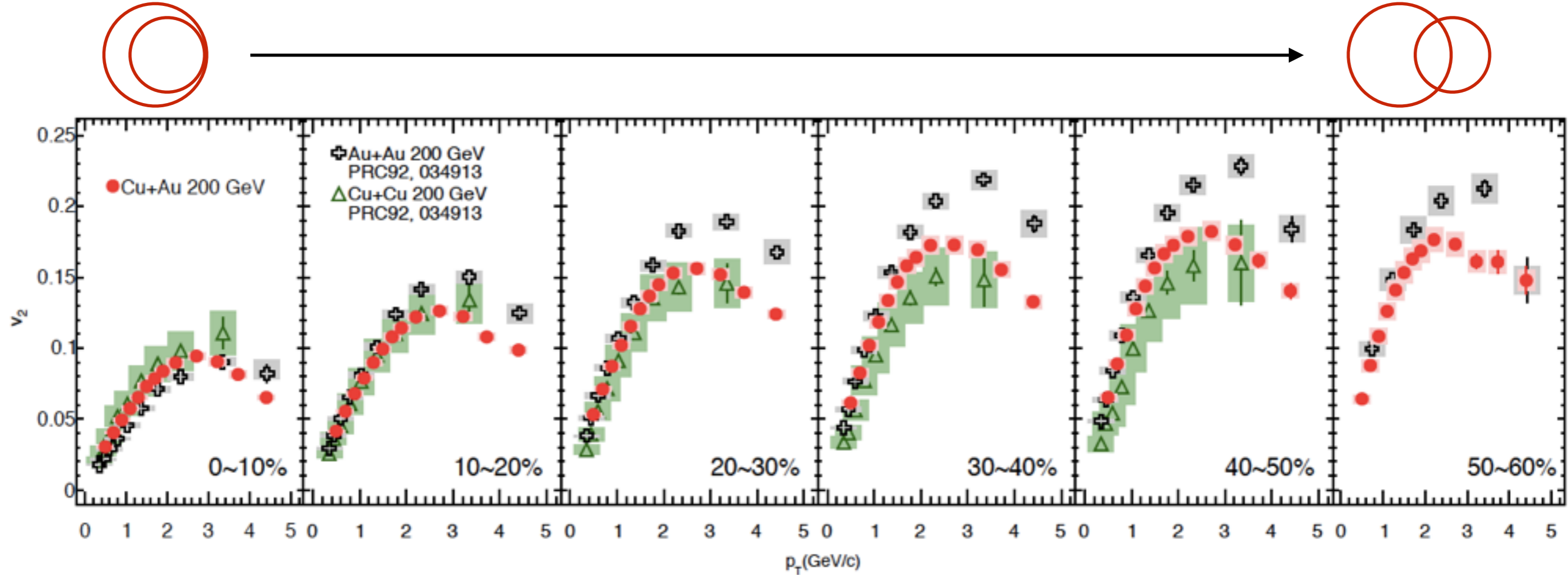


✓ v_1 at mid-rapidity is observed for 10-50%
 ✓ Negative v_1 indicates high p_T particles are emitted to Au side

- Magnitude decreases from central to more peripheral events
- In peripheral events, Left/Right path length becomes similar

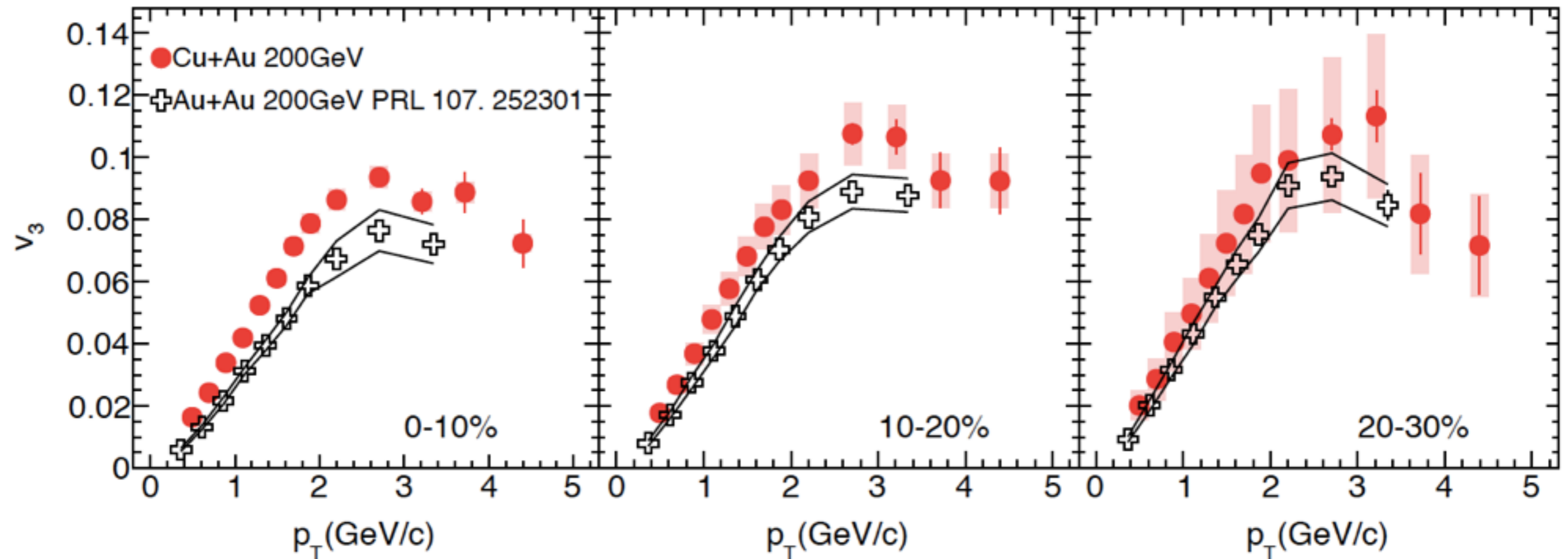
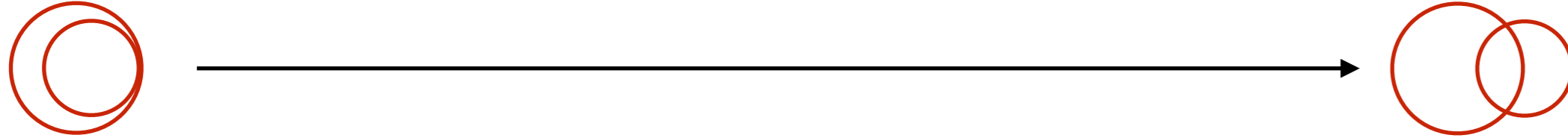


Charged hadron $v_2(p_T)$ in Cu+Au collisions



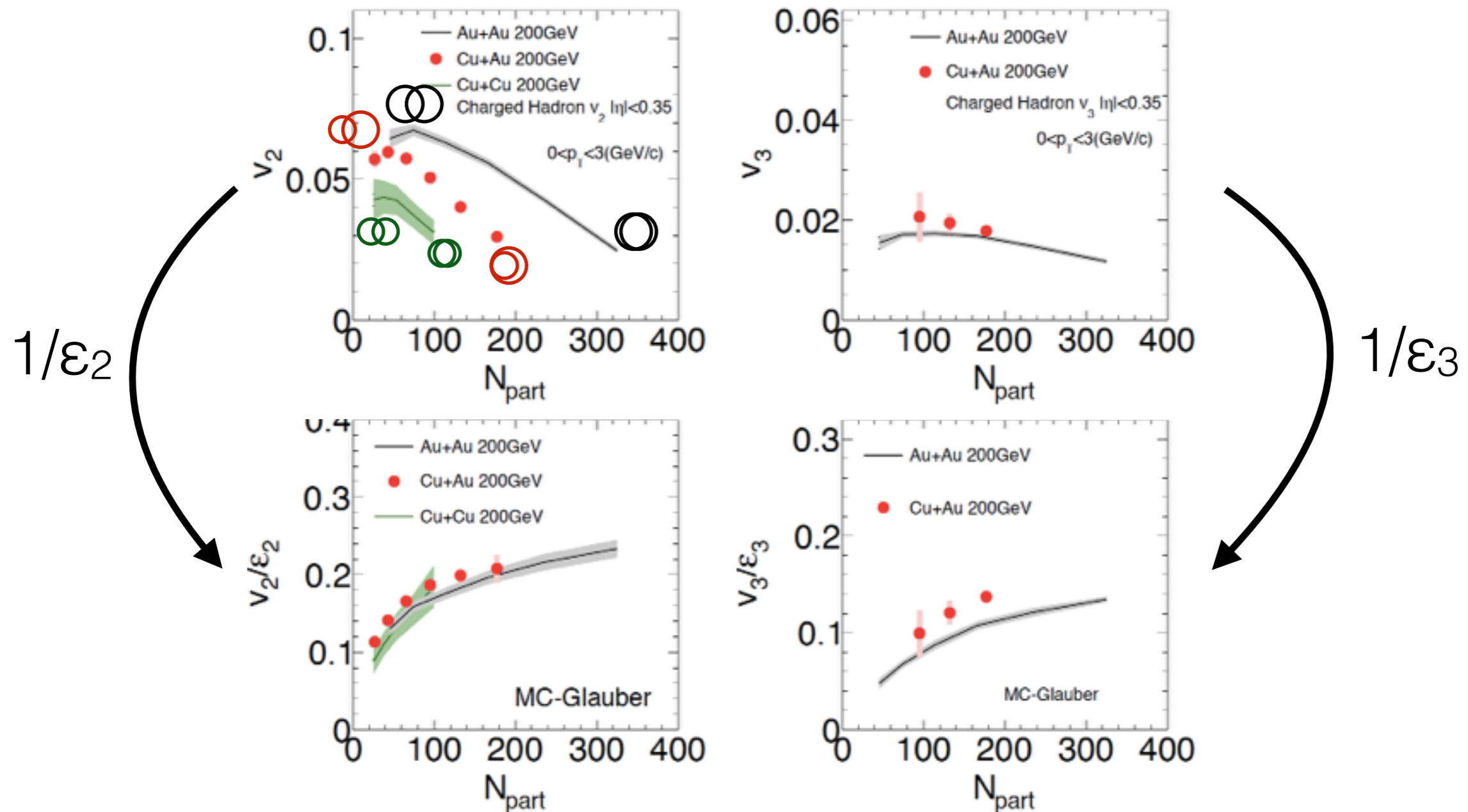
- ✓ Similar p_T and centrality dependence of v_2 as seen in symmetric collisions
- Strong centrality dependence, magnitude increase from central to peripheral
- Cu+Au v_2 is between symmetric Au+Au and Cu+Cu collisions

Charged hadron $v_3(p_T)$ in Cu+Au collisions



- ✓ Similar p_T and centrality dependence of v_3 as seen in symmetric collisions
- Weak centrality dependence, magnitude slightly increase from central to peripheral
- Cu+Au v_3 shows larger values than Au+Au results

System size dependence of $v_n(N_{\text{part}})$



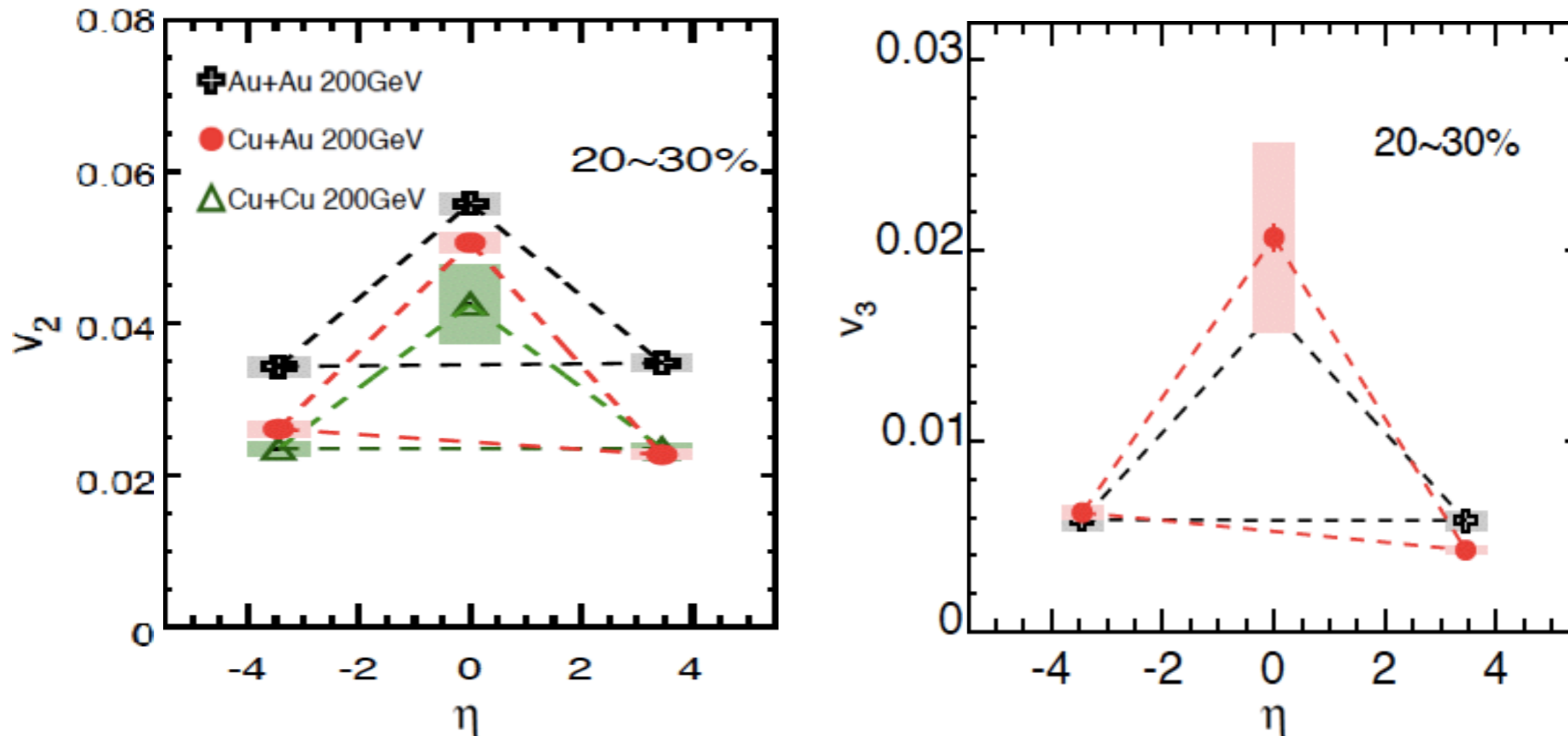
- ✓ Cu+Au v_2/ϵ_2 is consistent with Au+Au and Cu+Cu results
- ✓ Unlike v_2 , Cu+Au v_3 is slightly larger than Au+Au v_3
 - Cu+Au v_3 arises from not fluctuations but also intrinsic triangularity of overlap zone ?
- ✓ Cu+Au v_3/ϵ_3 is not consistent with Au+Au results
 - MC-Glauber might not reproduce ϵ_3 correctly

Results

Discussions

- v_1, v_2, v_3 at mid- η
- v_2, v_3 at F/B- η
- Initial condition study
- v_1, v_2, v_3 theory comparison

Rapidity dependence of v_n in Cu+Au collisions



✓ In Cu+Au collisions, F/B asymmetry of v_n is observed.

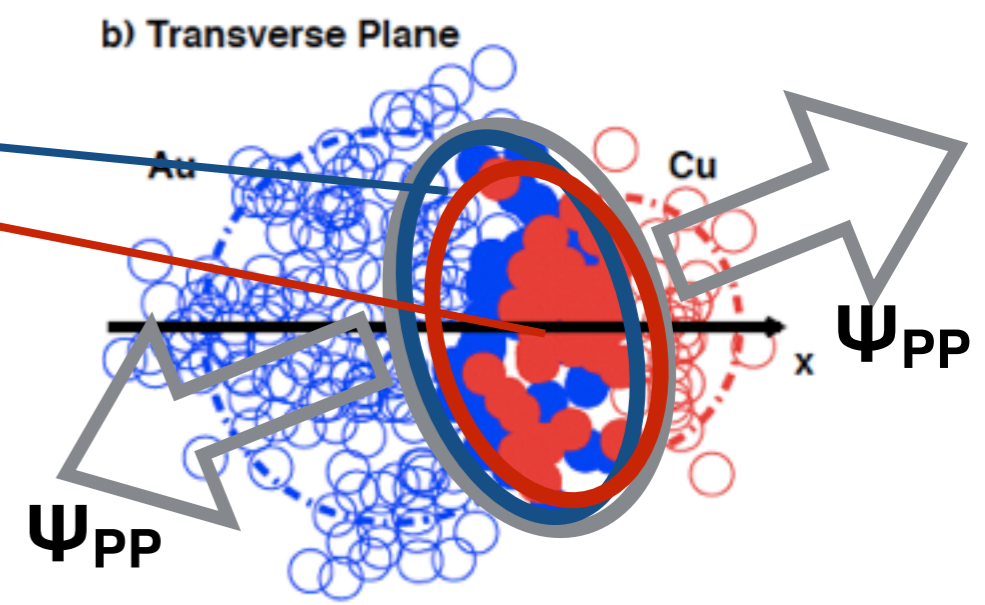
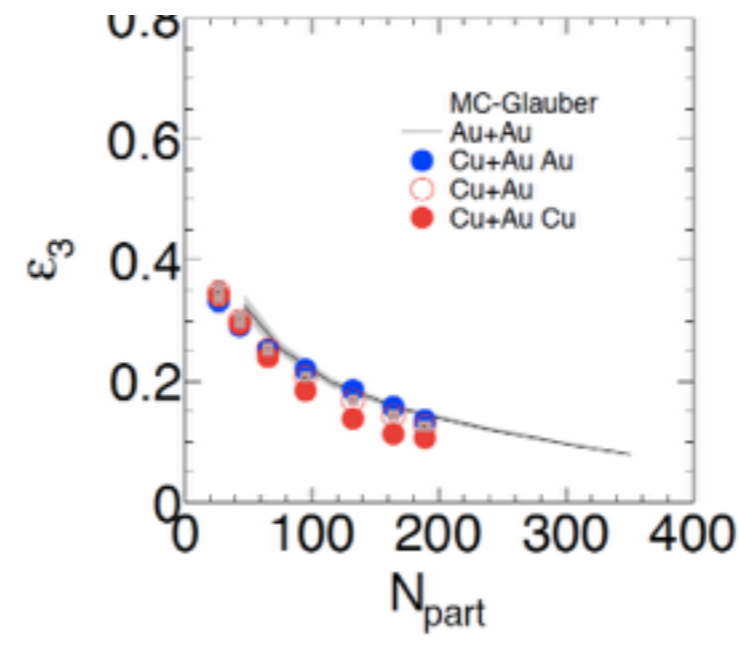
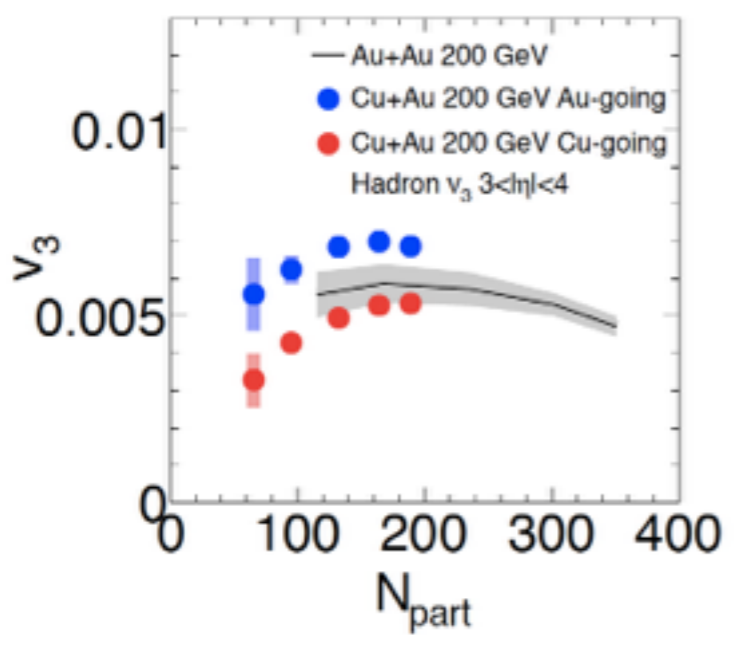
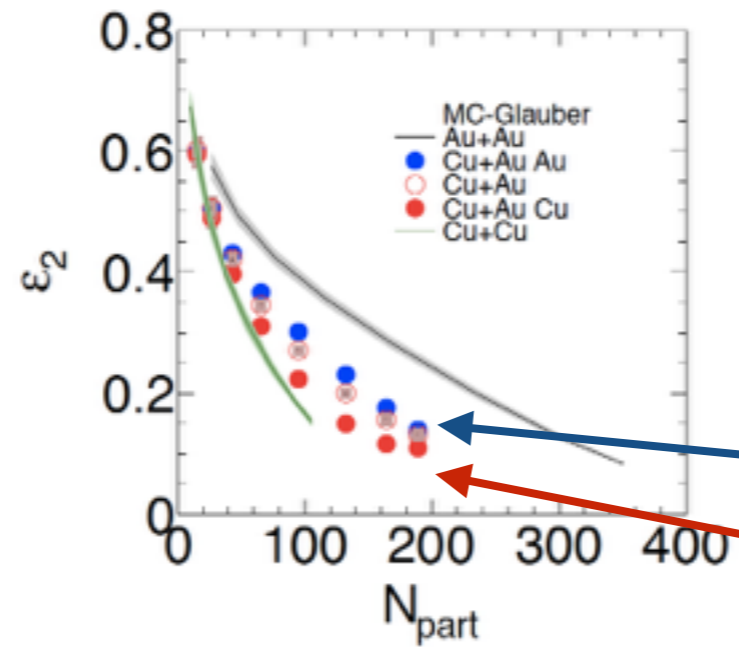
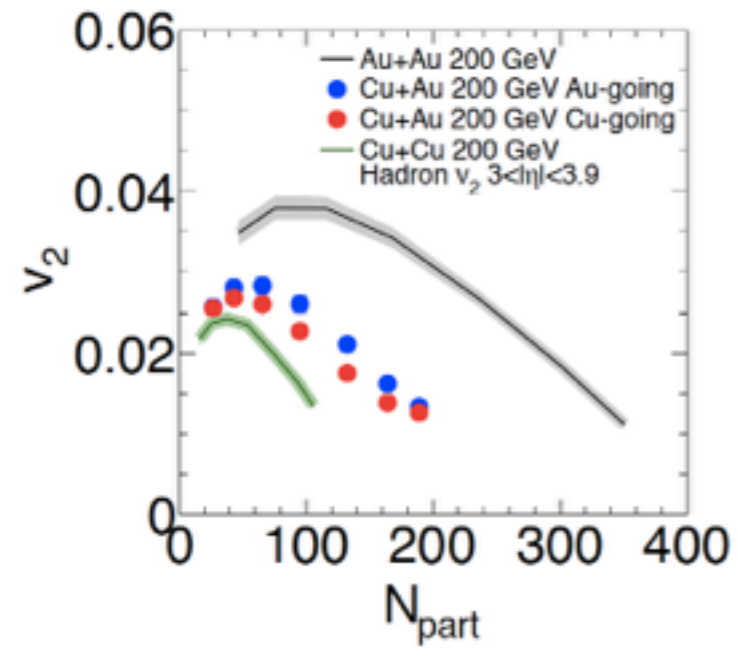
- $v_2(\text{Au-going}) > v_2(\text{Cu-going})$

- $v_3(\text{Au-going}) > v_3(\text{Cu-going})$

-> caused by different initial geometries in Au and Cu ?

✓ Unlike v_2 , Au-going v_3 in Cu+Au show similar values of Au+Au v_3

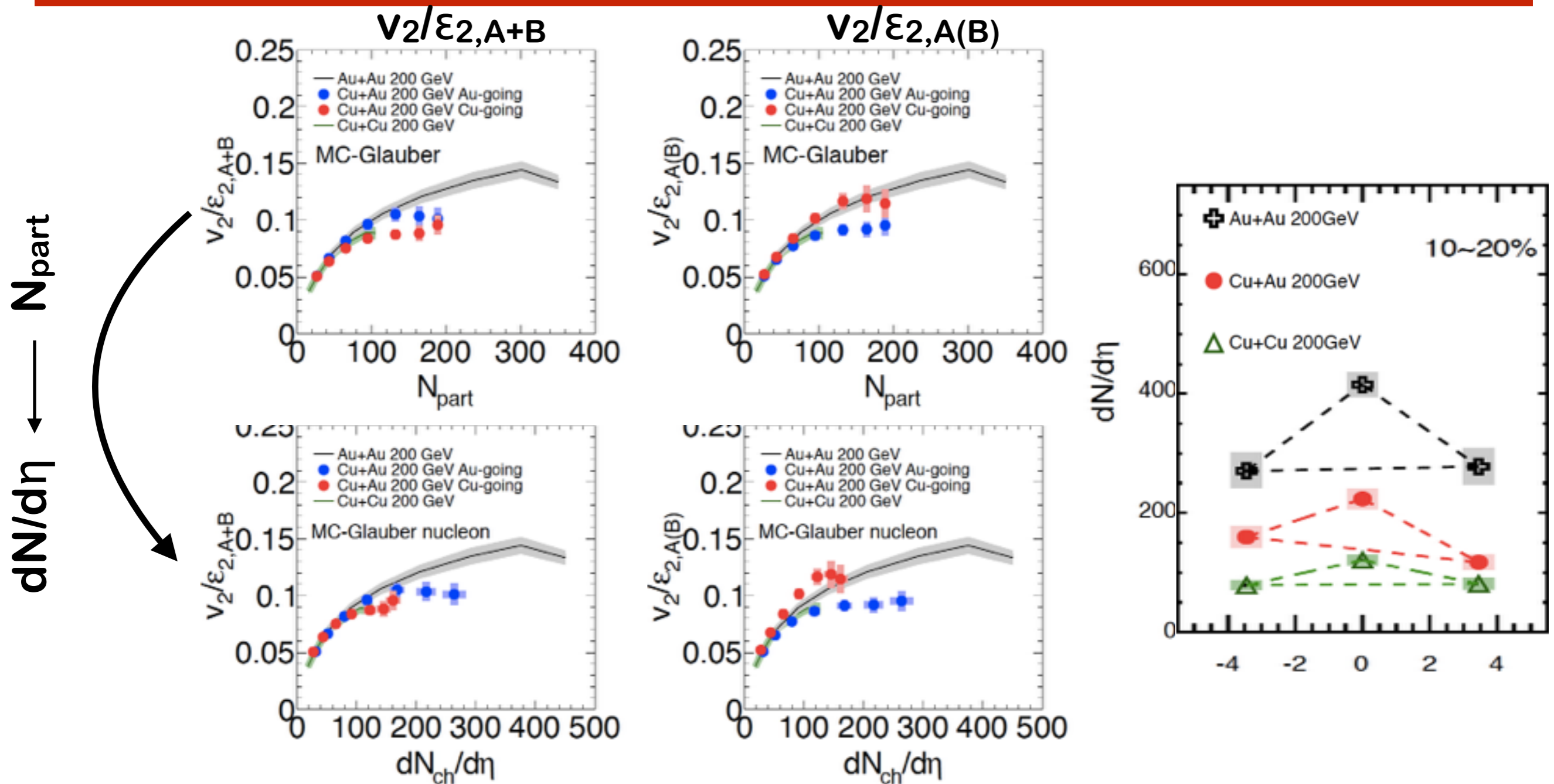
System size dependence of $v_n(N_{part})$ at F/B rapidity



✓ F/B asymmetry of v_2 is consistent that of ϵ_2
 $-\epsilon_{n,Au}$ and $\epsilon_{n,Cu}$ are estimated from Au and Cu participants separately

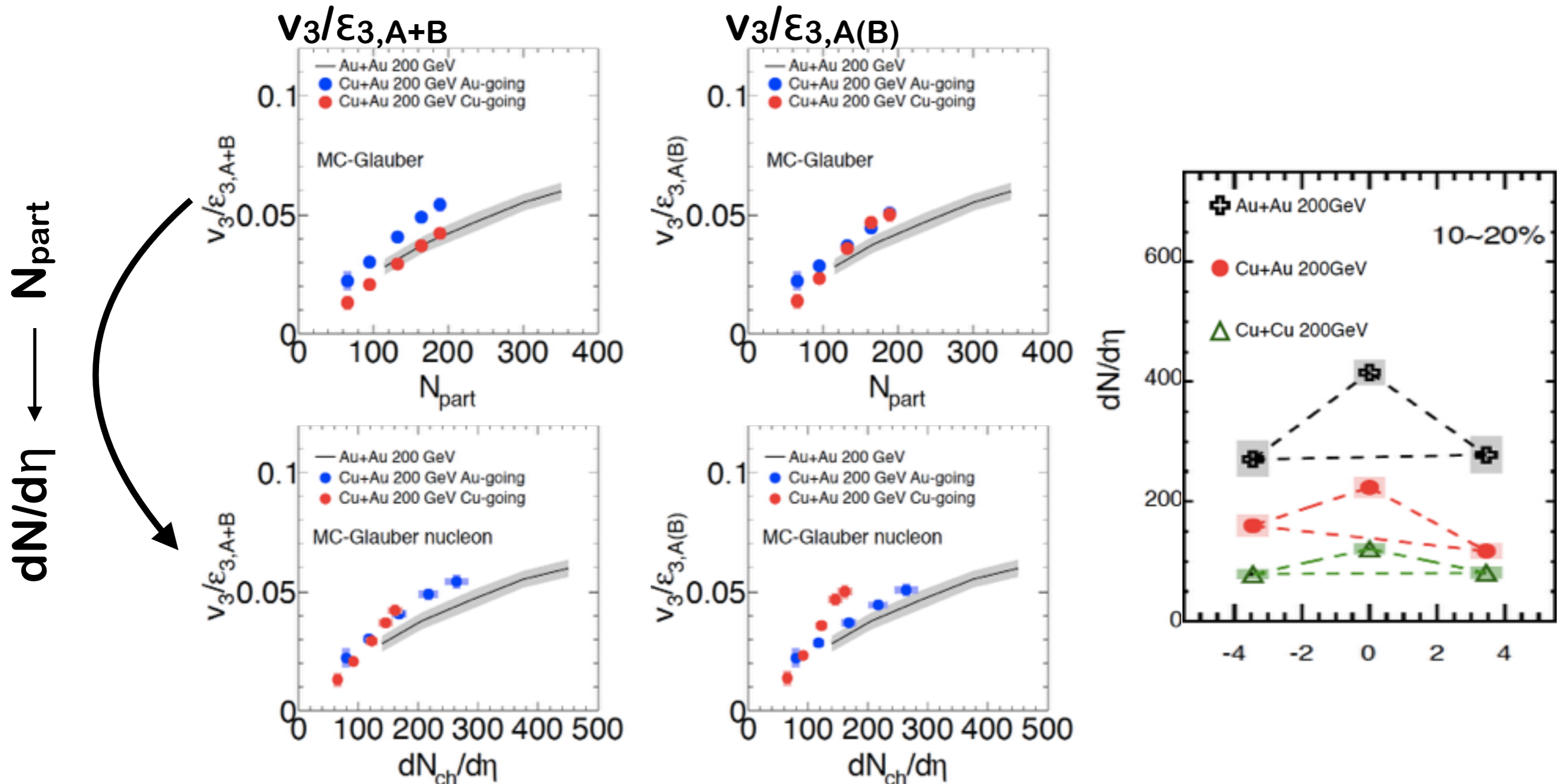
$\epsilon_{n,Au} > \epsilon_{n,Cu} \rightarrow v_{n,Au} > v_{n,Cu} ?$

Eccentricity scaling of v_2 at F/B rapidity



- ✓ In both cases, $v_2/\epsilon_2 (N_{part})$ in Au-going side and Cu-going side are not consistent \rightarrow Need take into account different energy ?
- ✓ $dN/d\eta(\text{Au-going}) > dN/d\eta(\text{Cu-going}) \rightarrow v_n(\text{Au-going}) > v_n(\text{Cu-going})$
- ✓ Scaled $v_2/\epsilon_{2,A+B}$ are consistent between Au-going and Cu-going

Eccentricity scaling of v_3 at F/B rapidity



✓ In both cases, v_3/ϵ_3 (N_{part}) in Au-going side and Cu-going side are not consistent

✓ Scaled $v_3/\epsilon_{3,A+B}$ are consistent between Au-going and Cu-going

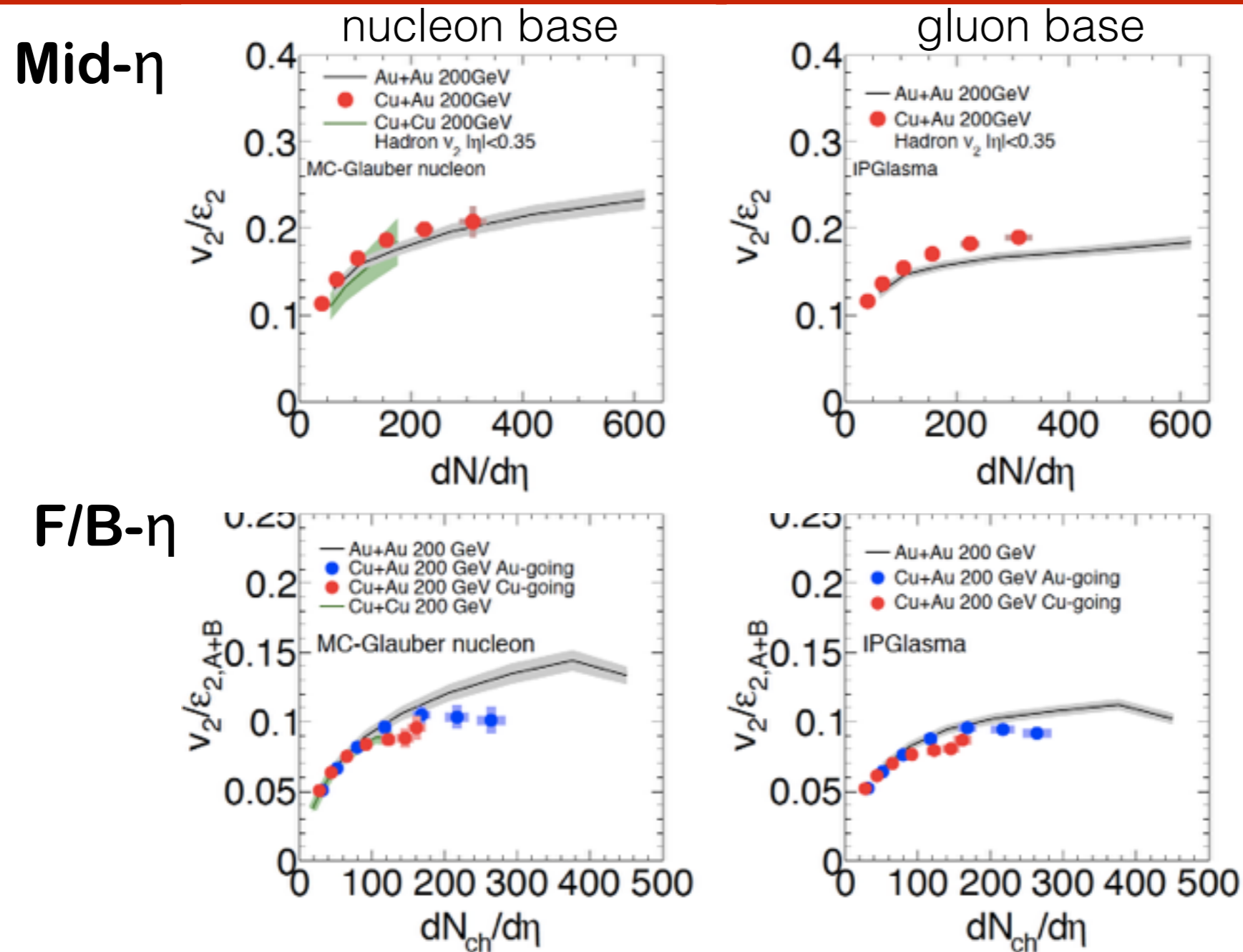
✓ F/B asymmetry of v_n arise from F/B asymmetry of density($dN/d\eta$)

Results

Discussions

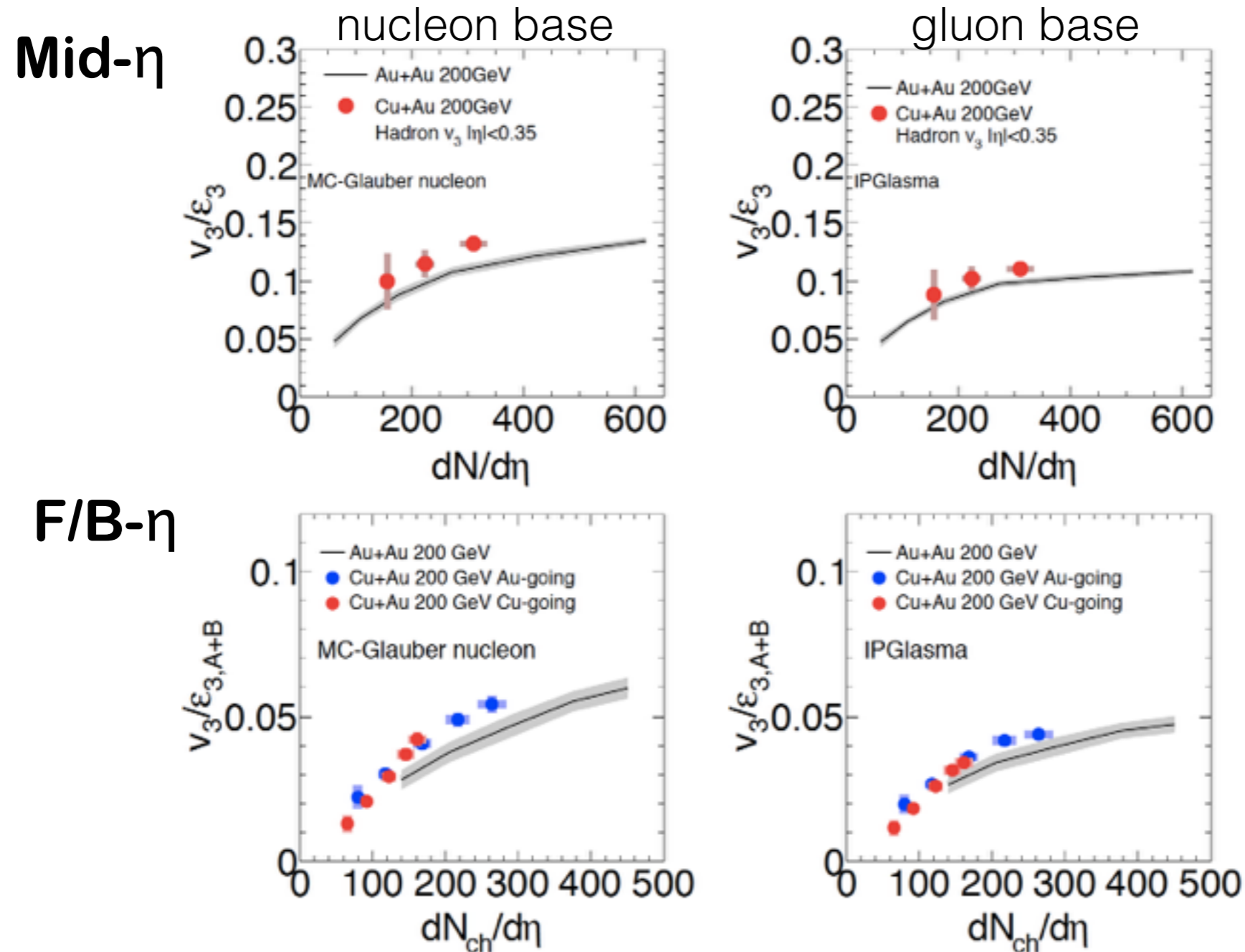
- v_1, v_2, v_3 at mid- η
- v_2, v_3 at large- η
- **Initial condition study**
- v_1, v_2, v_3 theory comparison

v_2/ε_2 scaling with Glauber and IPGlasma



- ✓ At-mid η , the v_2 scaled with nucleon base model are consistent among three collision systems
- ✓ At-F/B η , the v_2/ε_2 with gluon base model in Cu+Au is closer to that in Au+Au

v_3/ϵ_3 scaling with Glauber and IPGlasma



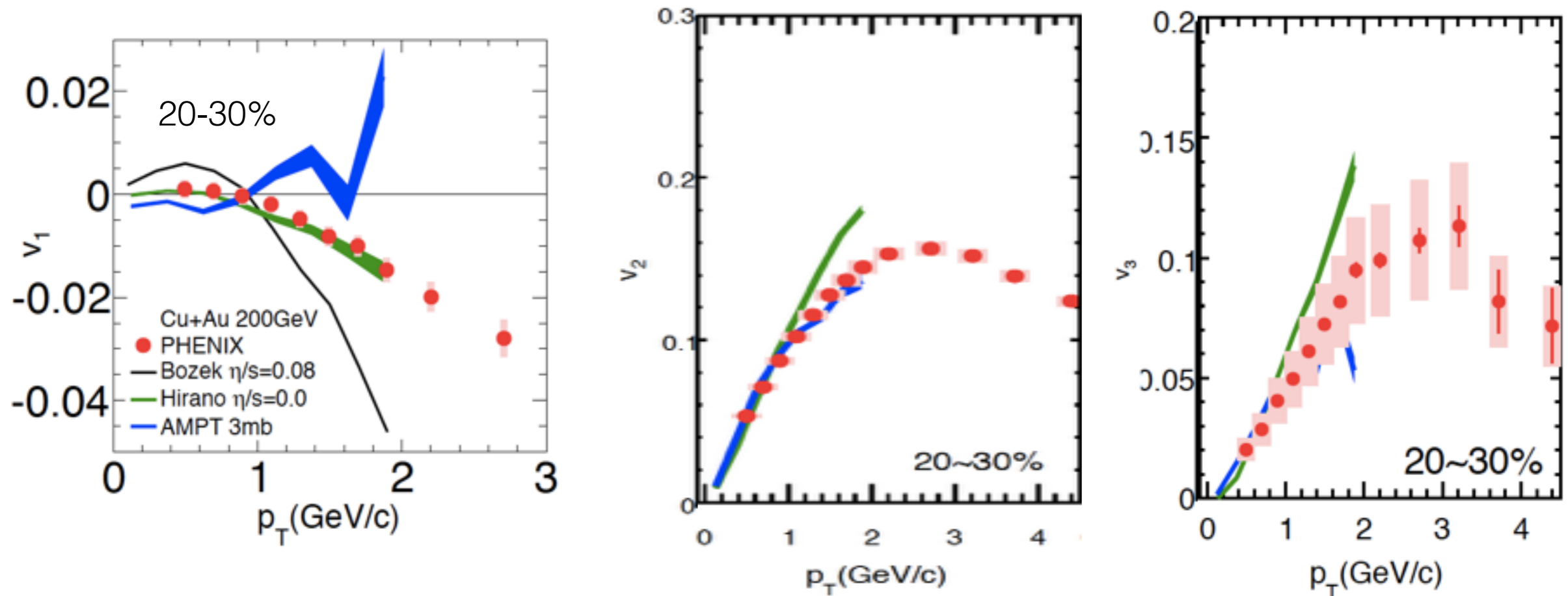
- ✓ At-mid η , the v_3 scaled with gluon base model in Cu+Au is closer to that in Au+Au
- ✓ At-F/B η , the v_3/ϵ_3 with gluon base model in Cu+Au is closer to that in Au+Au

Results

Discussions

- v_1, v_2, v_3 at mid- η
- v_2, v_3 at F/B- η
- Initial condition study
- **v_1, v_2, v_3 theory comparison**

Parton cascade and hydro $v_n(p_T)$

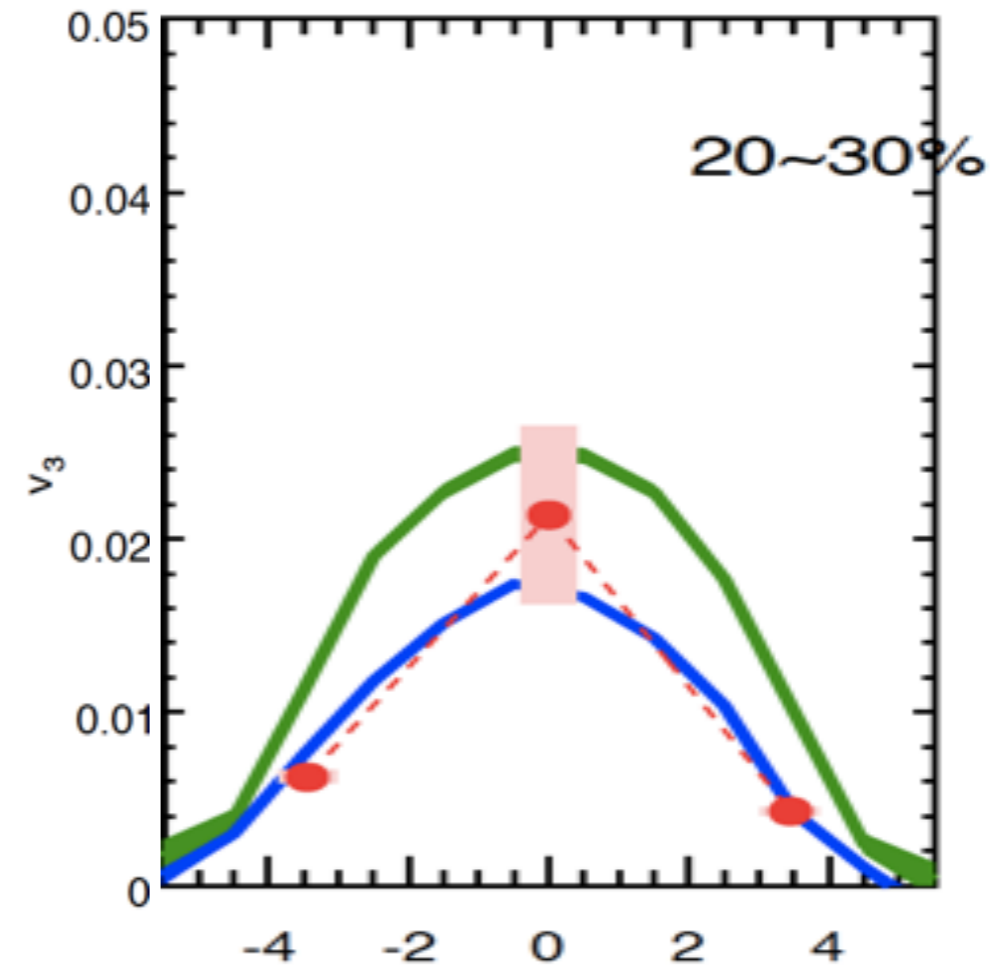
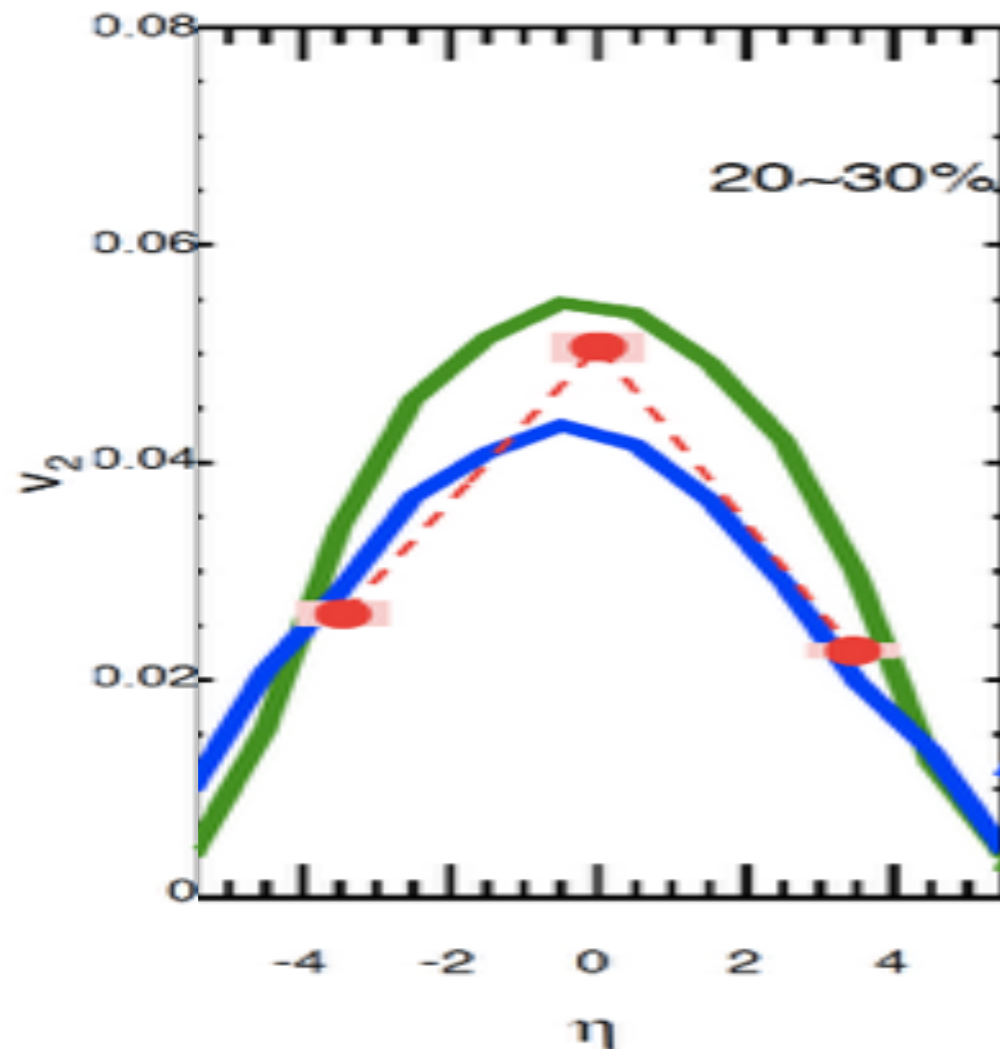


- Hydro(Bozek):Glauber + hydro
- Hydro(Hirano):Glauber + hydro + hadron cascade
- AMPT :Glauber + parton cascade + hadron cascade

✓ Hydrodynamic reproduce v_n

✓ AMPT model well reproduce v_2 and v_3 , but shows opposite sign of v_1

Parton cascade and hydro $v_n(\eta)$



- ✓ AMPT and Hydro predict the magnitude of v_2 at F/B rapidity well
- ✓ AMPT reproduce the magnitude of v_3 at F/B rapidity well
- ✓ Hydro overestimate the magnitude of v_3 at F/B rapidity
 - Hydro: Smooth longitudinal density+hydro
 - AMPT: Fluctuated longitudinal density+parton cascade

Summary

✓ v_1 at mid- η

High p_T particles are emitted to Au side

✓ v_2, v_3 at mid- η

- Similar centrality and p_T dependence as seen in symmetric collisions
- Cu+Au v_3 is larger than Au+Au results, which might arise from intrinsic triangularity of overlap zone

✓ v_2, v_3 at F/B- η

- Forward/Backward asymmetry of v_n in Cu+Au arise from Forward/Backward asymmetry of density ($dN/d\eta$)

✓ Initial model study

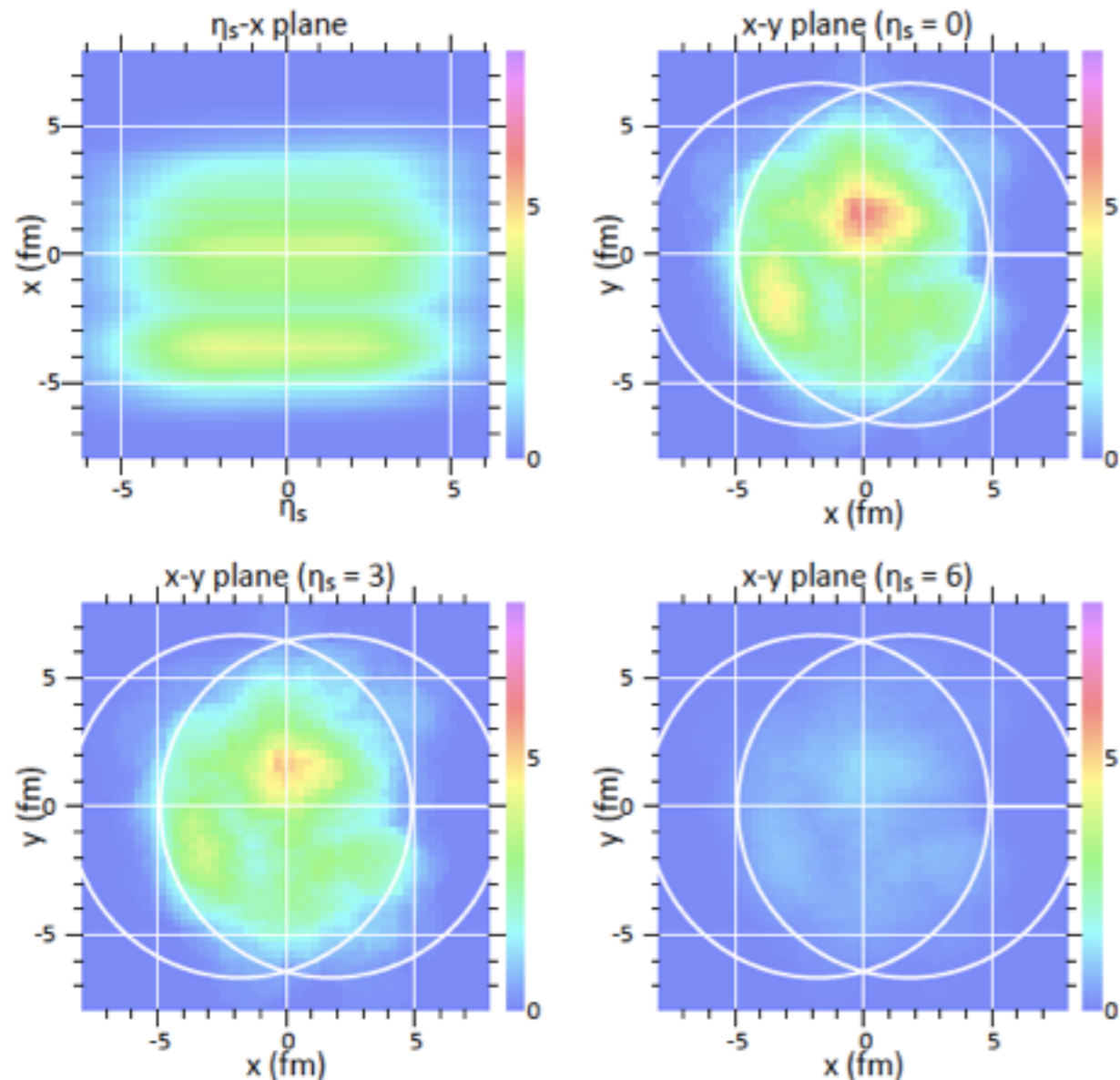
- Glauber model describes mid-rapidity v_2 well
- IPGlasma model describes mid-rapidity v_3 and preferred at F/B η , which might indicate different initial conditions between central and F/B η

✓ Theory comparison

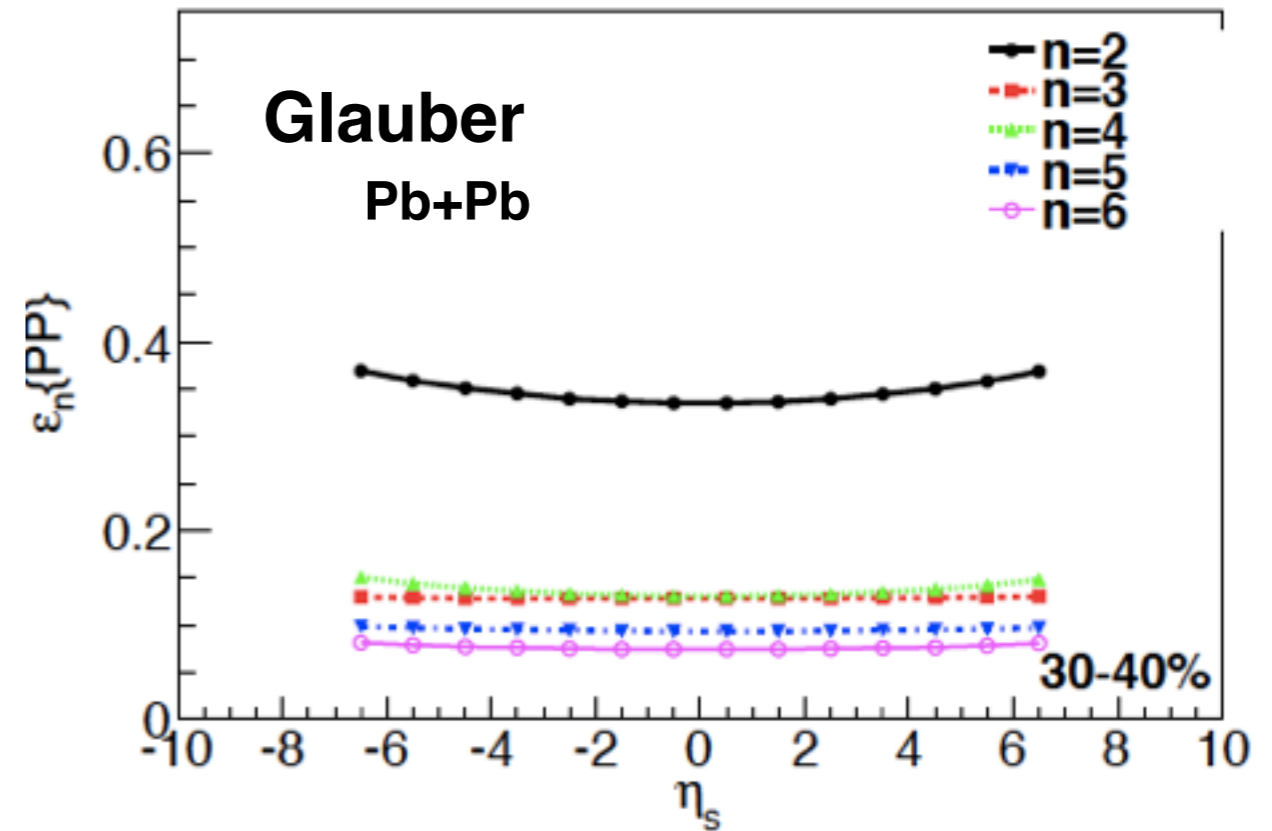
- Parton cascade (AMPT) does not well describe sign of v_1

Back Up

η_s dependence of ε_n



arXiv:12004.5814v2

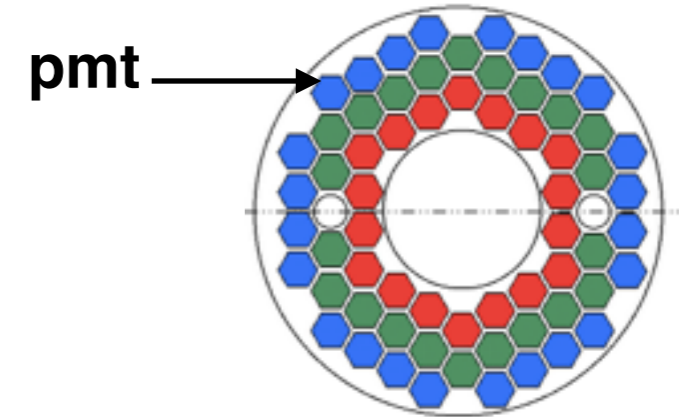


- ✓ Longitudinal structure is less understood
 - Transverse direction can be described by Glauber, CGC...
- ✓ Initial spatial geometry $\varepsilon_n(\eta)$ are η symmetric
 - Smooth longitudinal density profile, streak-like structure

v_n measurement at Bbc ($3 < |\eta| < 4$)

✓ v_n is measured using 64 Bbc pmts

- Bbc can't reconstruct tracks
- pmt based v_n include back ground



✓ Full Giant simulation with PHENIX configuration

- pmt based $v_n \rightarrow$ track based v_n

$$v_n^{track} = R_n * v_n^{pmt} \quad R_n = \frac{v_{n,input}^{Sim}}{v_{n,output}^{Sim}}$$

$v_{n,input}^{Sim}$

Input v_n from particle simulation

$v_{n,output}^{Sim}$

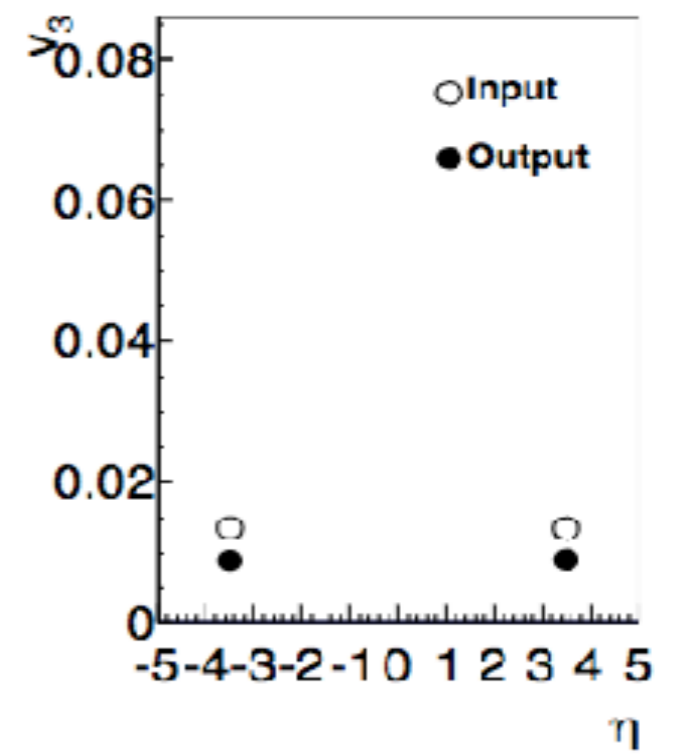
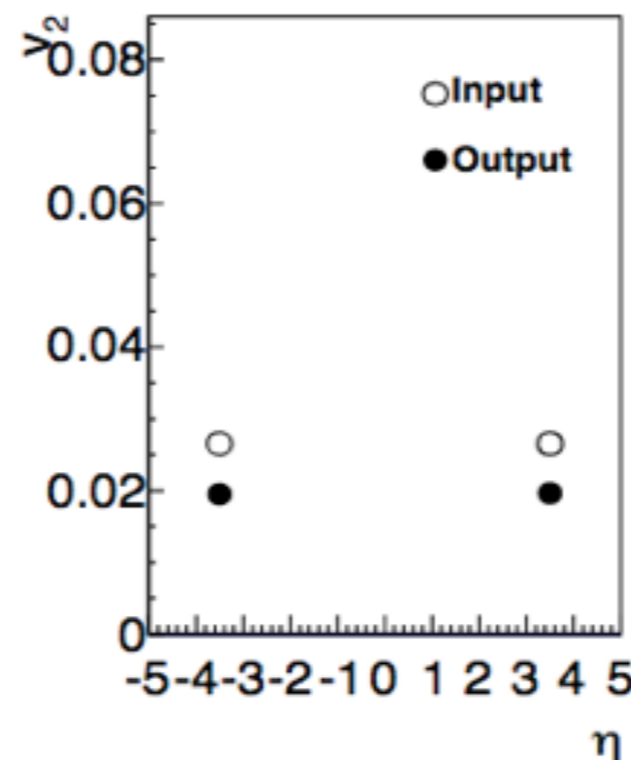
Output v_n from Giant simulation

✓ Correction factor R_n

- R_2 : 0.73
- R_3 : 0.65

✓ Systematic study

- $dN/d\eta$
- pT spectra
- $v_n(pT)$
- $v_n(\eta)$



Initial spatial anisotropy

Glauber Monte Carlo simulation

-Wood Saxon density profile

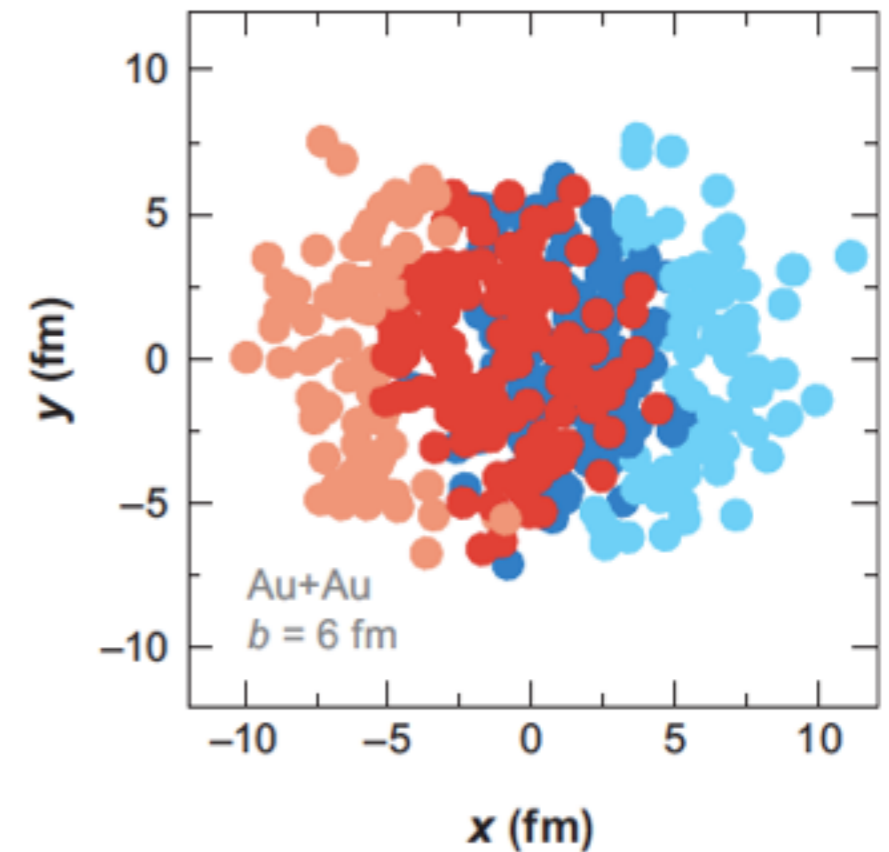
- collision is occurred, if $d < \sqrt{(\sigma_{nn}/\pi)}$

d : distance between nucleons

σ_{nn} : total cross section(pp collision)

$$\epsilon_n = \frac{\langle r^2 \cos[n(\phi - \Psi_{n,PP})] \rangle}{\langle r^2 \rangle}$$

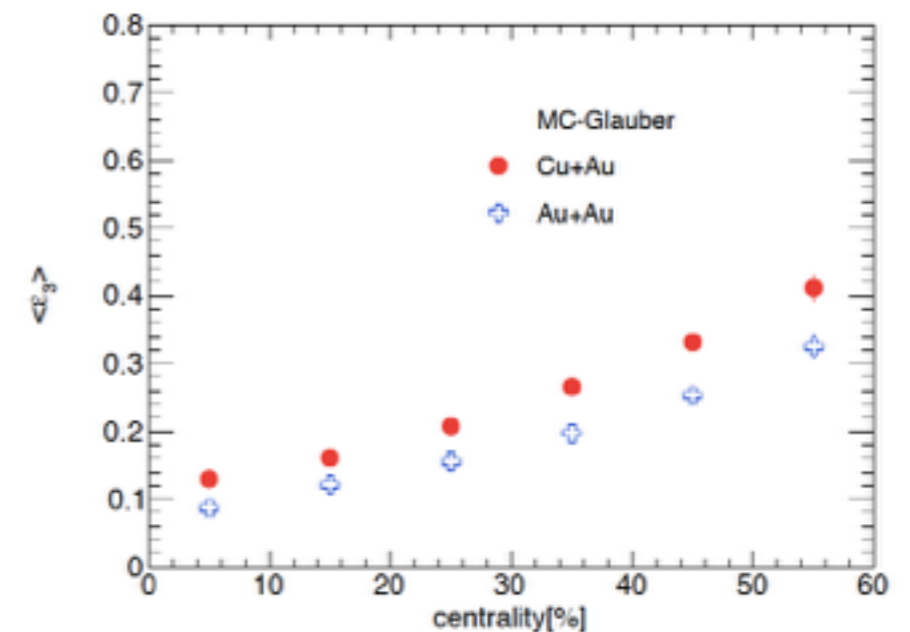
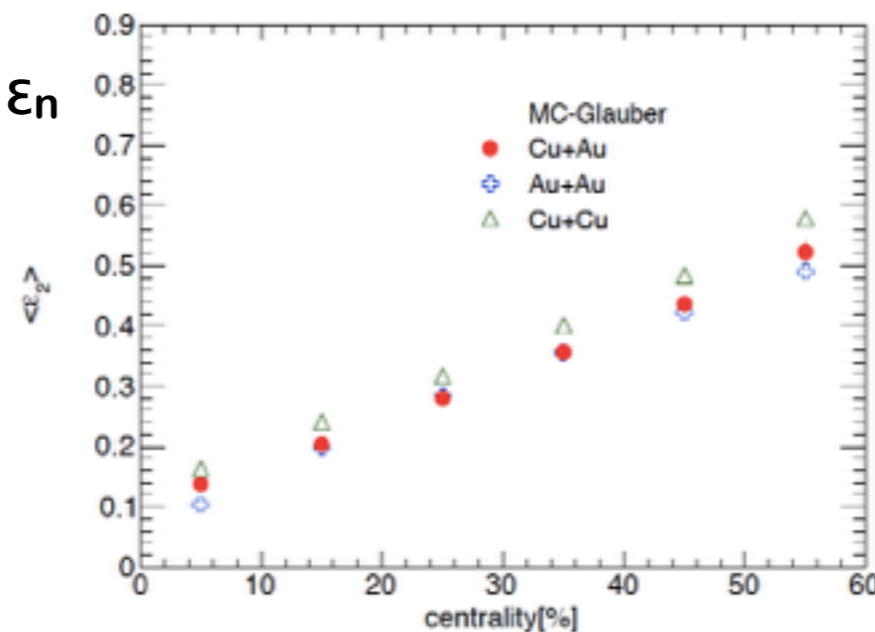
$$\Psi_{n,PP} = \frac{1}{n} \left[\tan^{-1} \frac{\langle r^2 \sin(n\phi) \rangle}{\langle r^2 \cos(n\phi) \rangle} + \pi \right]$$



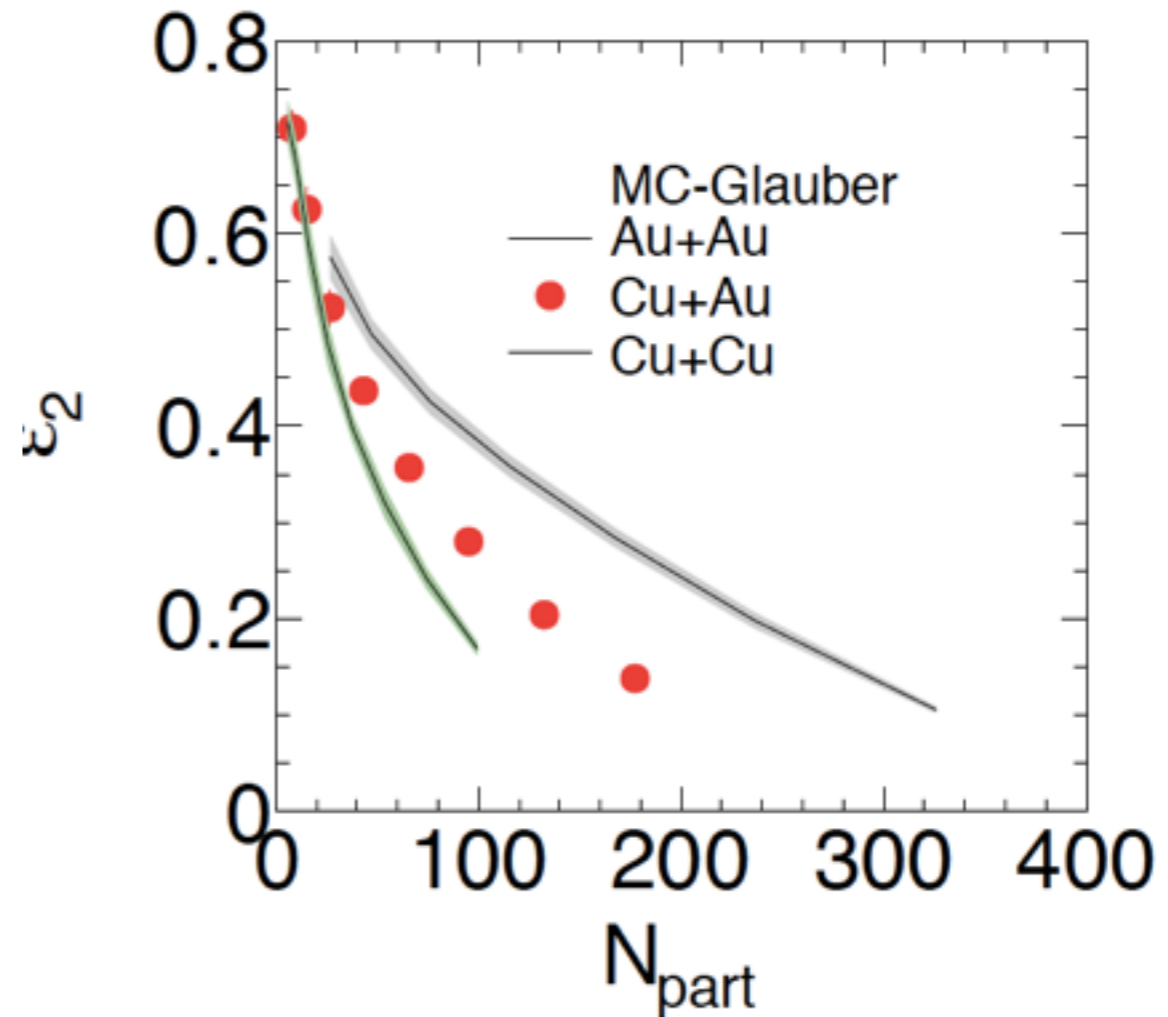
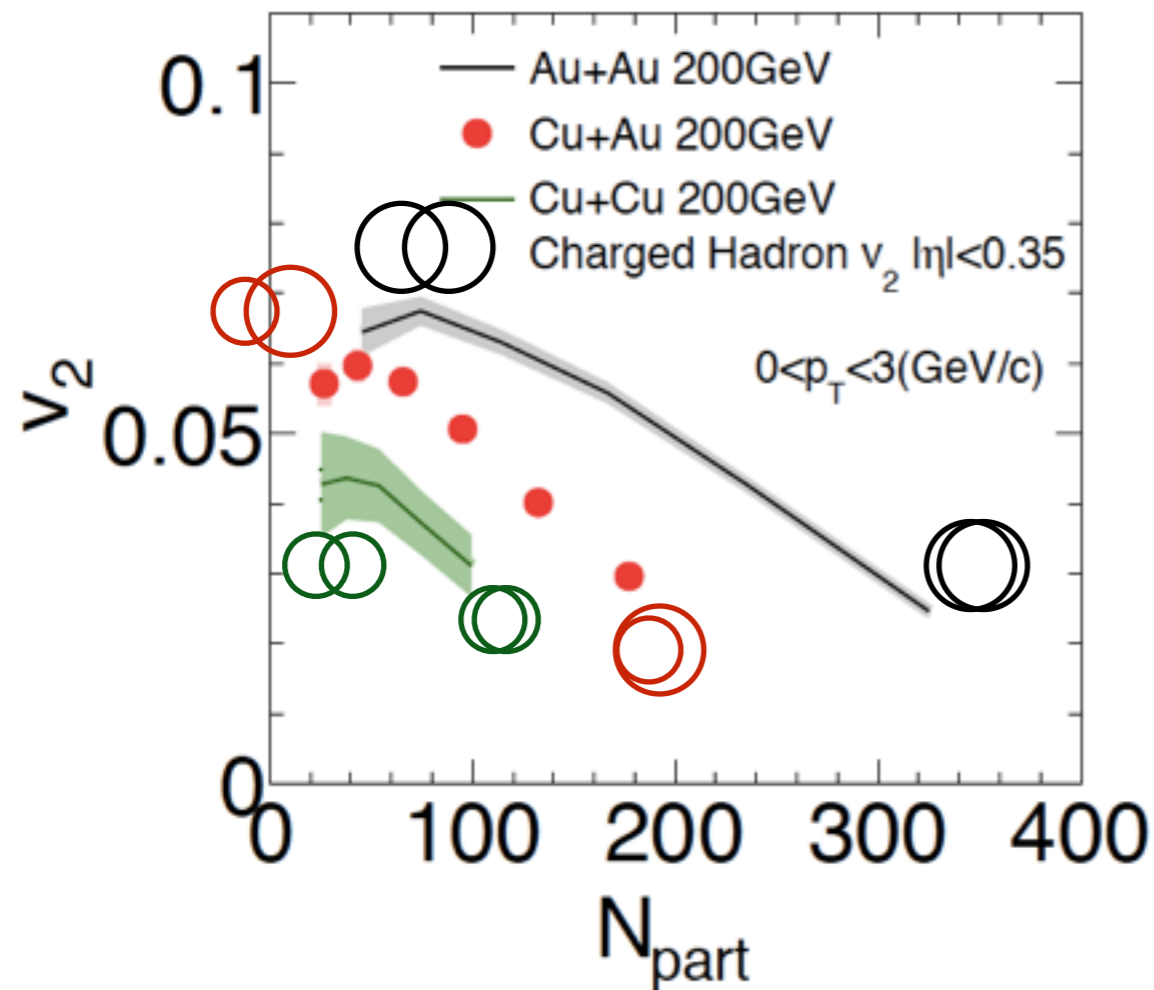
Centrality dependence of ϵ_n

ϵ_2 : CuCu > CuAu ~ AuAu

ϵ_3 : CuAu > AuAu

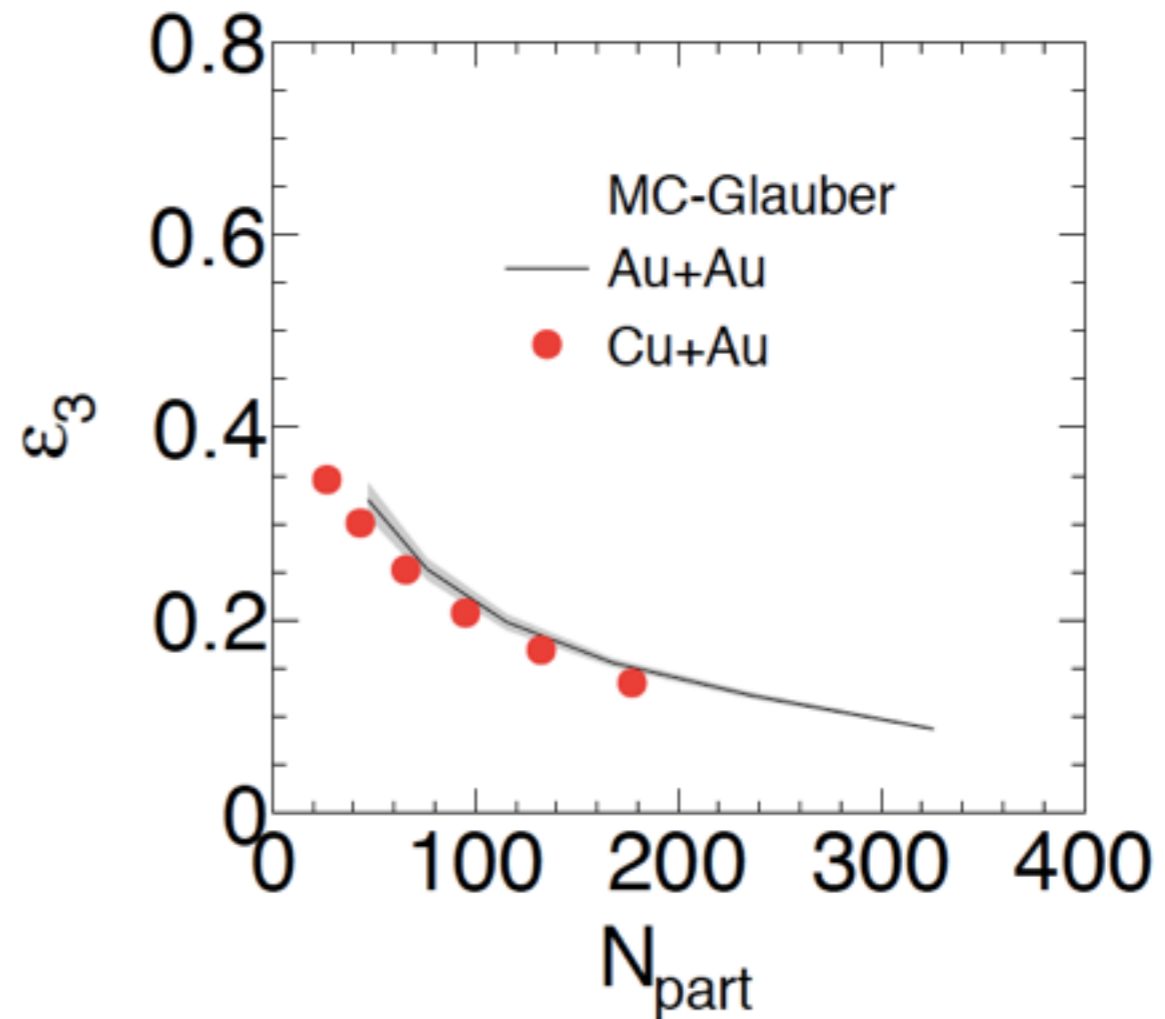
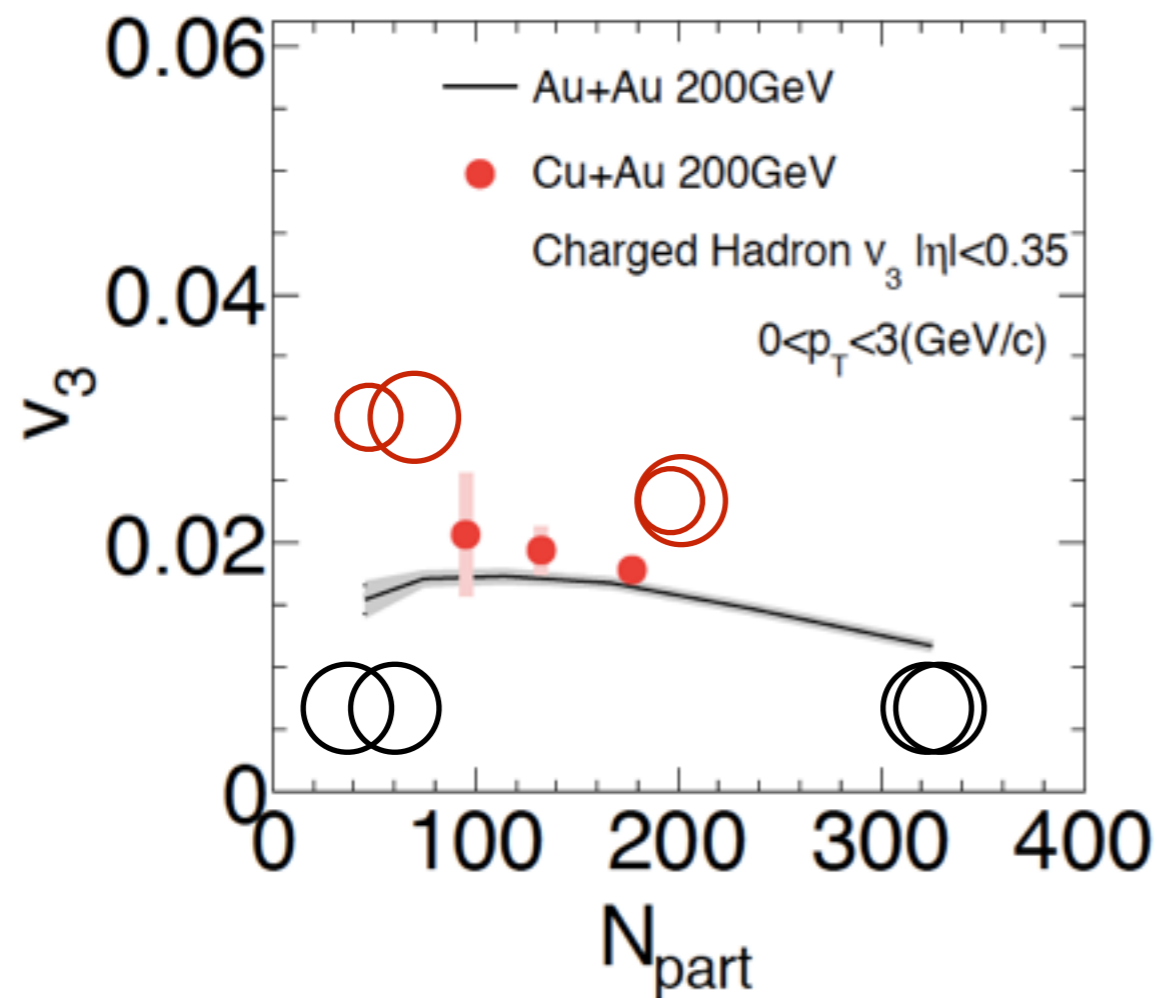


System size dependence of $v_2(N_{\text{part}})$ and $\varepsilon_2(N_{\text{part}})$



- ✓ $v_2(N_{\text{part}})$ and $\varepsilon_2(N_{\text{part}})$ are similar system size dependence
- N_{part} : Number of participants from MC-Glauber
- $v_2(\text{AuAu}) > v_2(\text{CuAu}) > v_2(\text{CuCu}) \sim \varepsilon_2(\text{AuAu}) > \varepsilon_2(\text{CuAu}) > \varepsilon_2(\text{CuCu})$

System size dependence of $v_3(N_{\text{part}})$ and $\varepsilon_3(N_{\text{part}})$



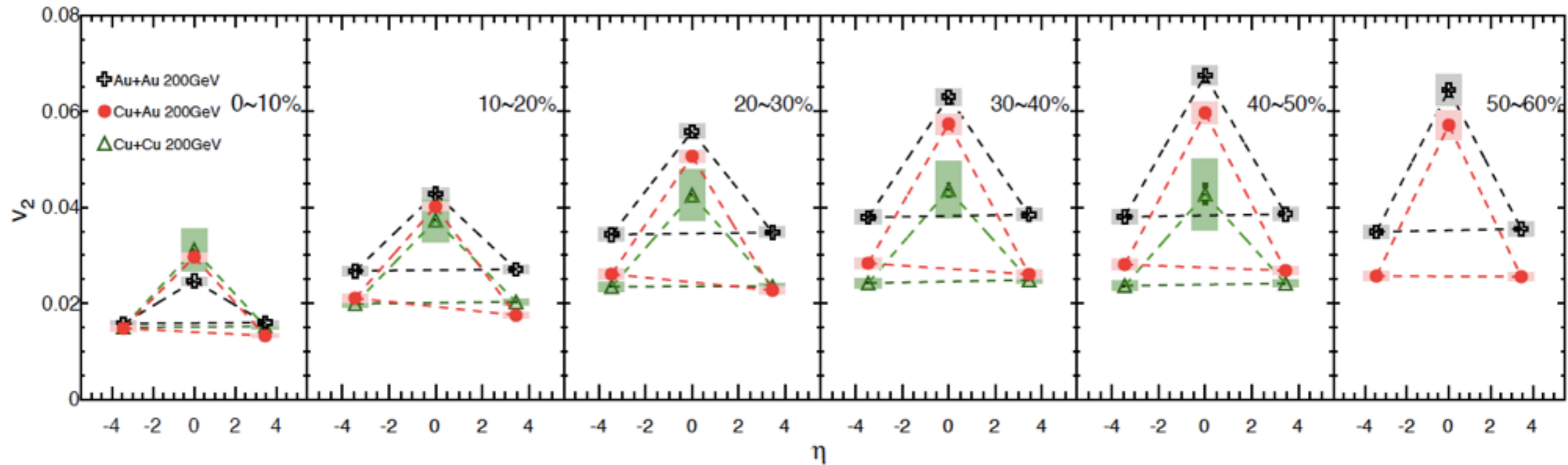
✓ Unlike $v_2(N_{\text{part}})$, no significant system size dependence of $v_3(N_{\text{part}})$ and $\varepsilon_3(N_{\text{part}})$

- The ordering of the magnitude of v_3 is reversed with that of ε_3

- v_3 in Cu+Au are almost same or slightly larger than those in Au+Au

-> intrinsic triangularity of asymmetric overlap zone?

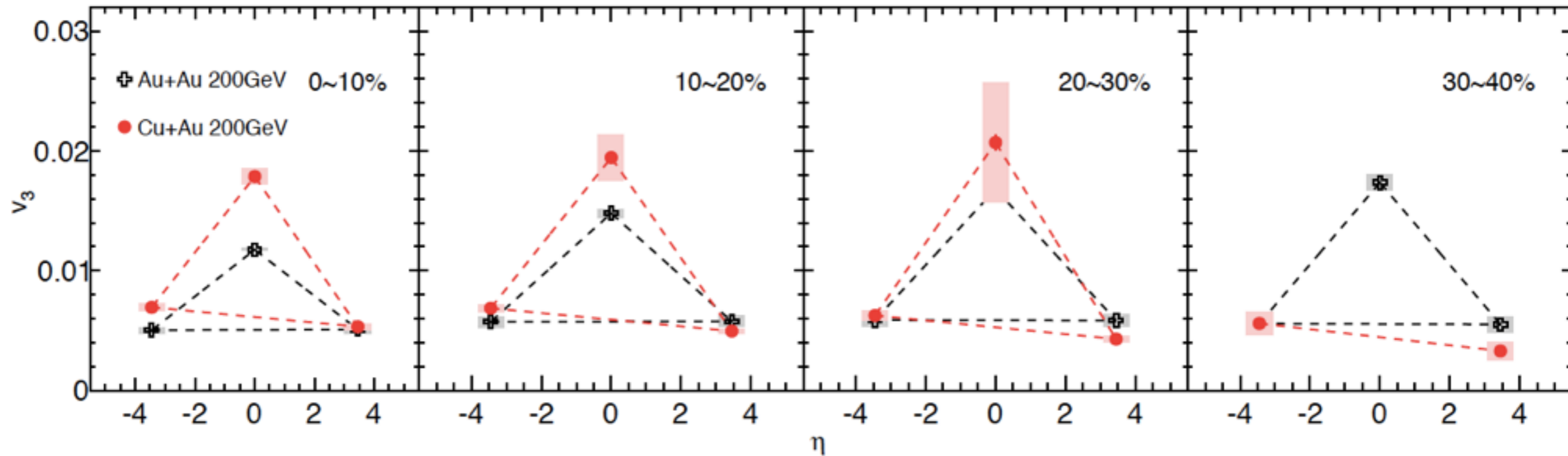
System size dependence of v_2 at F/B



✓ In Cu+Au collisions, F/B asymmetry of v_2 is observed.

- central & peripheral collisions: $v_2(\text{Au-going}) \sim v_2(\text{Cu-going})$
- mid-central collisions : $v_2(\text{Au-going}) > v_2(\text{Cu-going})$
- >caused by different initial geometries in Au and Cu ?

System size dependence of v_3 at F/B



✓ Weak centrality dependence of v_3 is seen for all collision systems

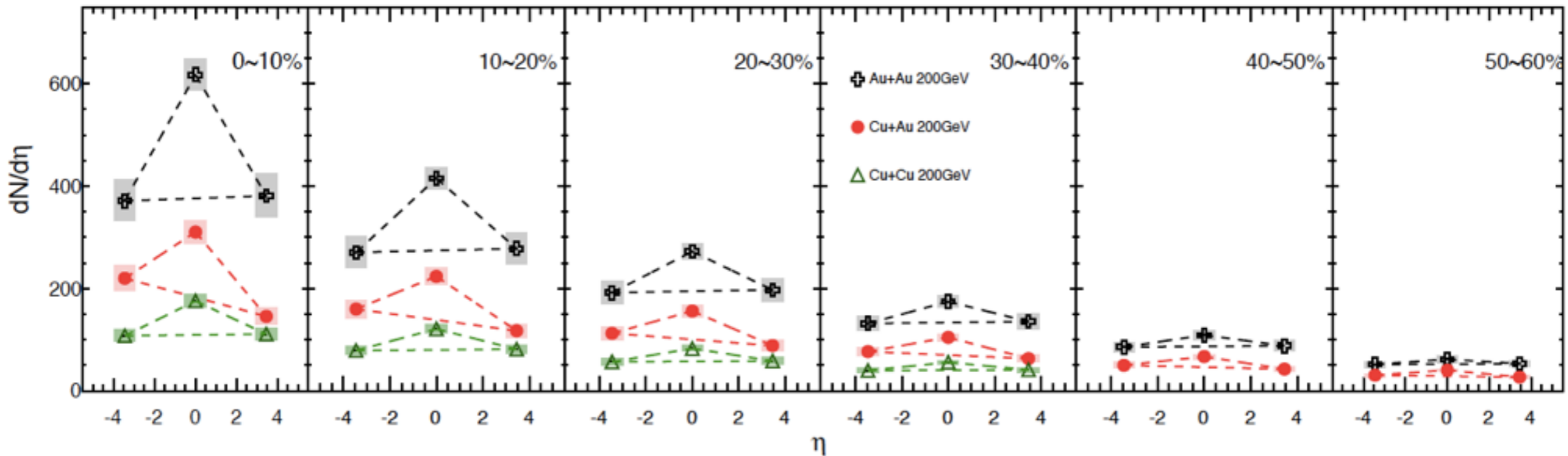
- AuAu: same centrality dependence as seen mid η

- CuAu: v_3 decrease as centrality decrease

✓ In CuAu collisions, $v_3(\text{Au-going}) > v_3(\text{Cu-going})$ for all centrality bins

-> Like v_2 , the different initial geometry cause the different v_3 ?

F/B asymmetry of $dN/d\eta$

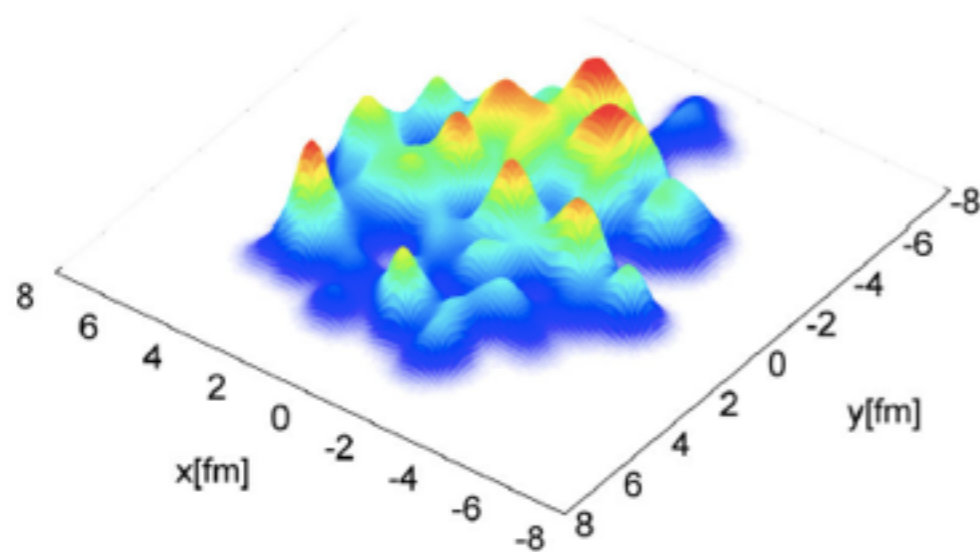


✓ Like the v_n , the $dN/d\eta$ in Au-going side is higher

✓ In 50-60%, the $dN/d\eta$ in Au-going side and Cu-going side are almost same due to similar N_{part} .

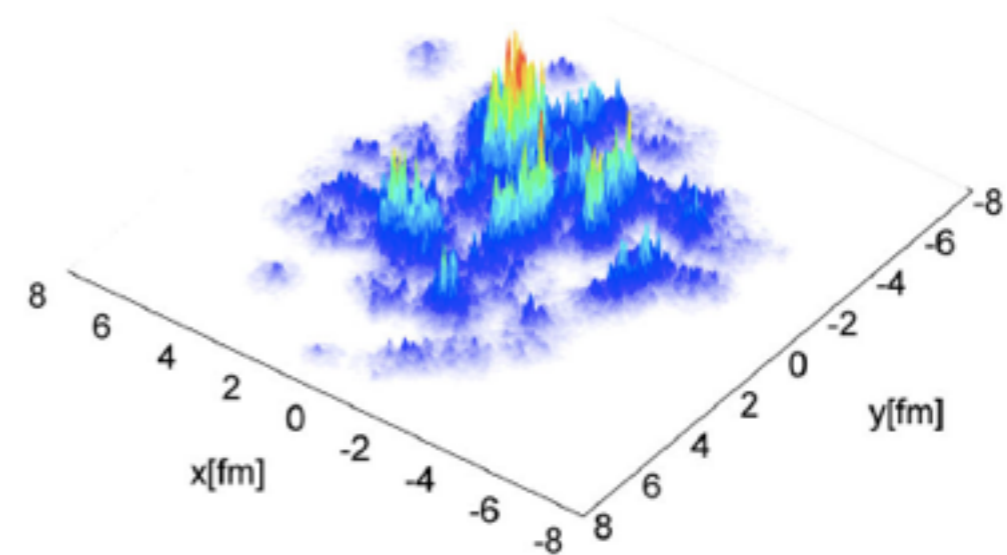
Initial geometry model

Glauber nucleon



Smooth structure

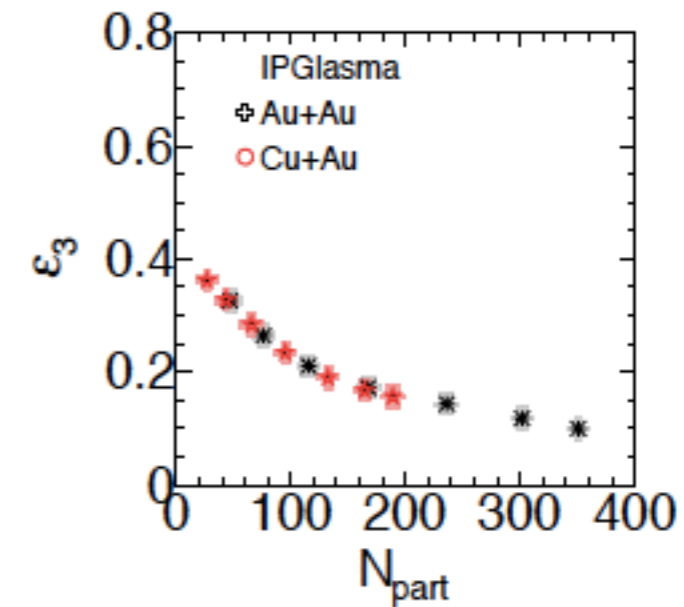
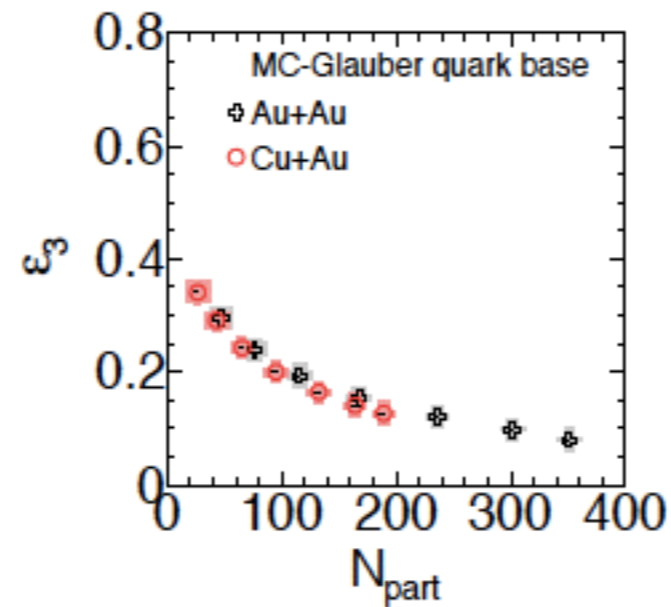
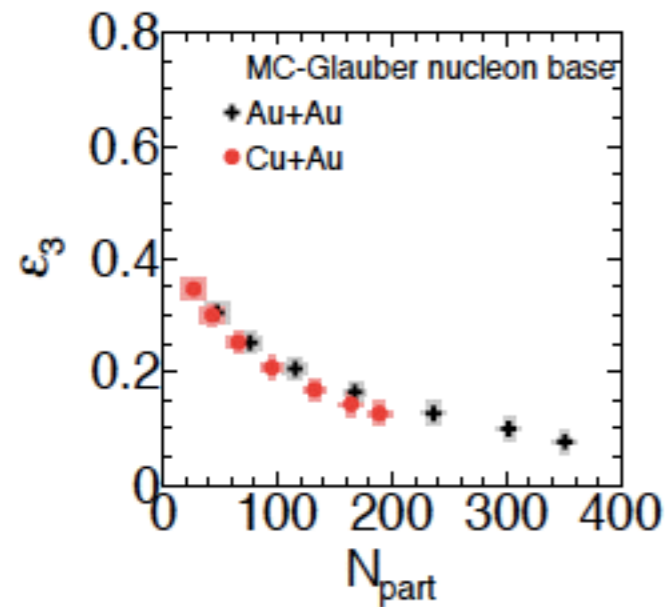
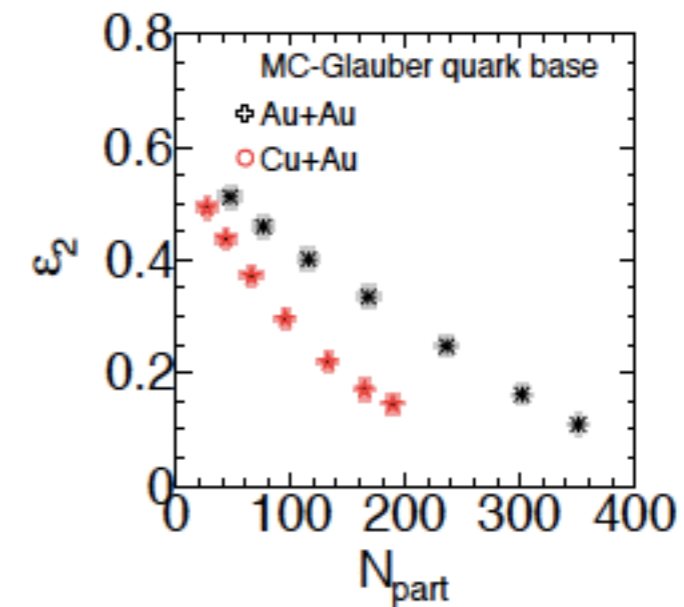
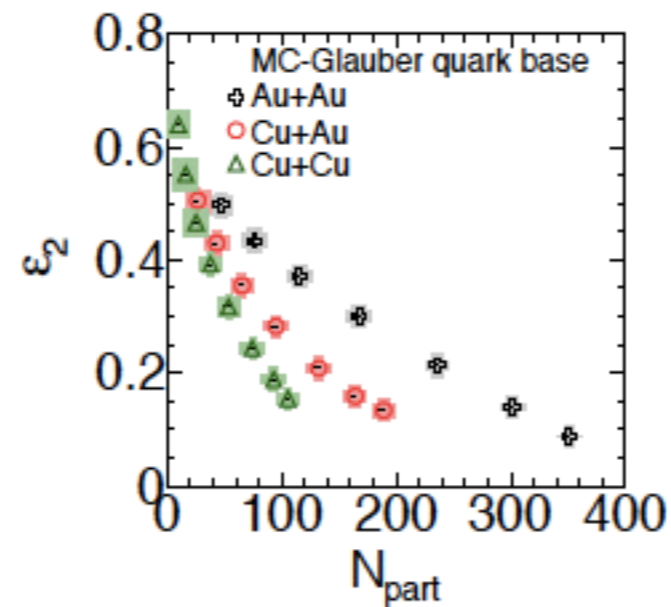
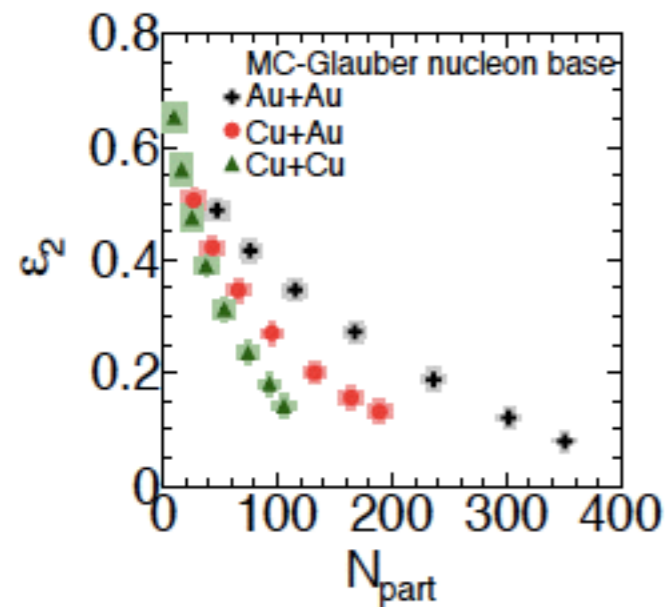
IPGlasma



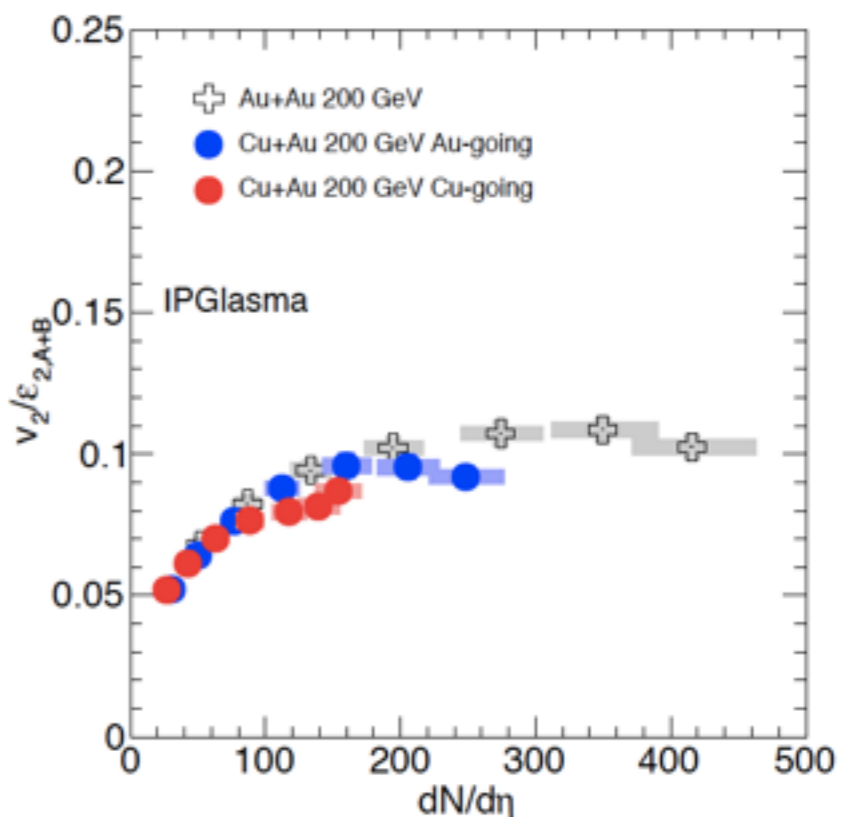
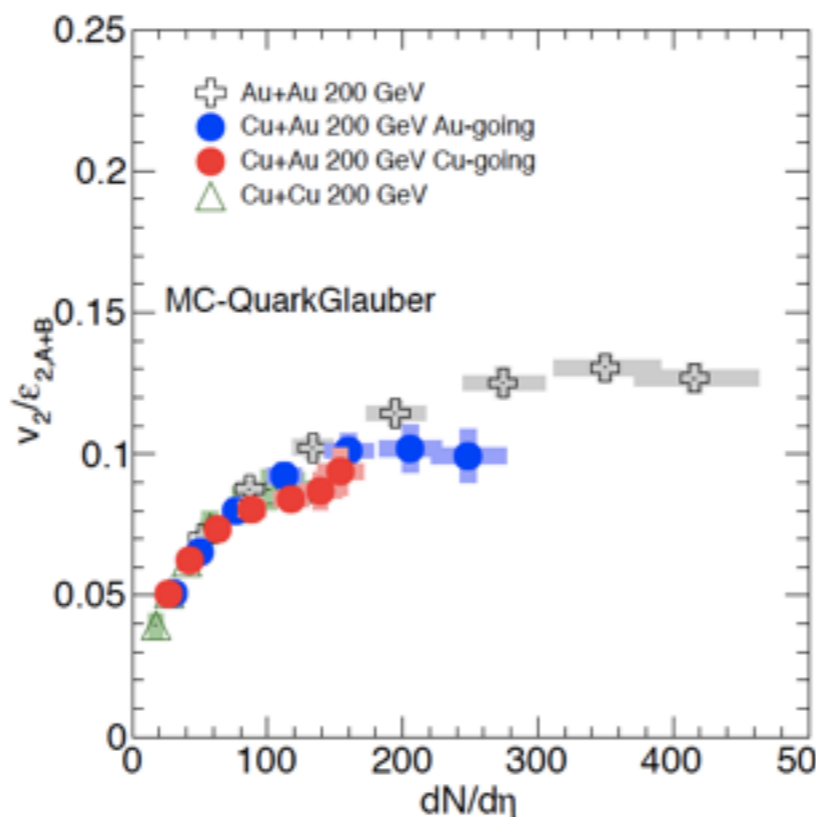
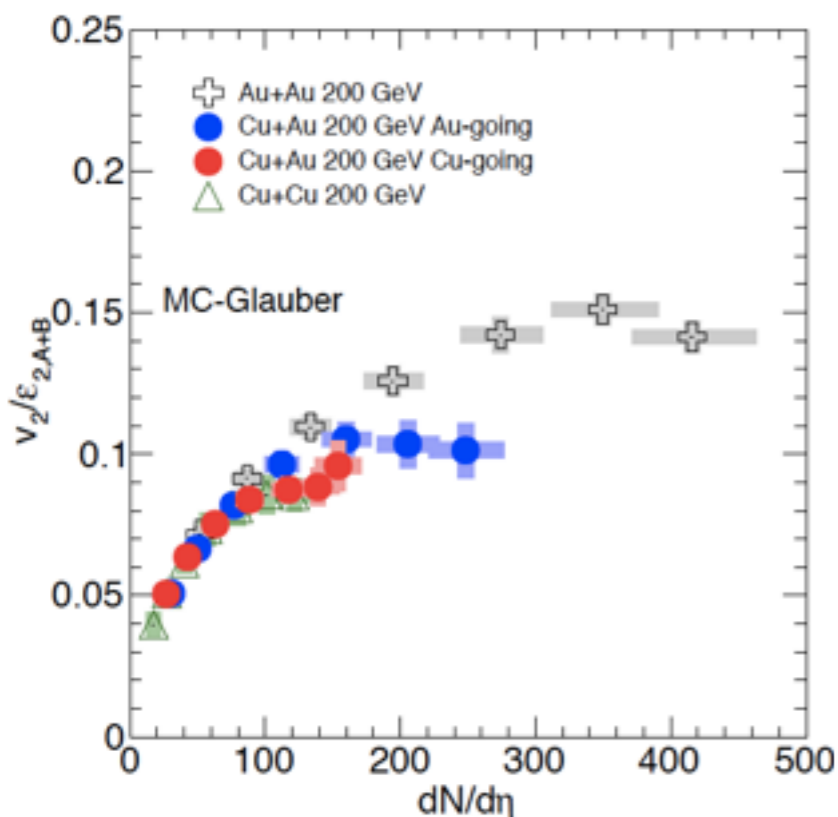
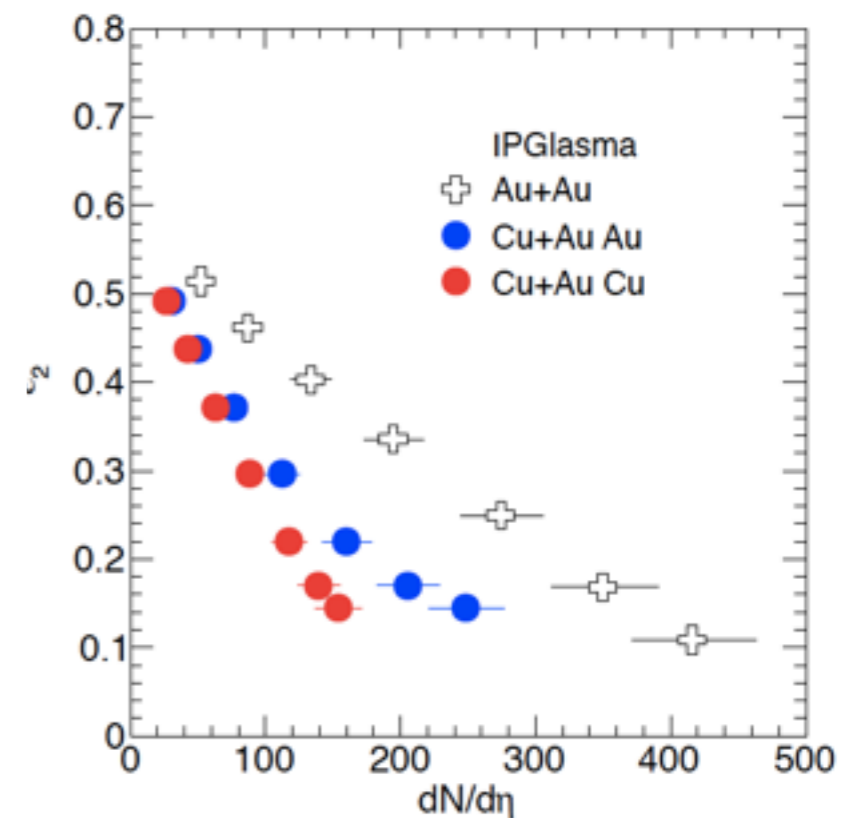
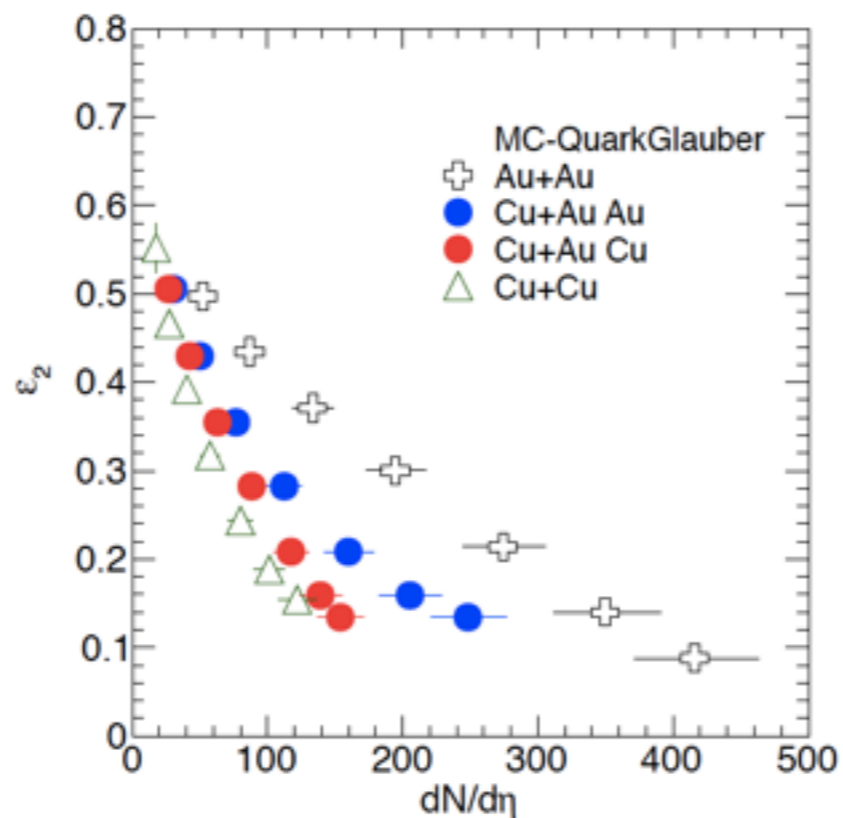
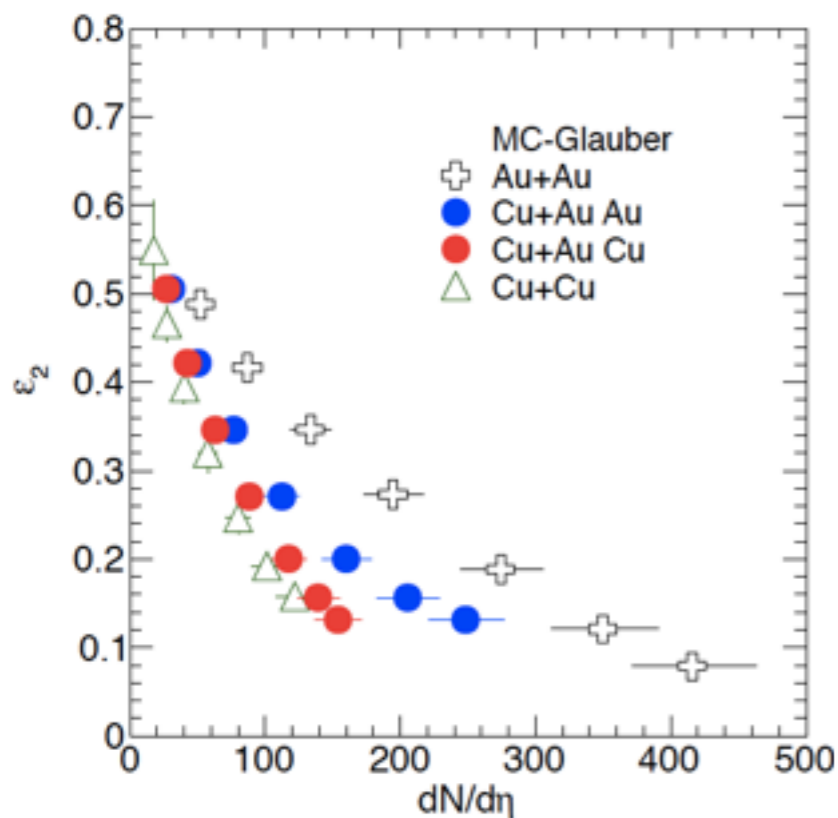
Fine structure

- ✓ Glauber Monte Carlo model:nucleon base
 - ✓ Glauber Monte Carlo model:Constituent quark base
PRC 93 024901
 - ✓ IPGlasma Model : gluon base(CGCG), PRC 89, 064908
- >fineness: gluon base>quark base > nucleon base

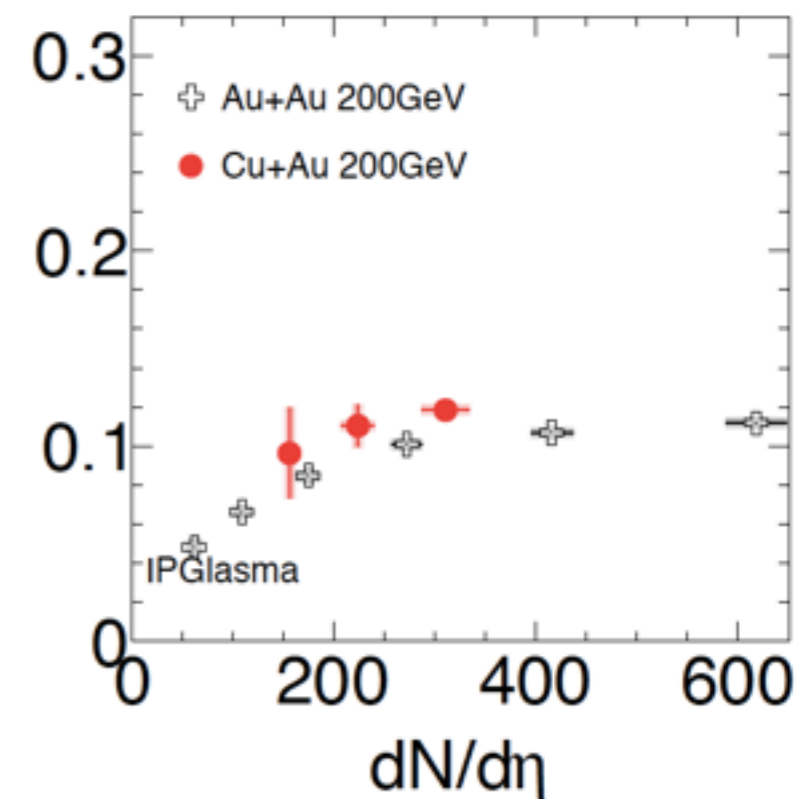
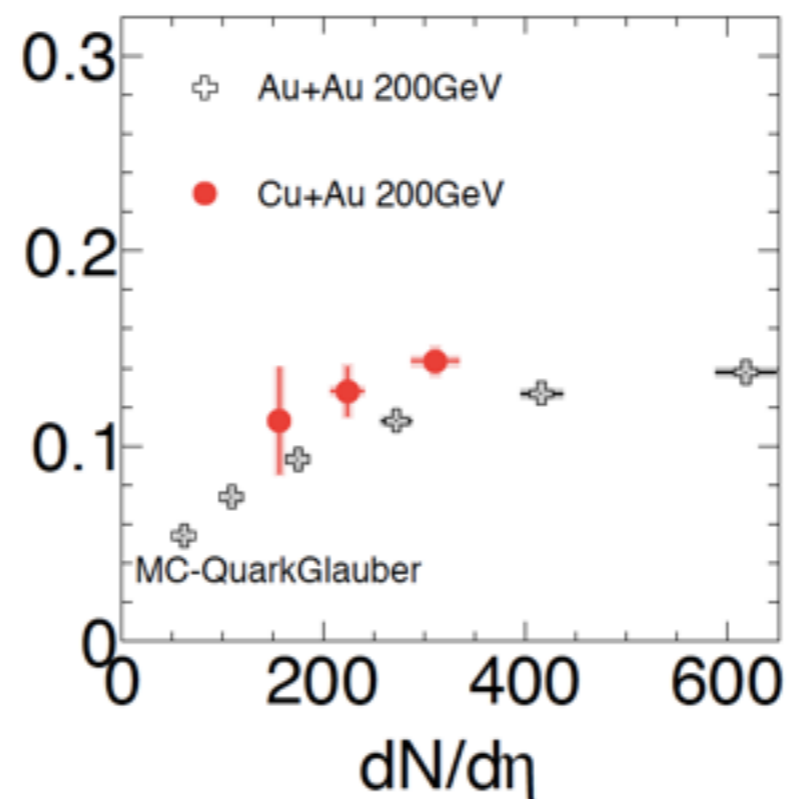
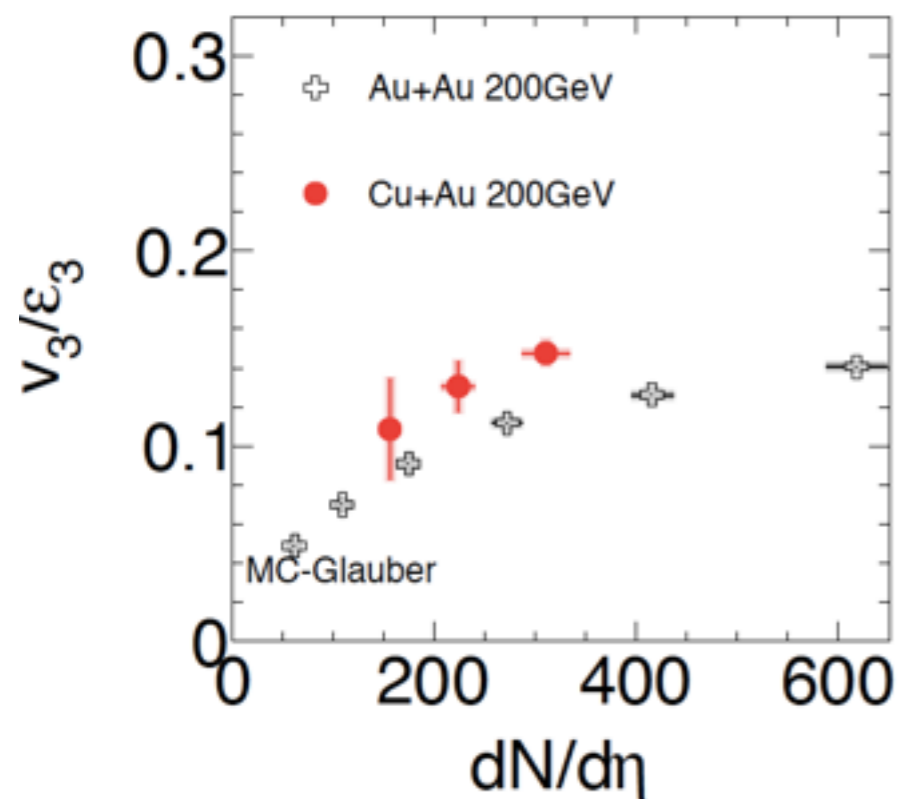
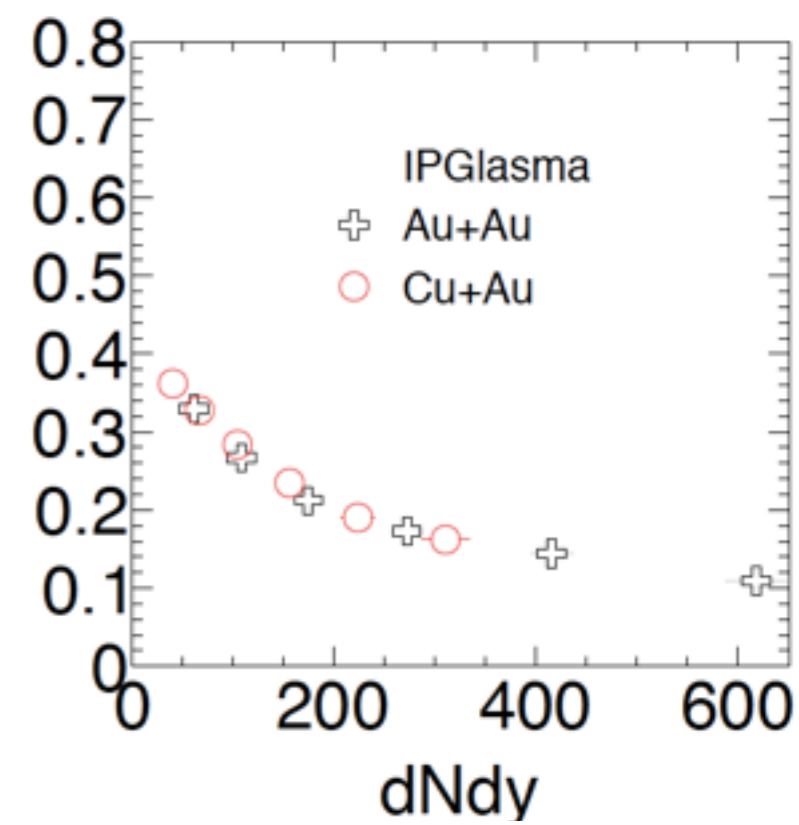
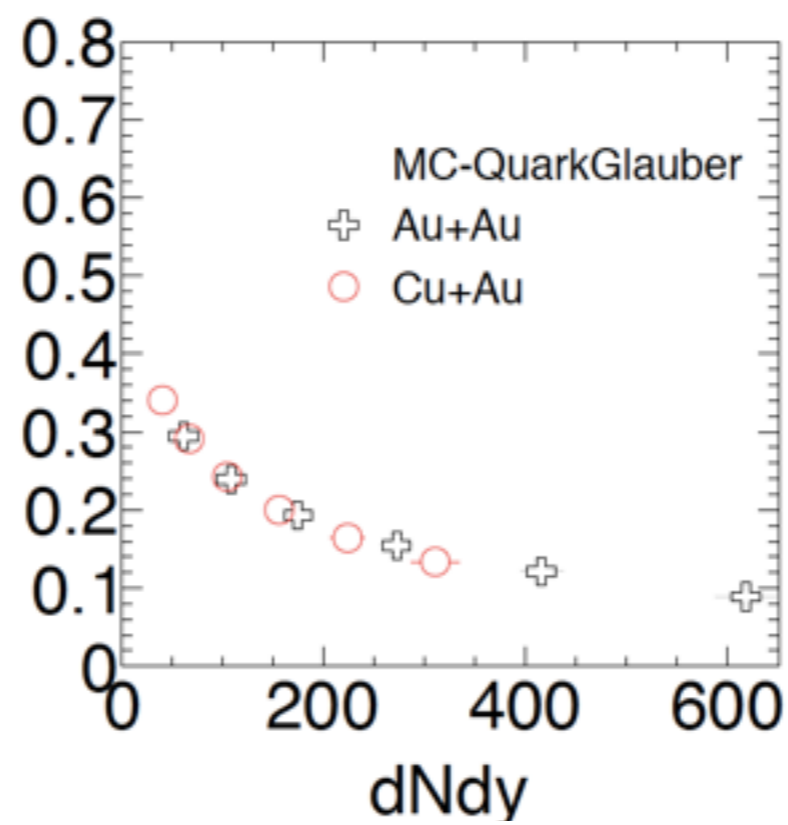
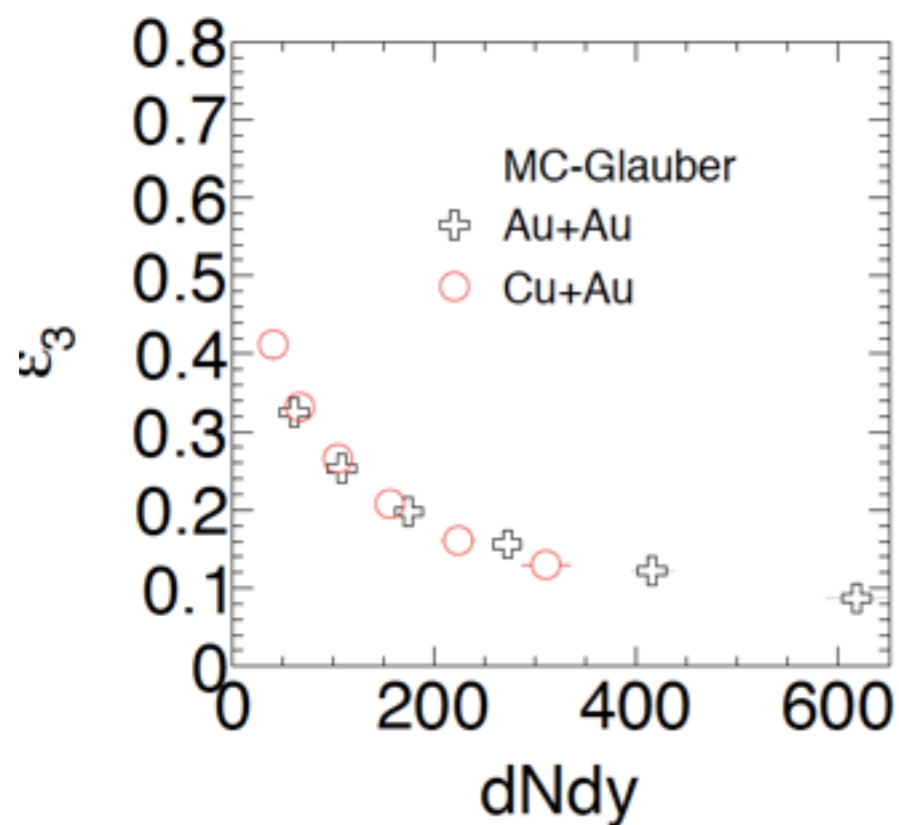
Model dependence of 2nd and 3rd Eccentricity



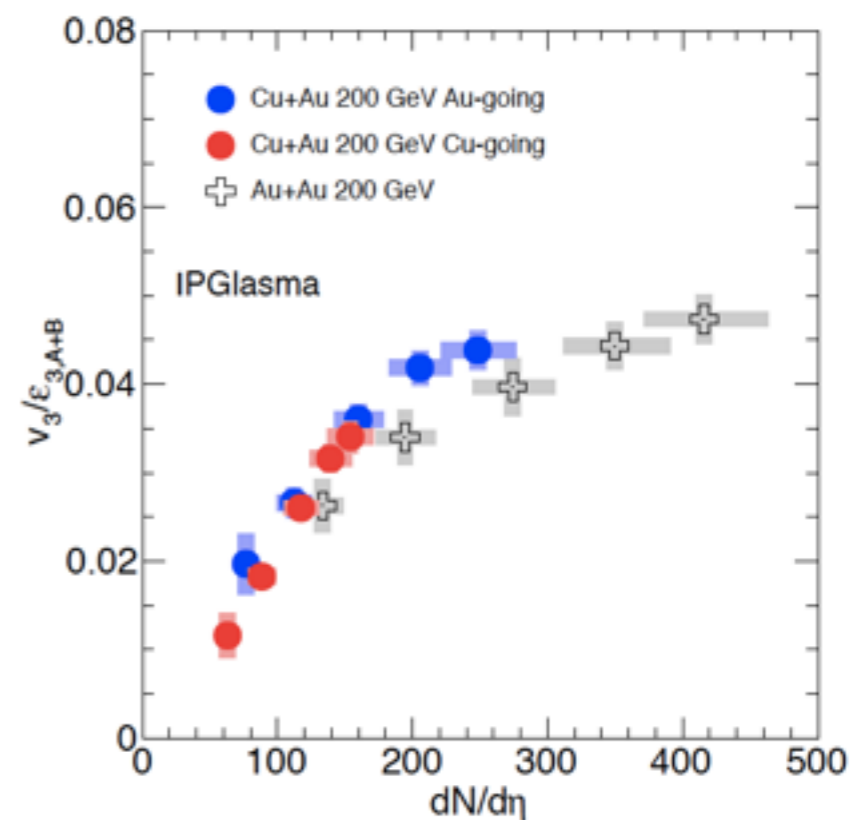
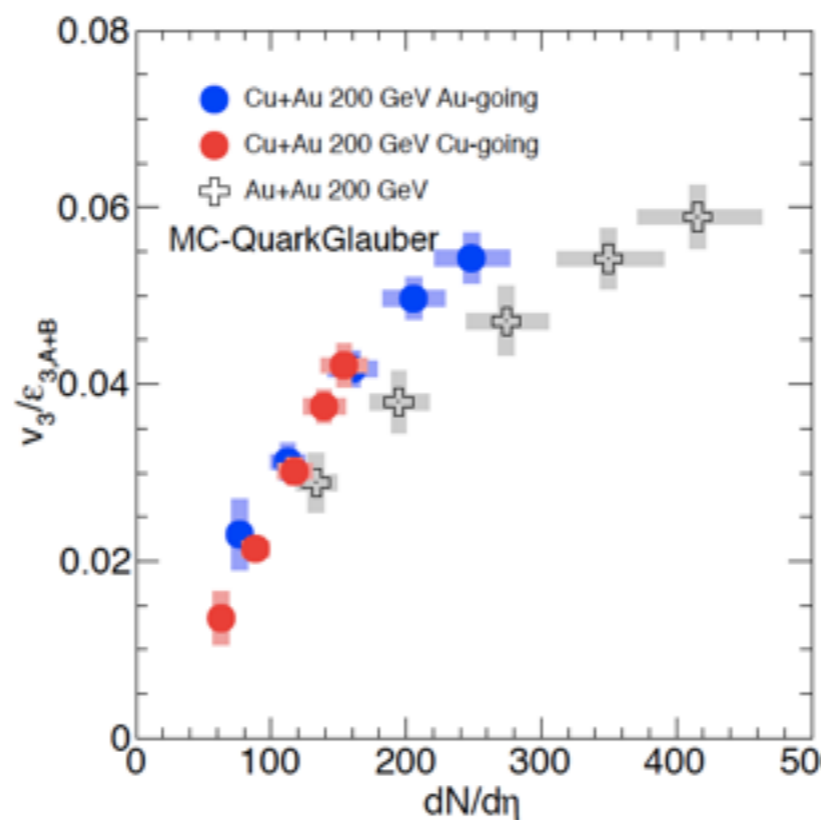
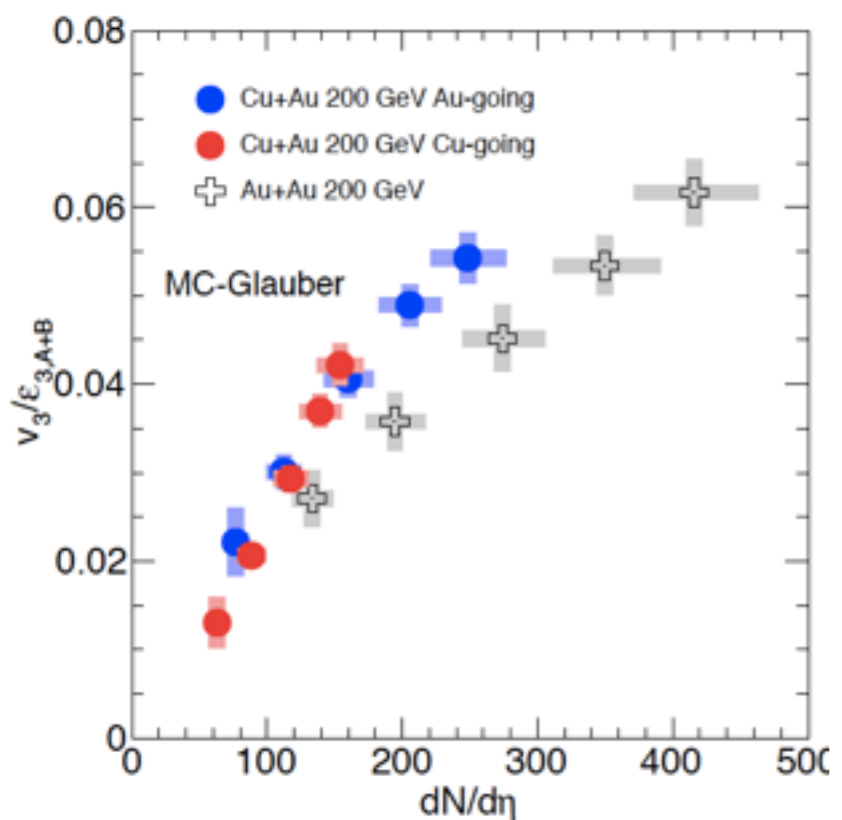
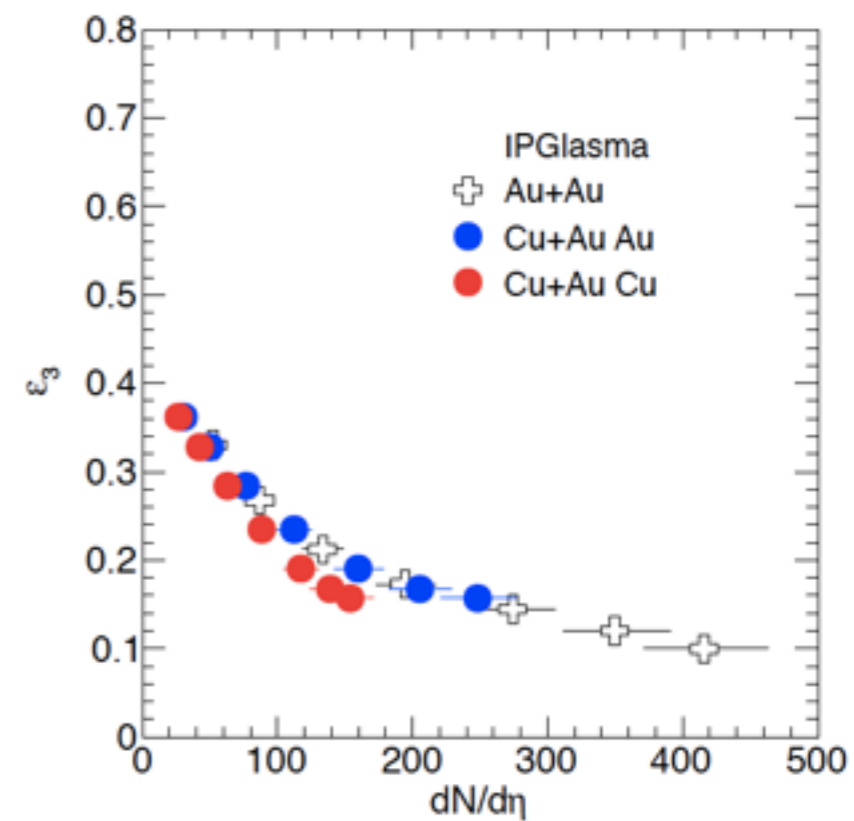
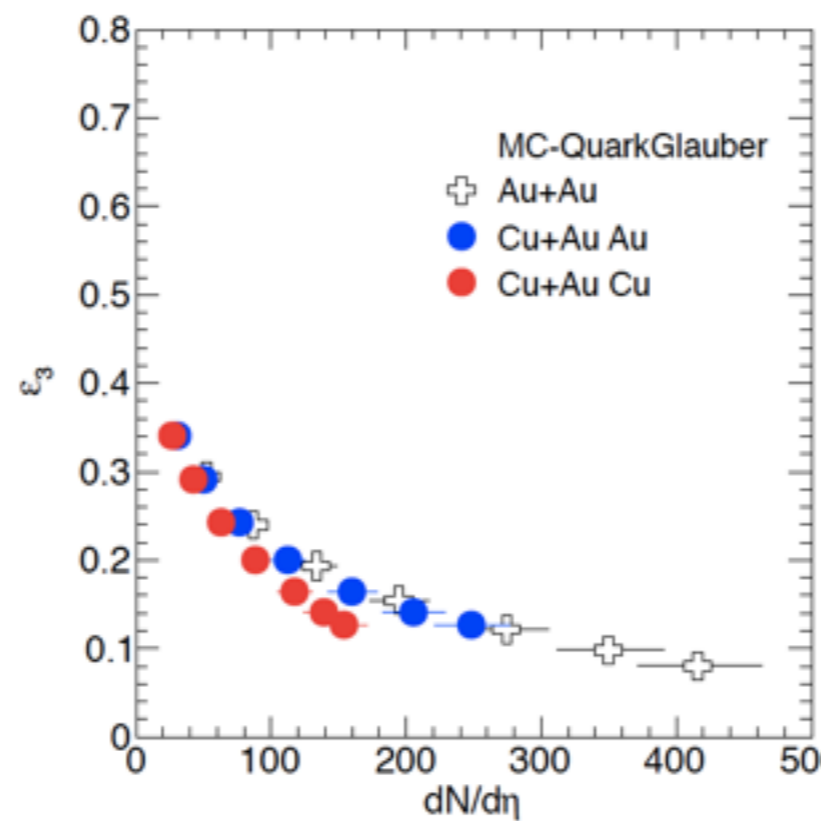
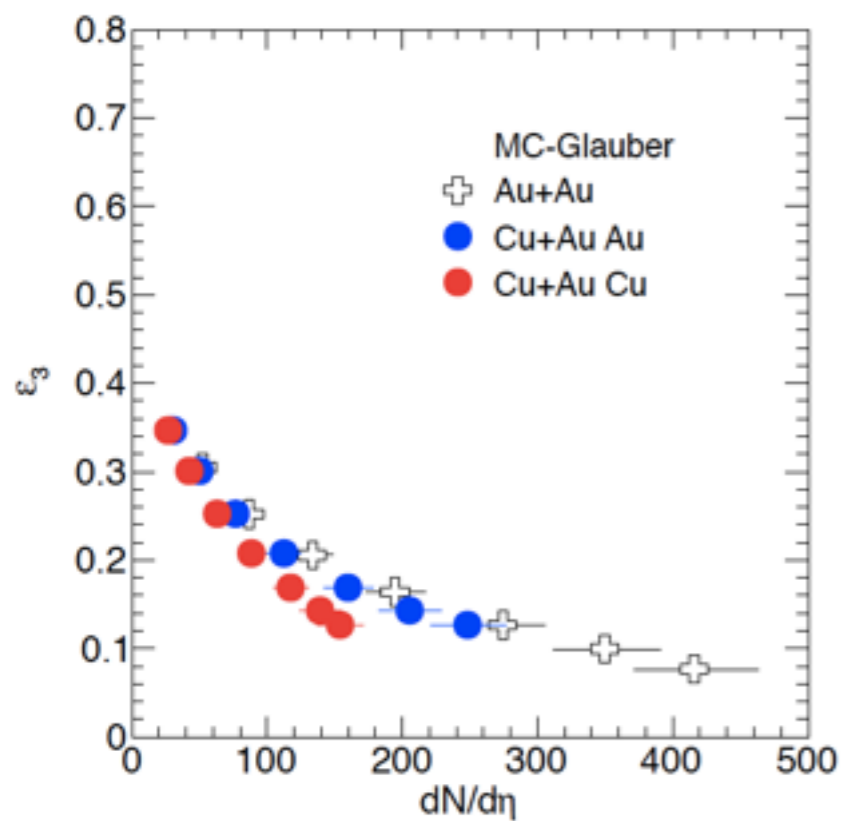
v_2/e_2 at f/b rapidity vs $dN/d\eta$



v_3/e_3 at mid rapidity vs dN/dy

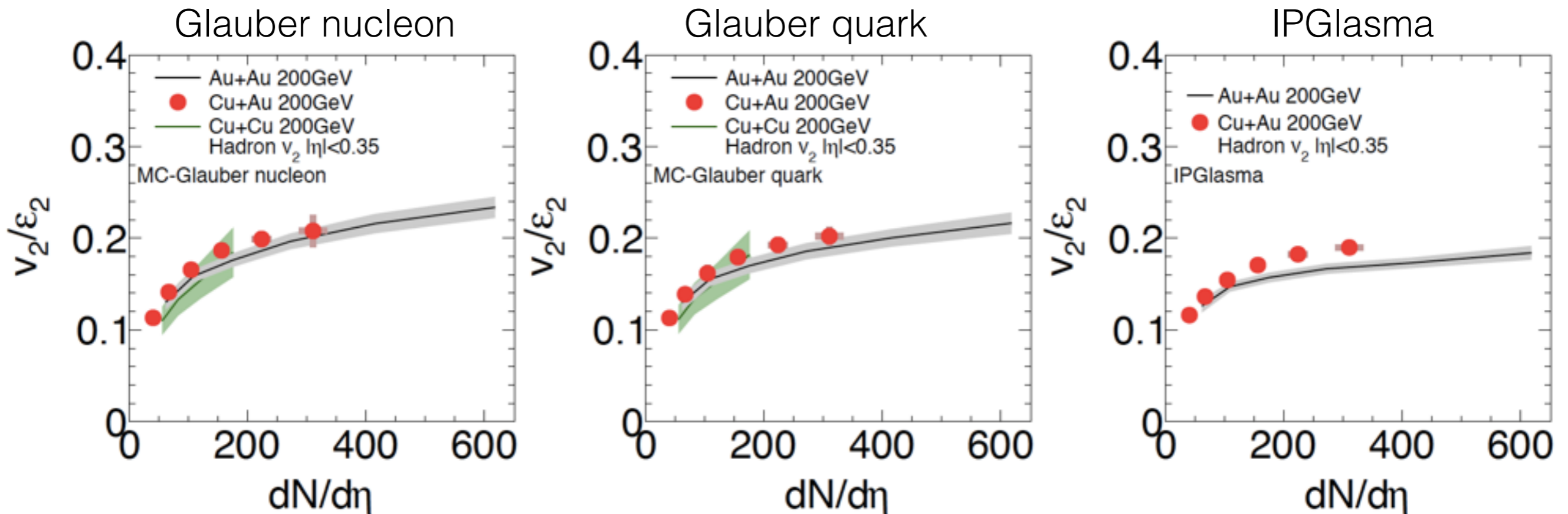


v_3/e_3 at f/b rapidity vs $dN/d\eta$



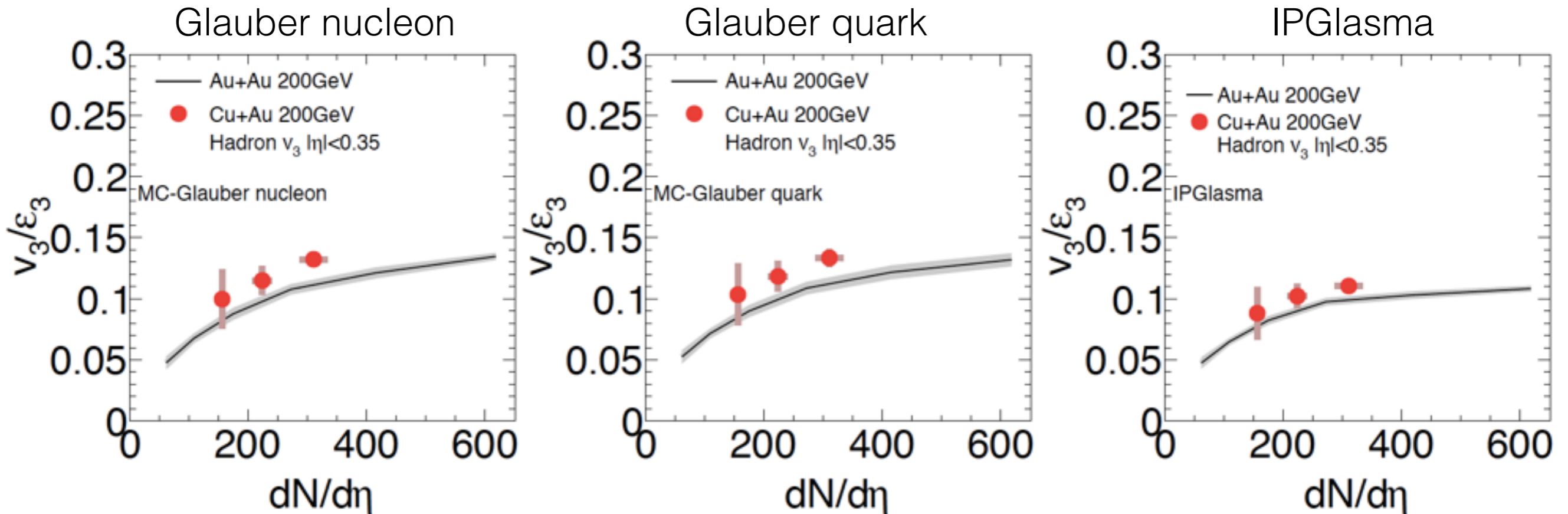
vn vs Npart

v_2/ε_2 scaling at mid-rapidity



- ✓ v_2 scaled with Glauber model (nucleon, quark) are consistent among three collision systems
- ✓ The deviation is seen in central for IPGlasma model

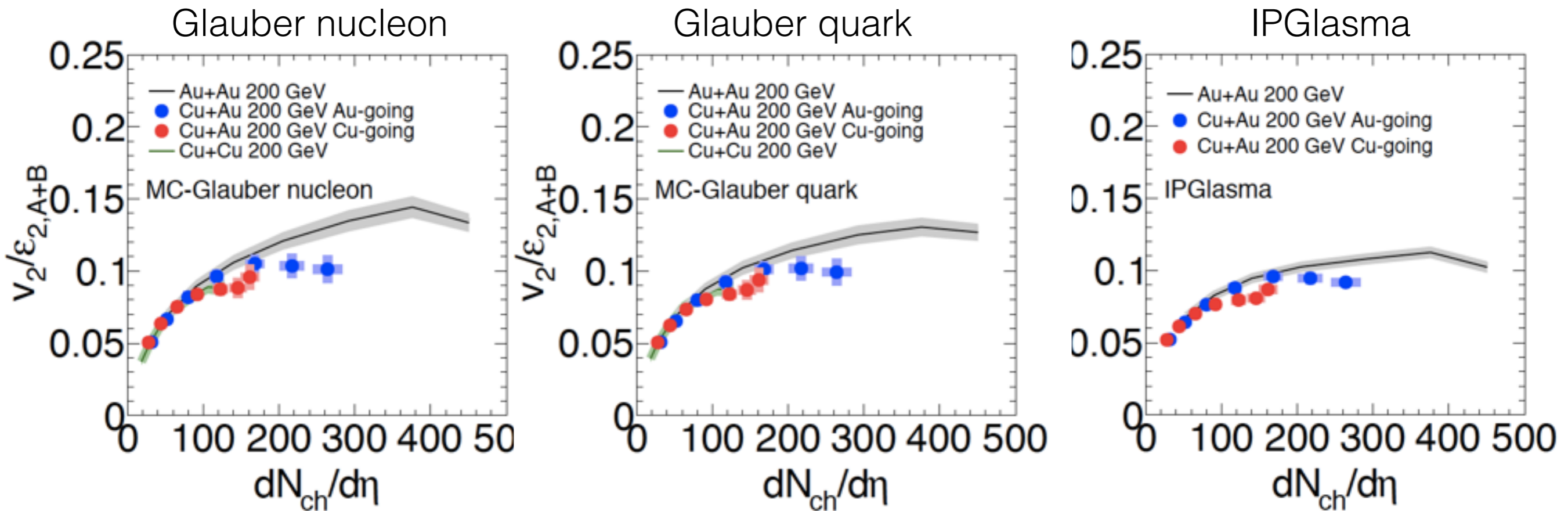
v_3/ϵ_3 scaling at mid-rapidity



✓ In Glauber model (nucleon, quark), the deviation is seen at central bin

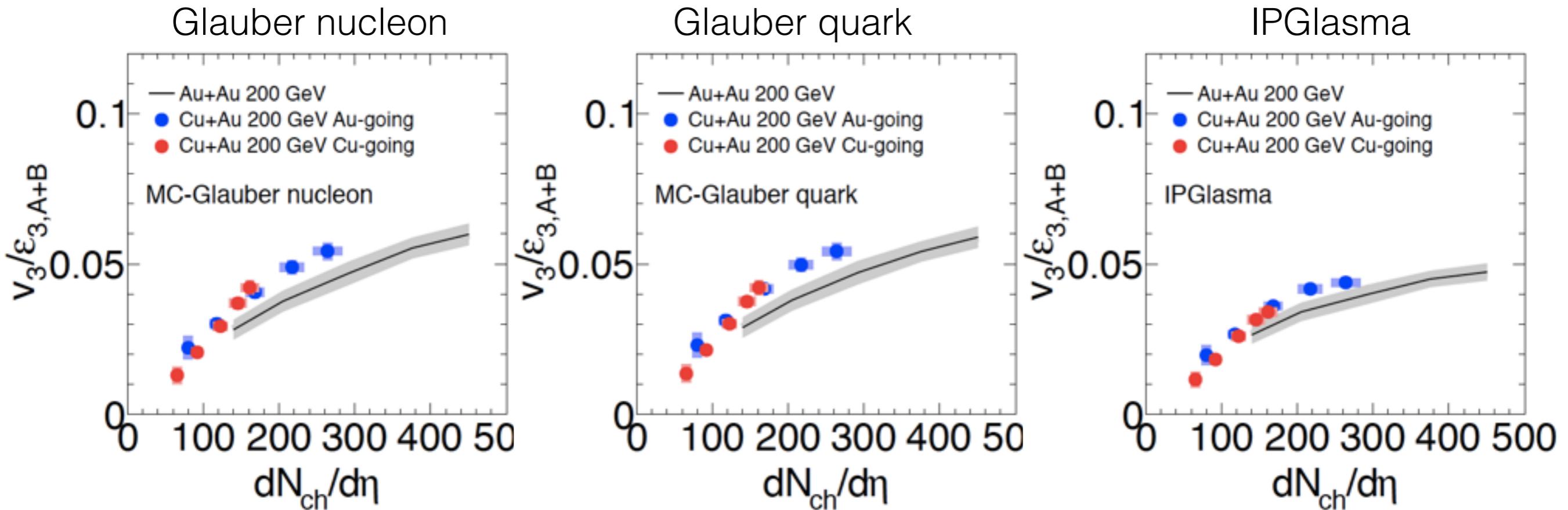
✓ In IPGlasma model, AuAu v_3/ϵ_3 and CuAu v_3/ϵ_3 are close to each other

v_2/ε_2 scaling at f/b-rapidity



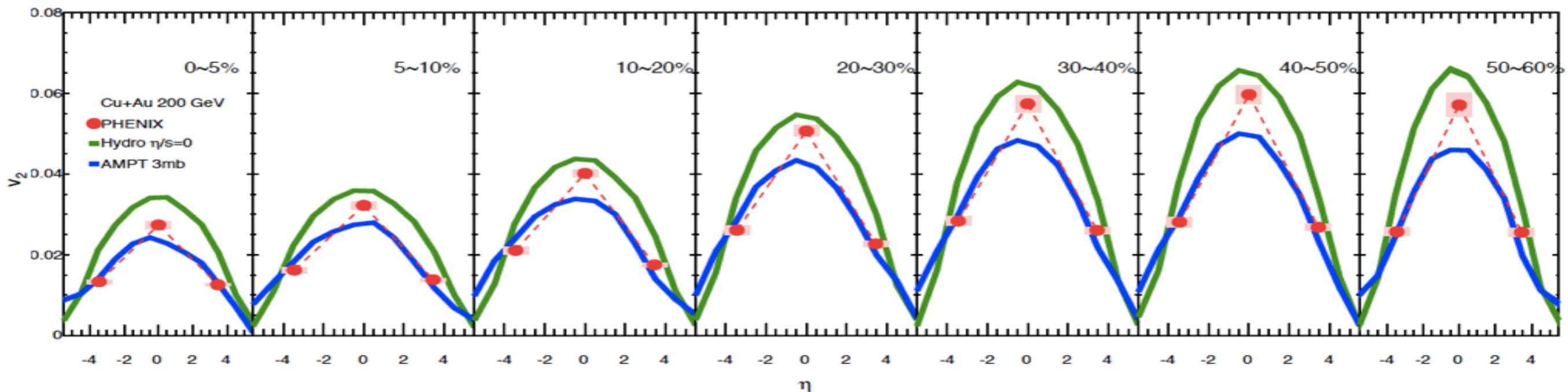
- ✓ In Glauber model (nucleon, quark), the deviations between CuAu and AuAu are seen at central bin
- ✓ In IPGlasma model, AuAu v_2/ε_2 and CuAu v_2/ε_2 are close to each other

v_3/ϵ_3 scaling at f/b-rapidity



- ✓ In Glauber model (nucleon, quark), the deviation is seen from central to mid-central
- ✓ In IPGlasma model, AuAu v_3/ϵ_3 and CuAu v_3/ϵ_3 are close to each other

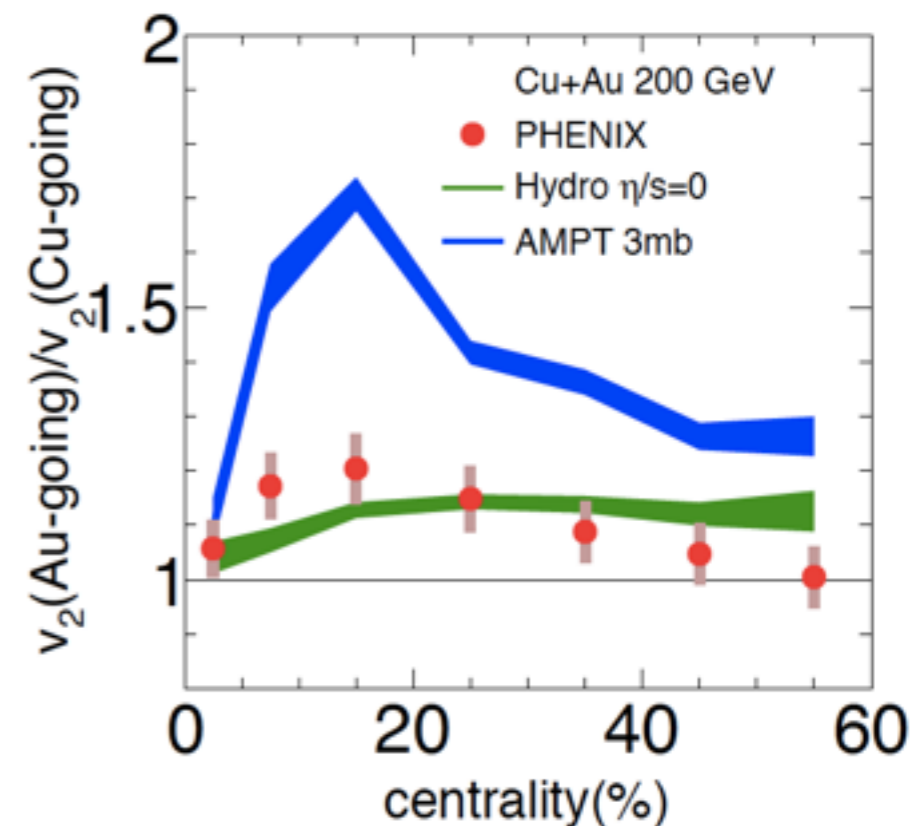
Parton cascade and hydro $v_2(\eta)$



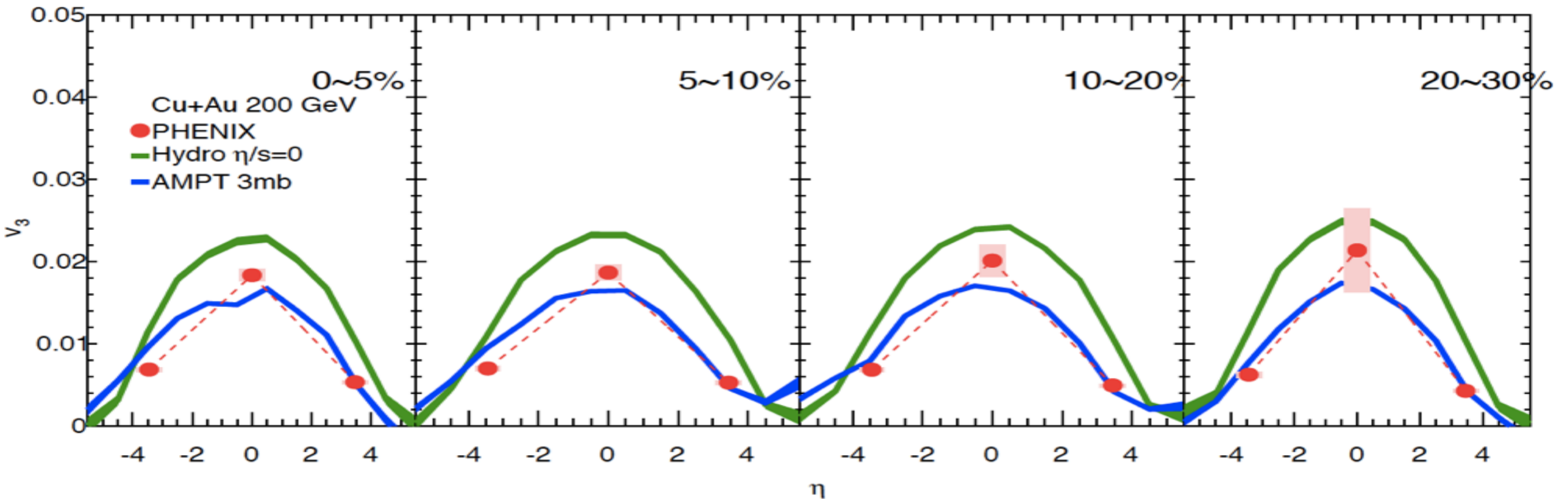
- ✓ AMPT and Hydro predict magnitude of v_2 at F/B rapidity well
- Hydro: Smooth longitudinal density + hydro
- AMPT: Fluctuated longitudinal density + parton cascade

- ✓ Hydro reproduces the ratio of F/B v_2
- In peripheral collisions, the F/B ratio becomes constant

- ✓ AMPT model over-estimate the ratio

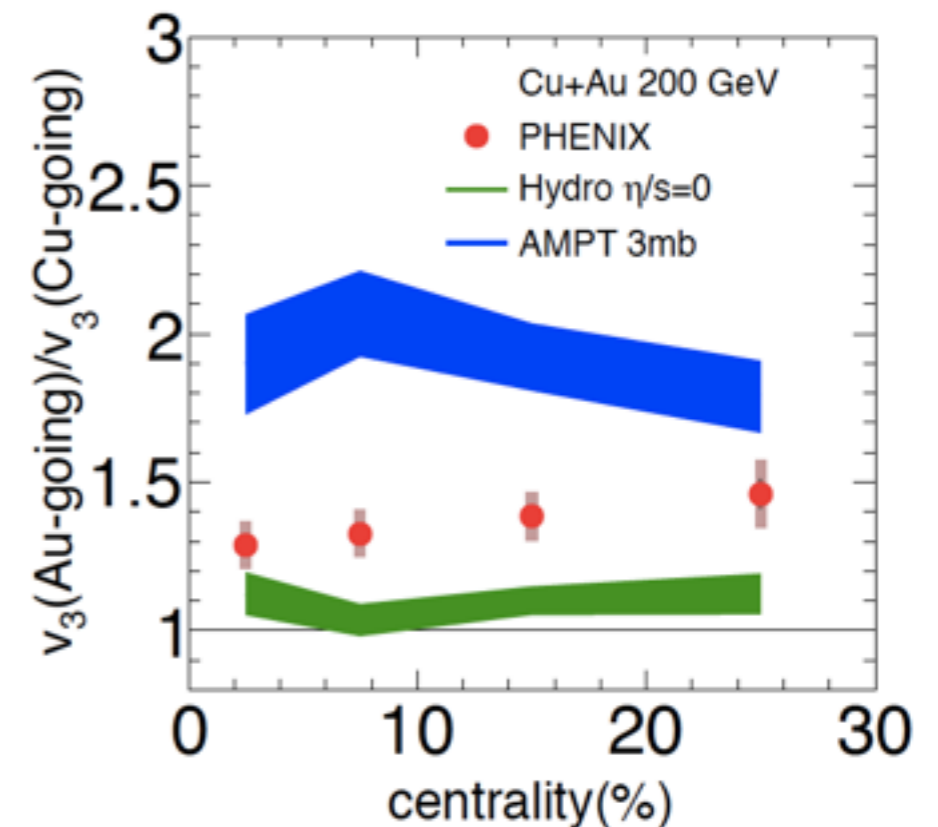


Parton cascade and hydro $v_3(\eta)$

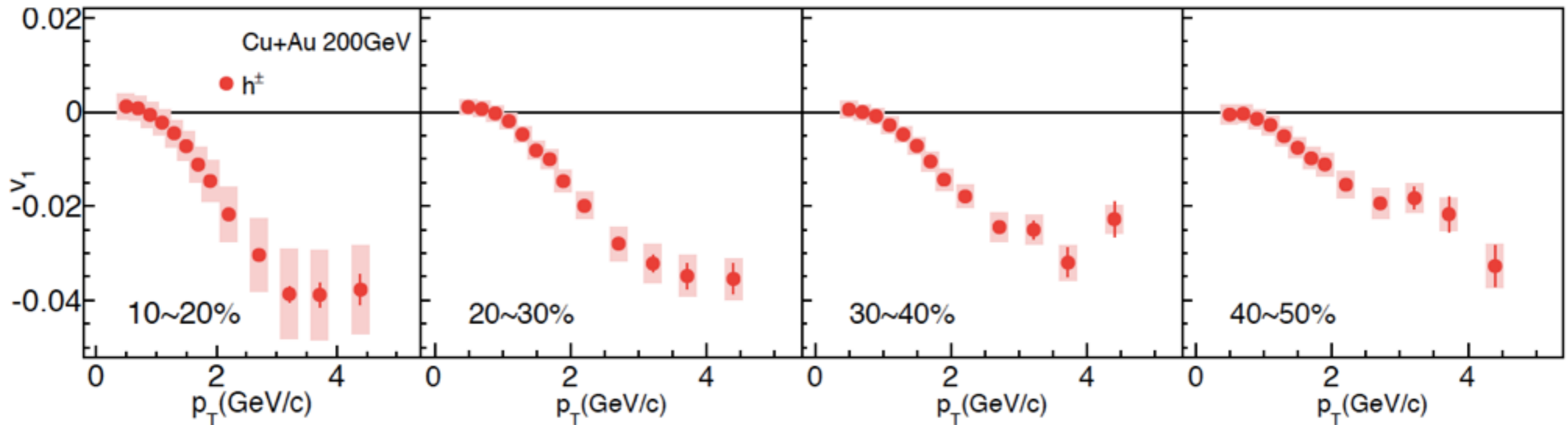
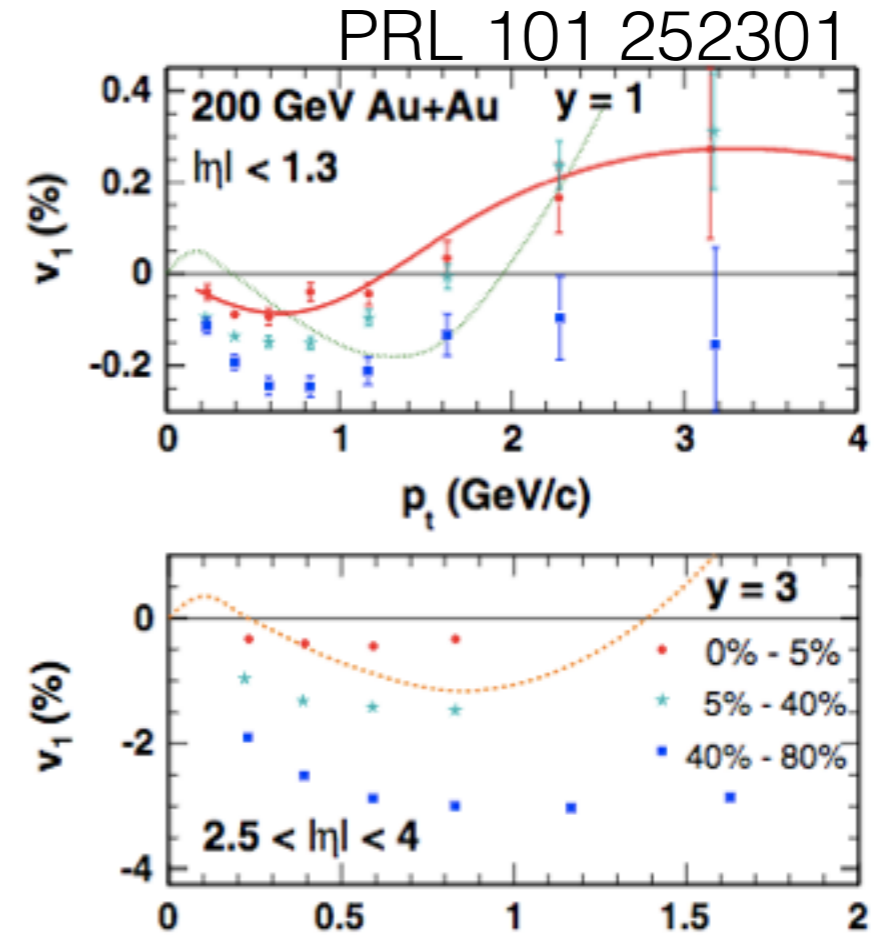
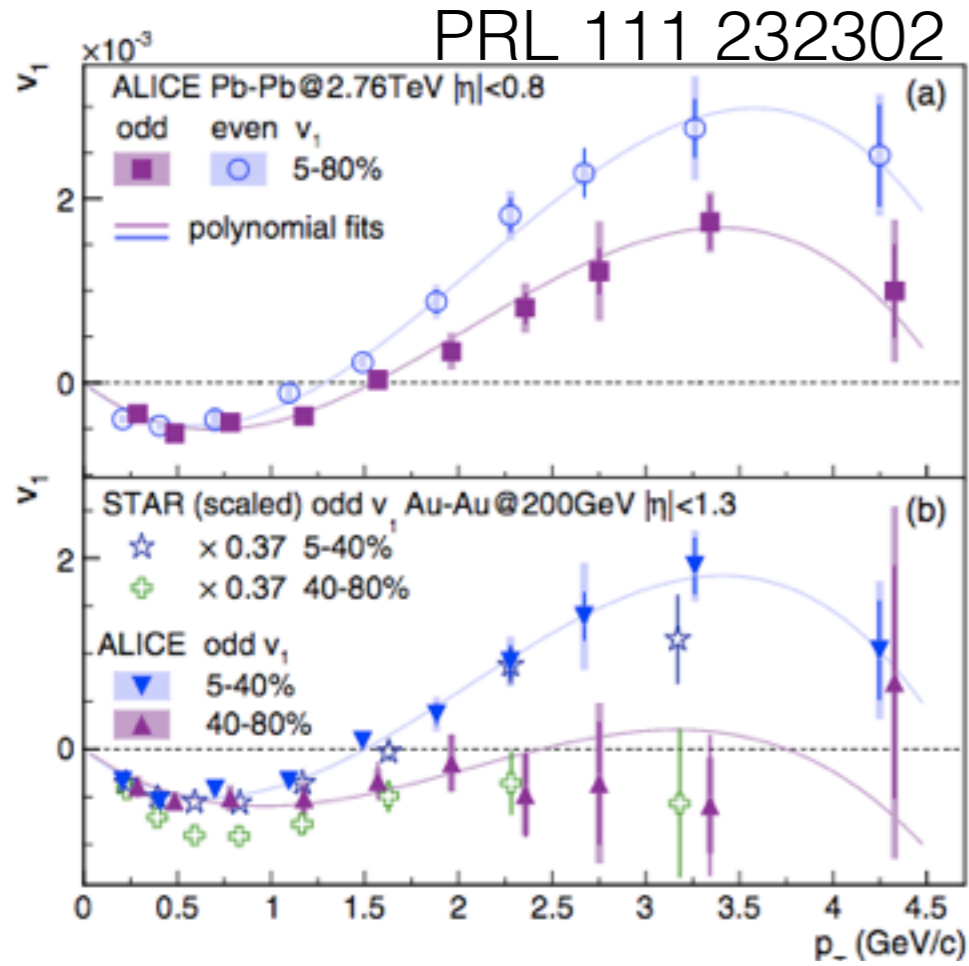


✓ AMPT show the F/B asymmetry of v_3
 - $v_3(\text{Au-going}) > v_3(\text{Cu-going})$
 -> Fluctuated longitudinal density show larger F/B asymmetry of v_n

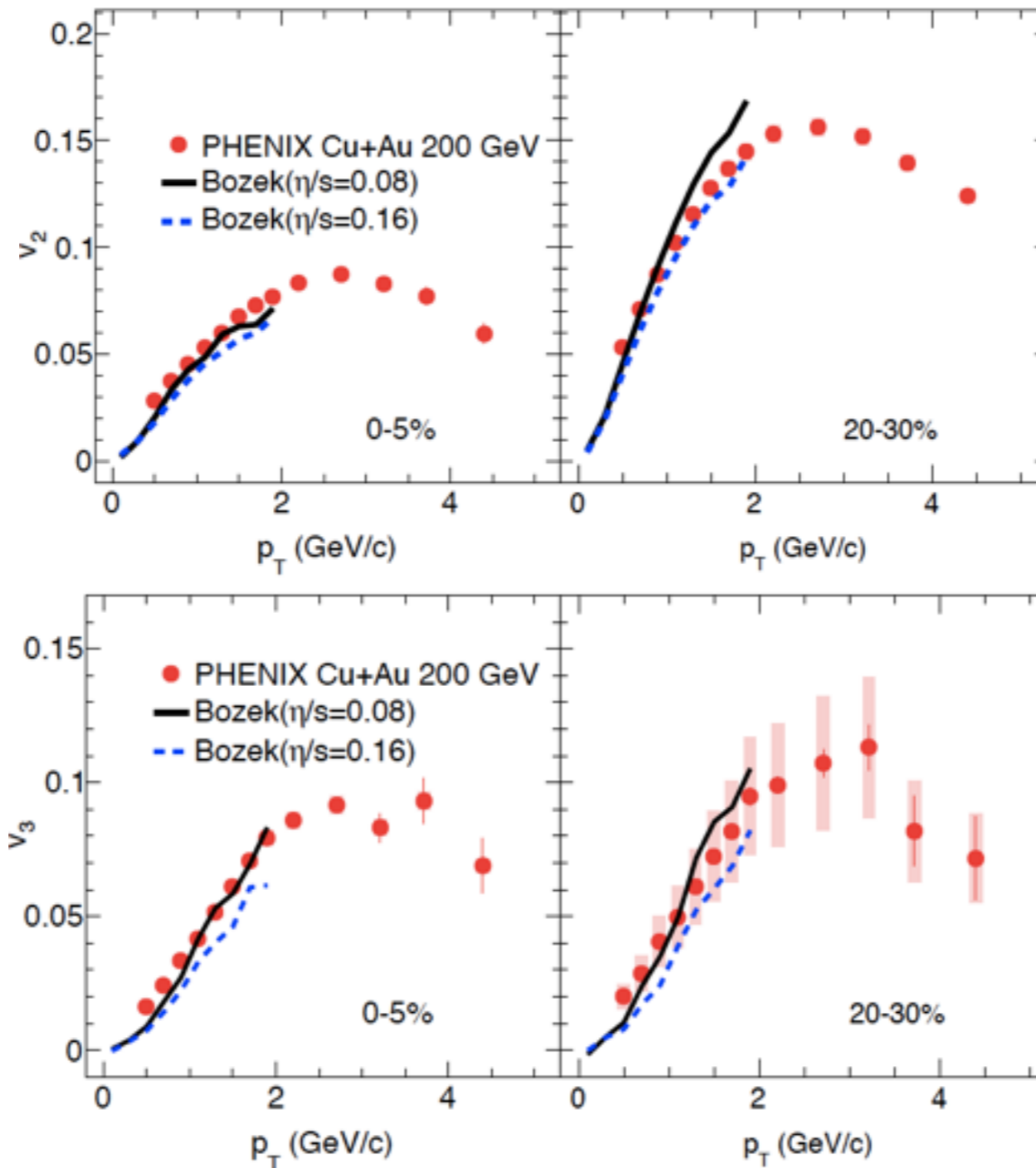
✓ Hydrodynamics show weak F/B asymmetry of v_3
 - $v_3(\text{Au-going}) \sim v_3(\text{Cu-going})$
 -> Smooth longitudinal density show weaker F/B asymmetry of v_n



Directed flow in comparison to STAR and ALICE

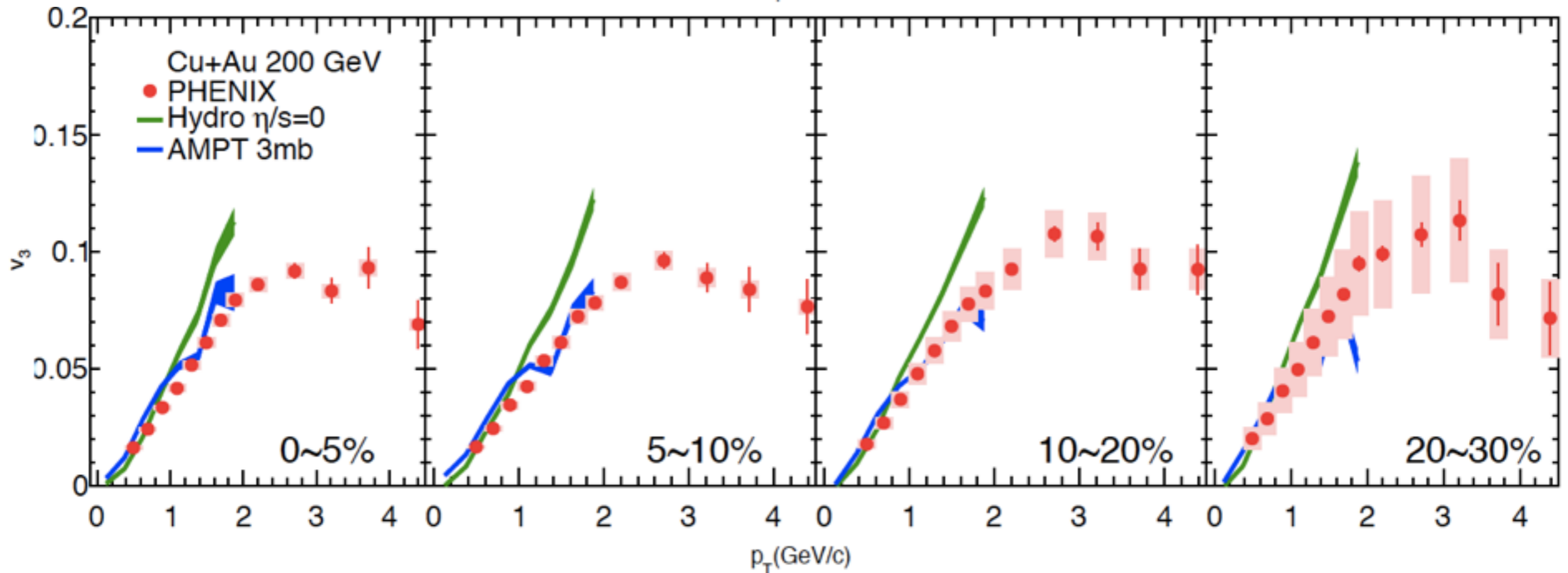
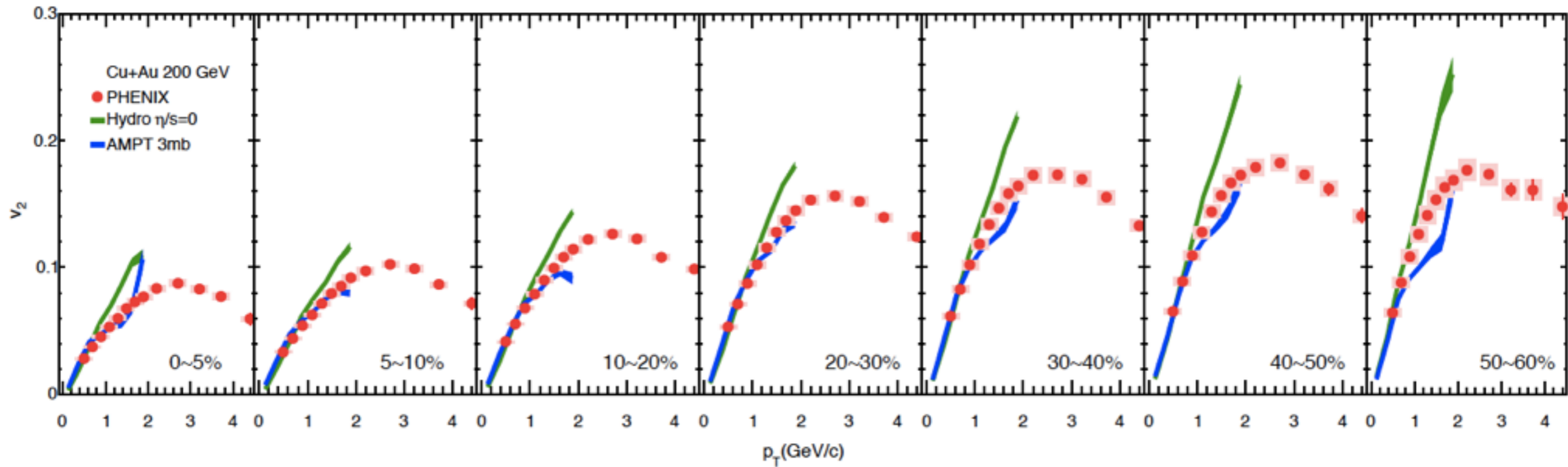


MC-Glauber E-by-E hydro v_2, v_3 at mid- η



For both centrality, both value of η/s agree with data

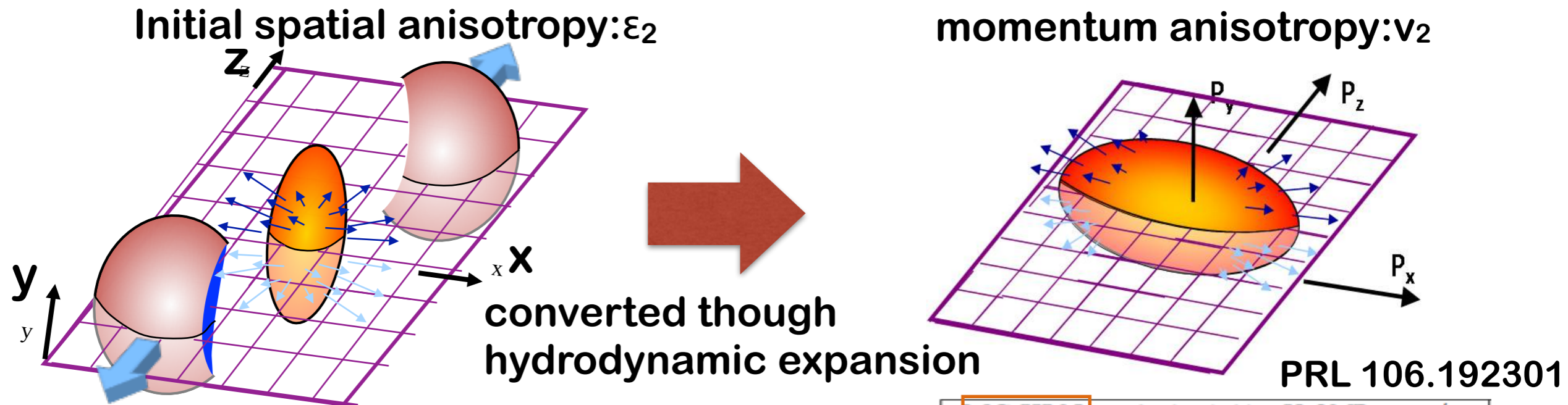
v_n : AMPT and Hydrodynamics





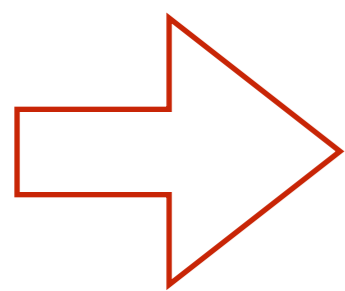


Azimuthal anisotropy: Elliptic flow



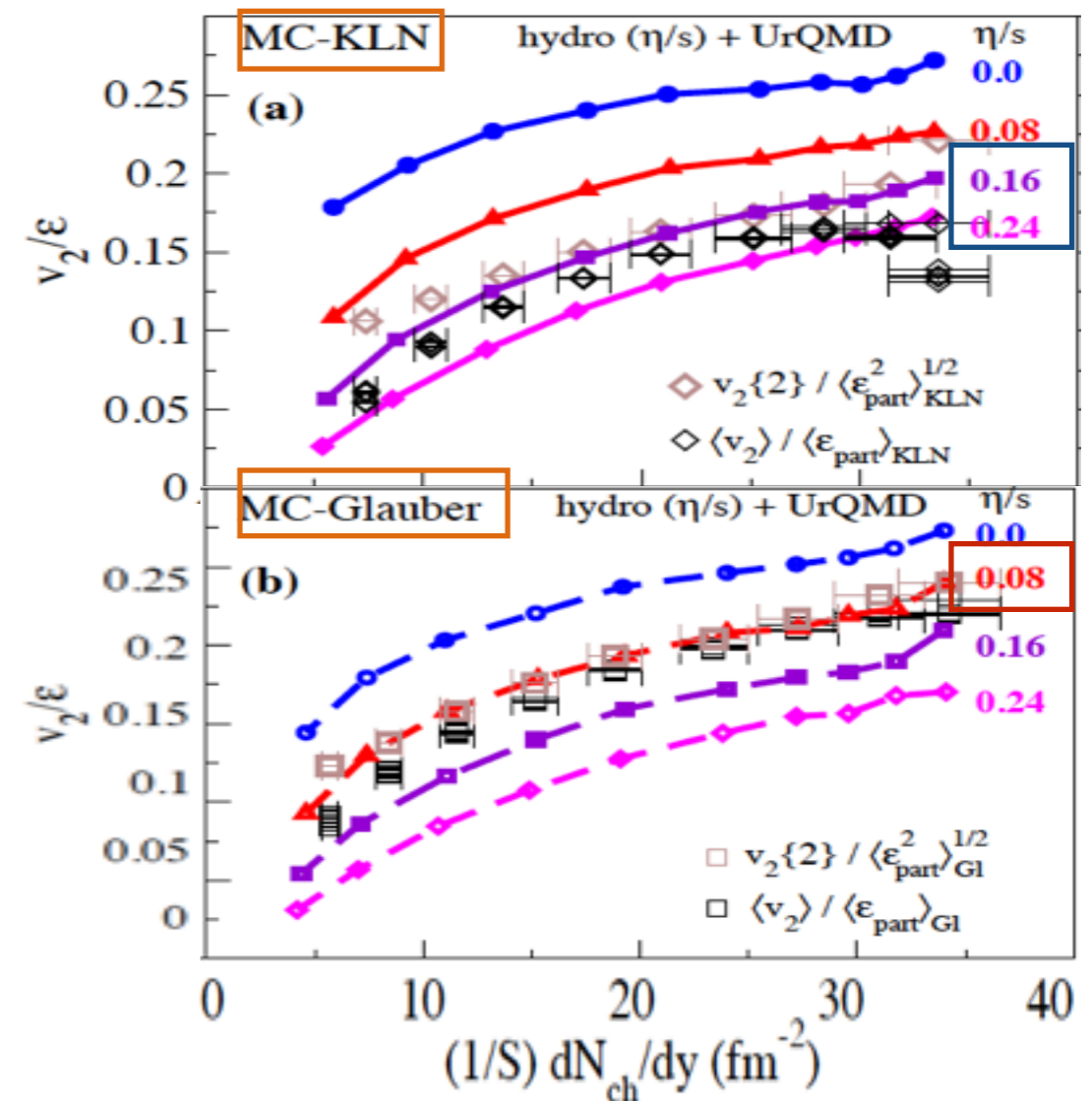
particle production will have an elliptical azimuthal distribution.

- Non-isotropic pressure gradient



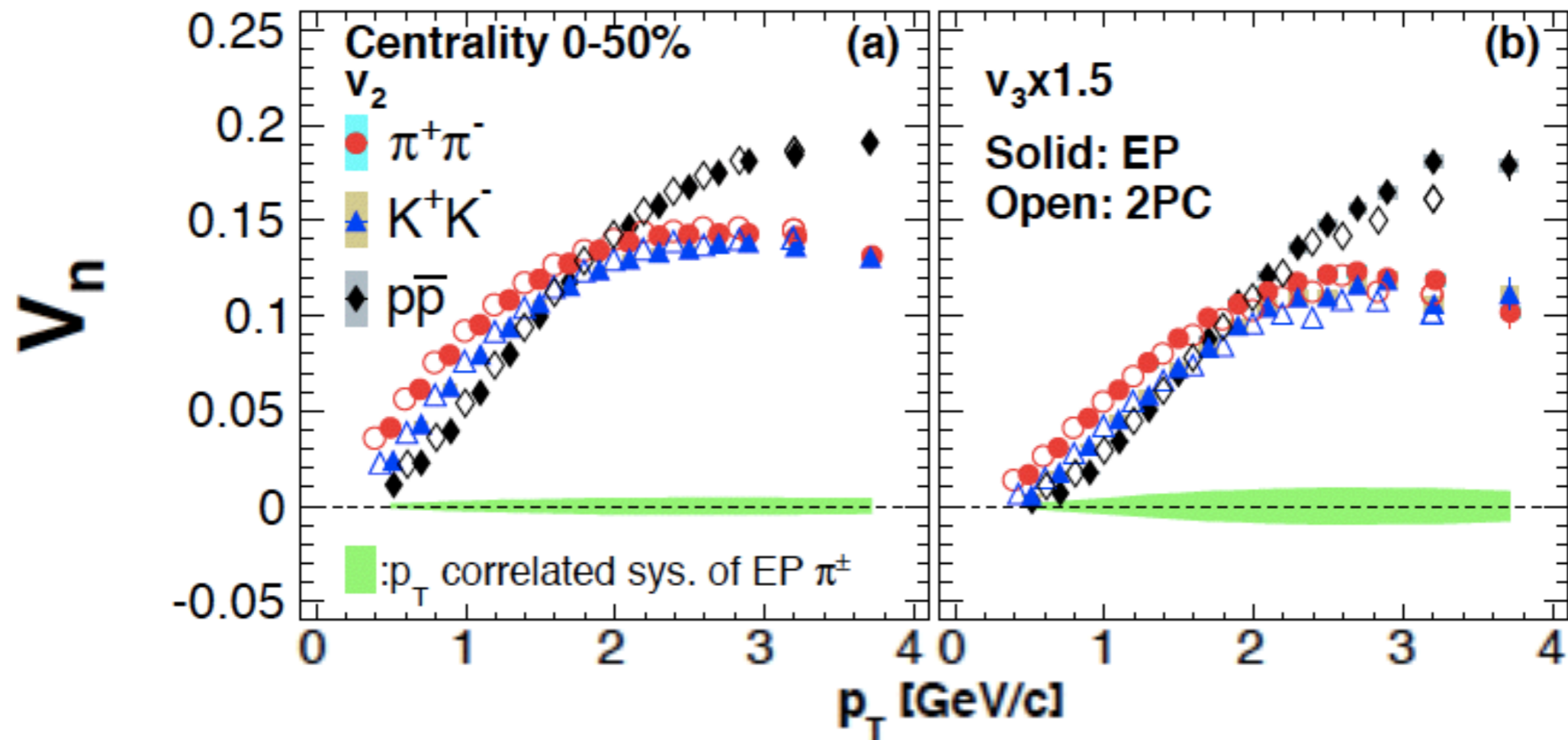
Sensitive to

- initial condition (Glauber, KLN..etc.)
- viscosity (η/s)



pi, K, p flow

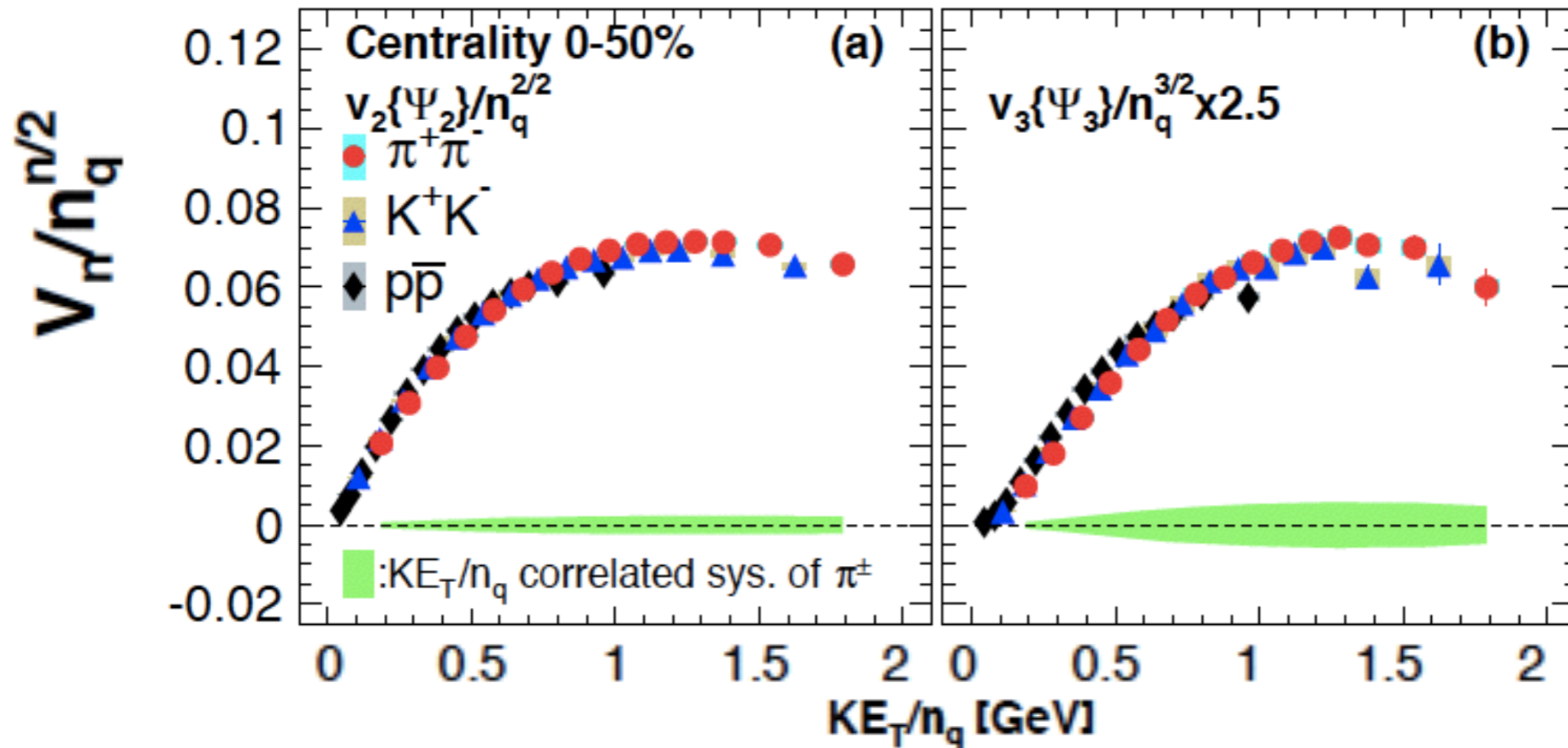
arXiv:1412.1038



v_2, v_3 have similar particle dependence
 v_3 scaled with $n_q^{3/2}$

Scaling property : quark number scaling

arXiv:1412.1038



v_2, v_3 have similar particle dependence
 v_3 scaled with $n_q^{3/2}$

Track identification at CNT ($|\eta| < 0.35$)

TOF.E and TOF.W are used

- TOF.E : Scintillation counter 130ps
- TOF.W : MRPC 95ps

Time of flight method

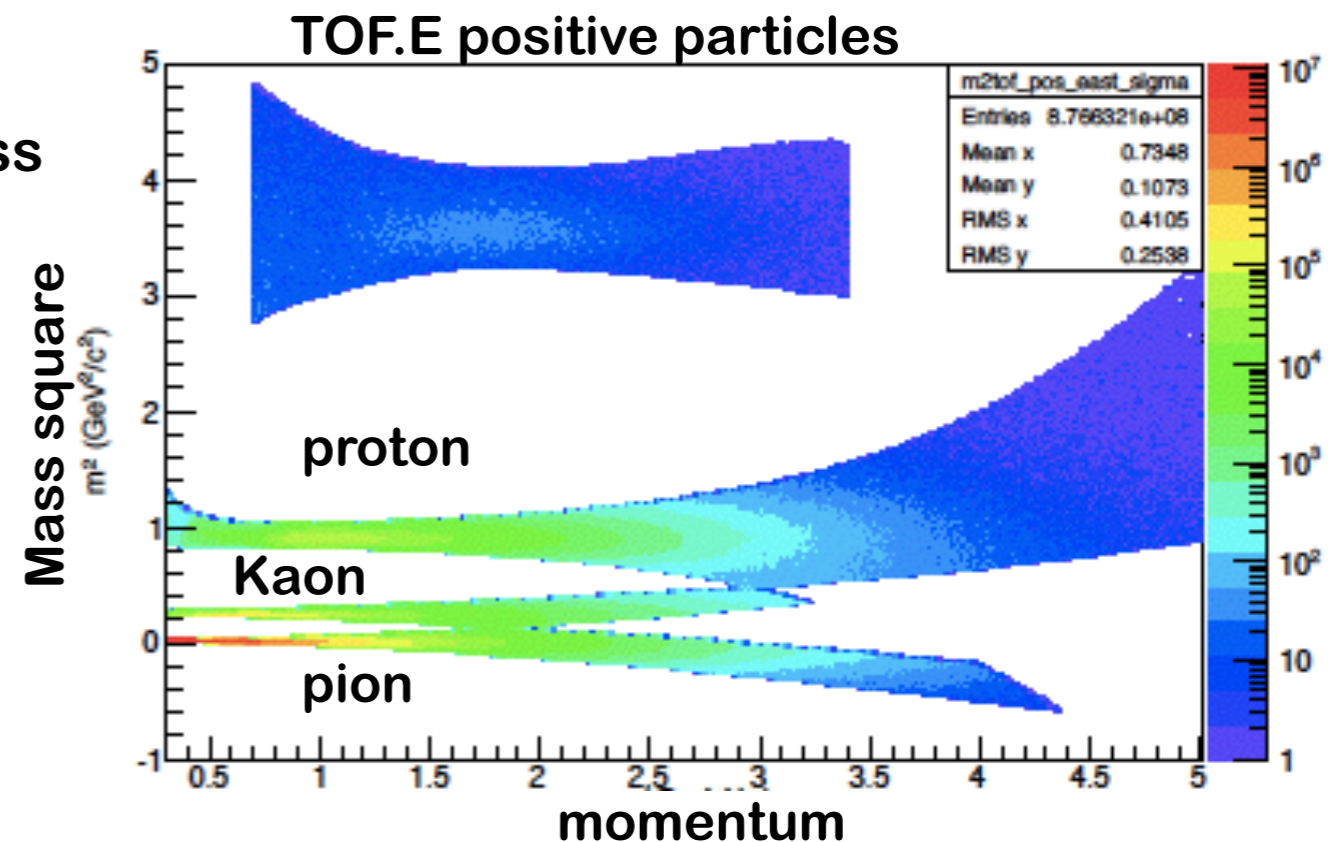
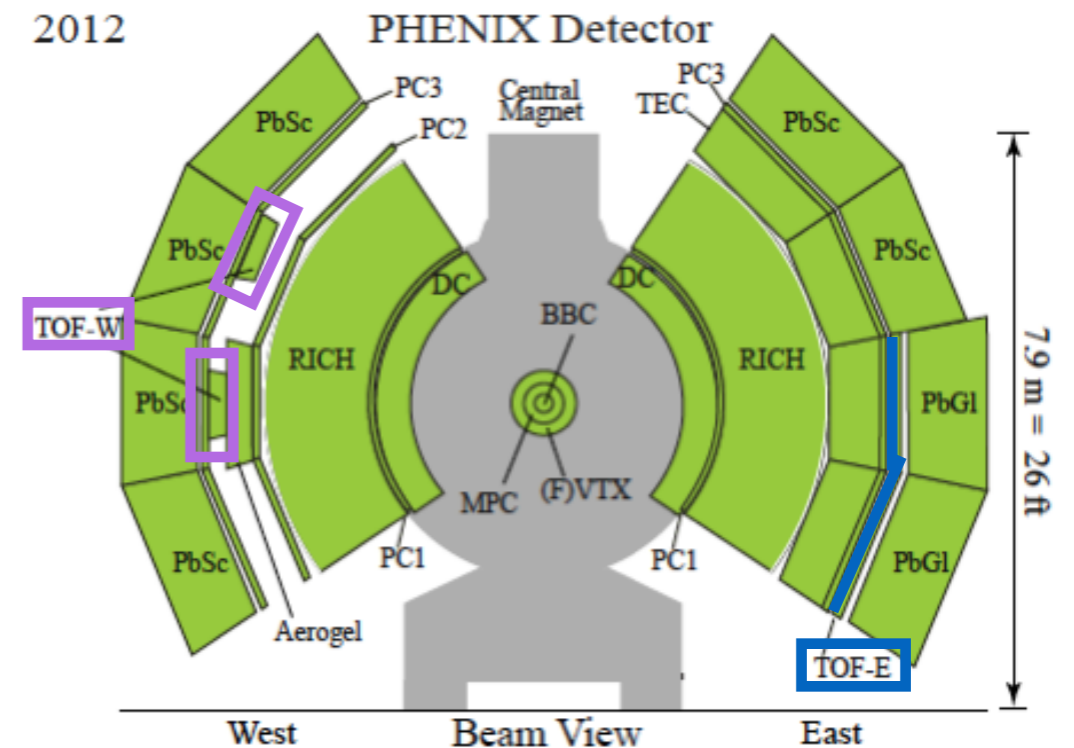
$$m^2 = p^2 \left(\left(\frac{ct}{L} \right)^2 - 1 \right)$$

m:particle mass, p:momentum, L:flight pass
c:light velocity, t:time of flight

Charged pi,K,p

-pi/K up to 3GeV

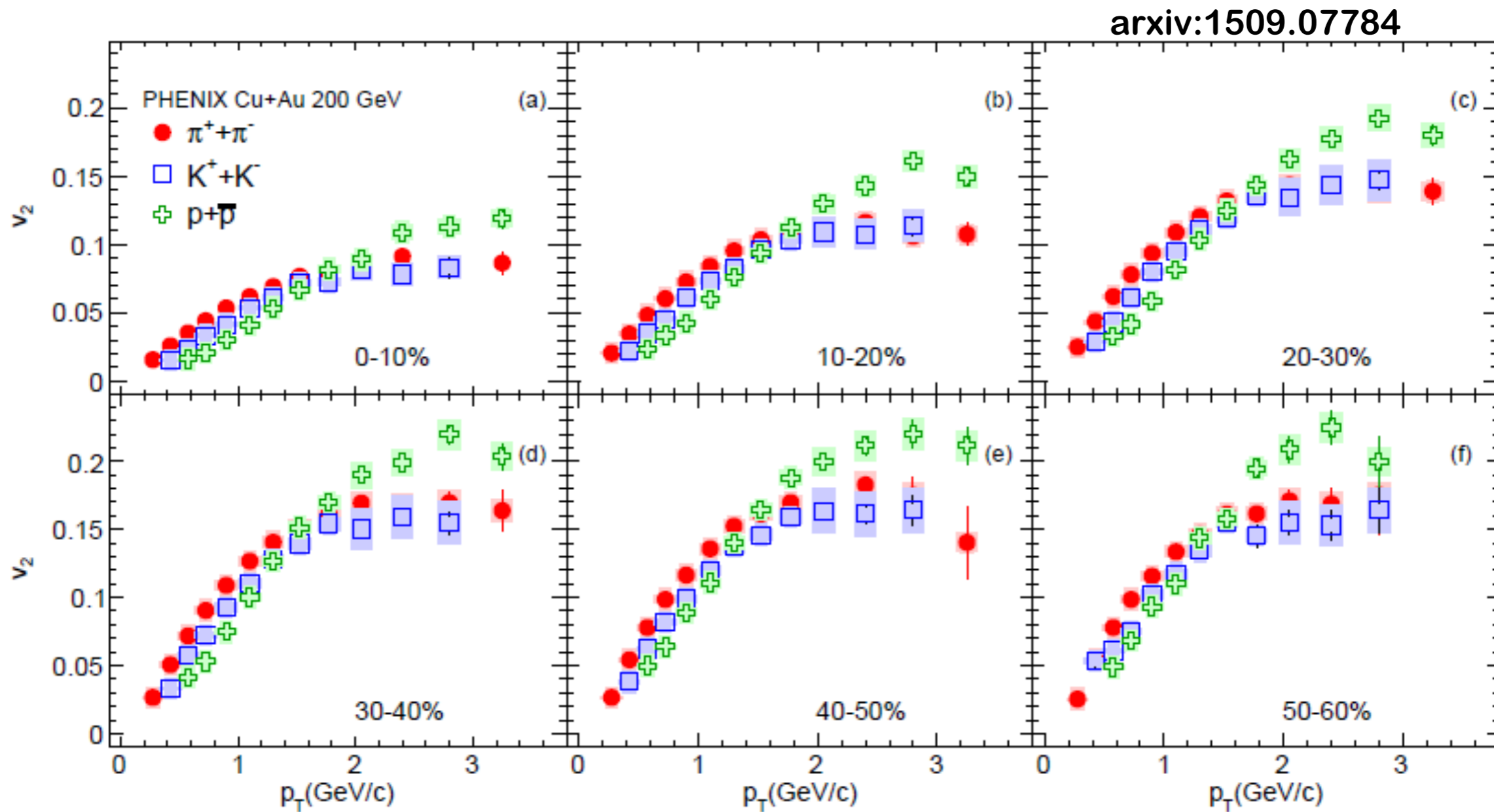
-K/p up to 4GeV



Results & Discussions

- System size dependence
- **PID** v_n
- Rapidity dependence
- Theory comparison

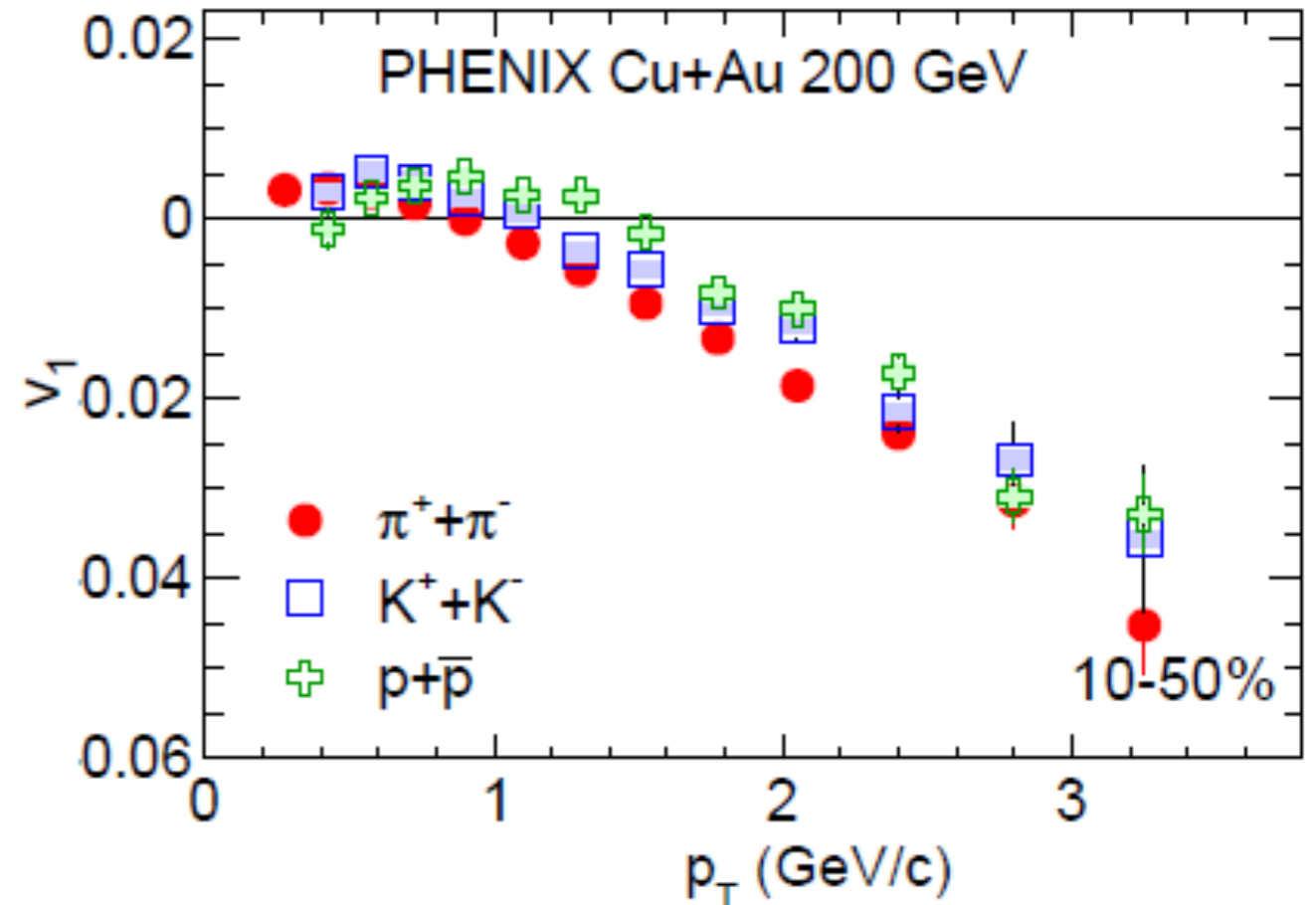
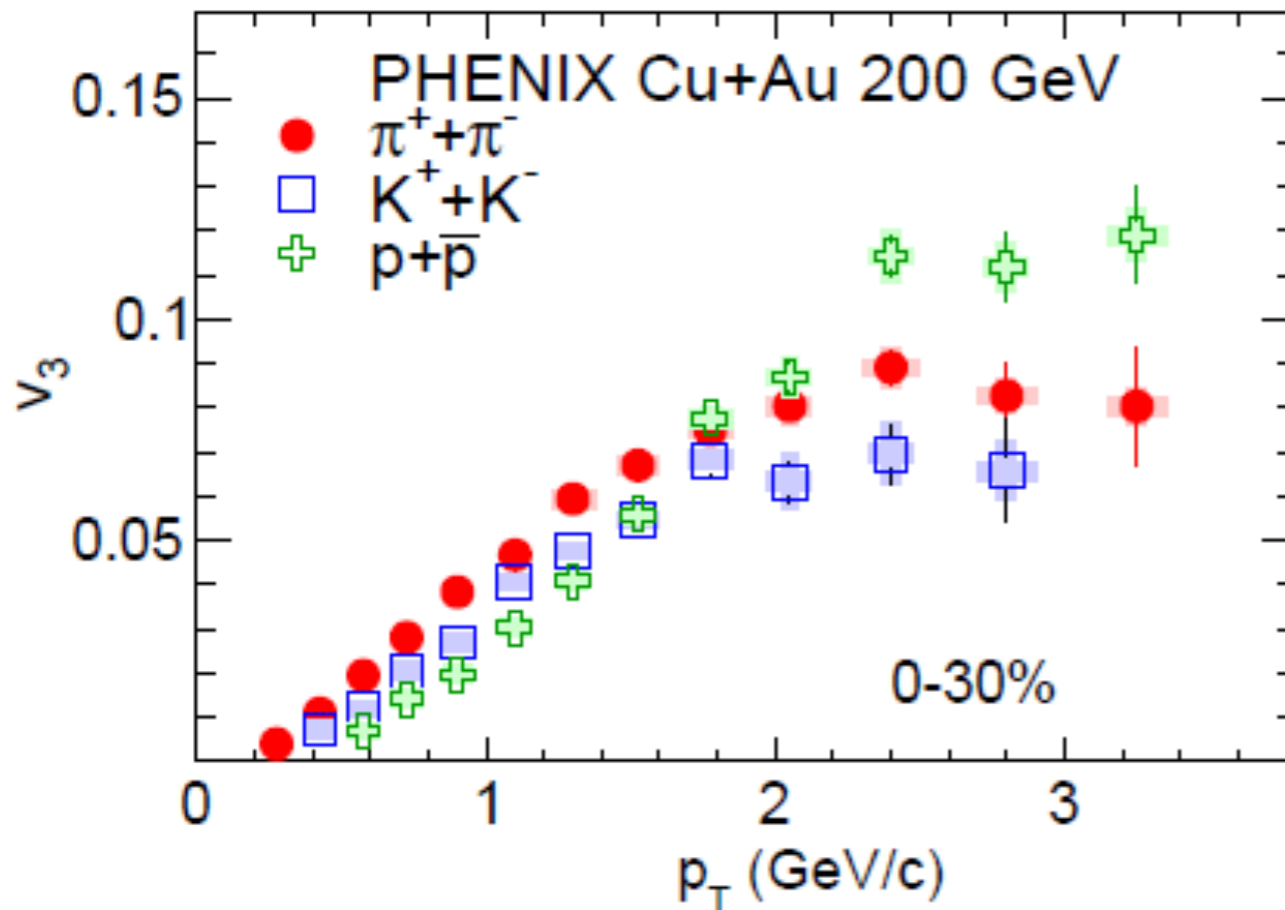
Identified particle v_2 in Cu+Au



Mass ordering at low p_T for v_2 for all centralities
Baryon and meson splitting at mid- p_T is seen

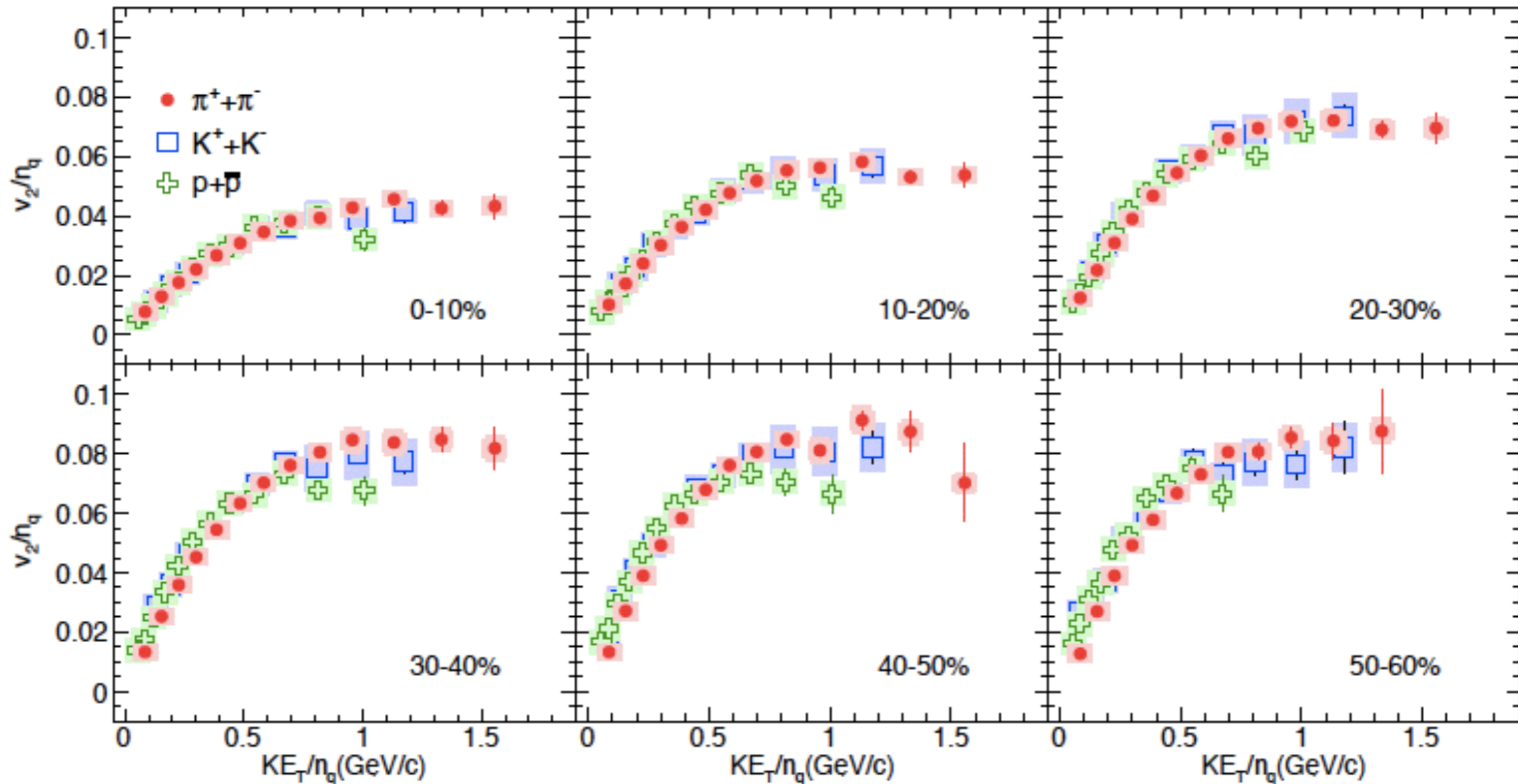
Identified particle v_1, v_3 in Cu+Au

arxiv:1509.07784



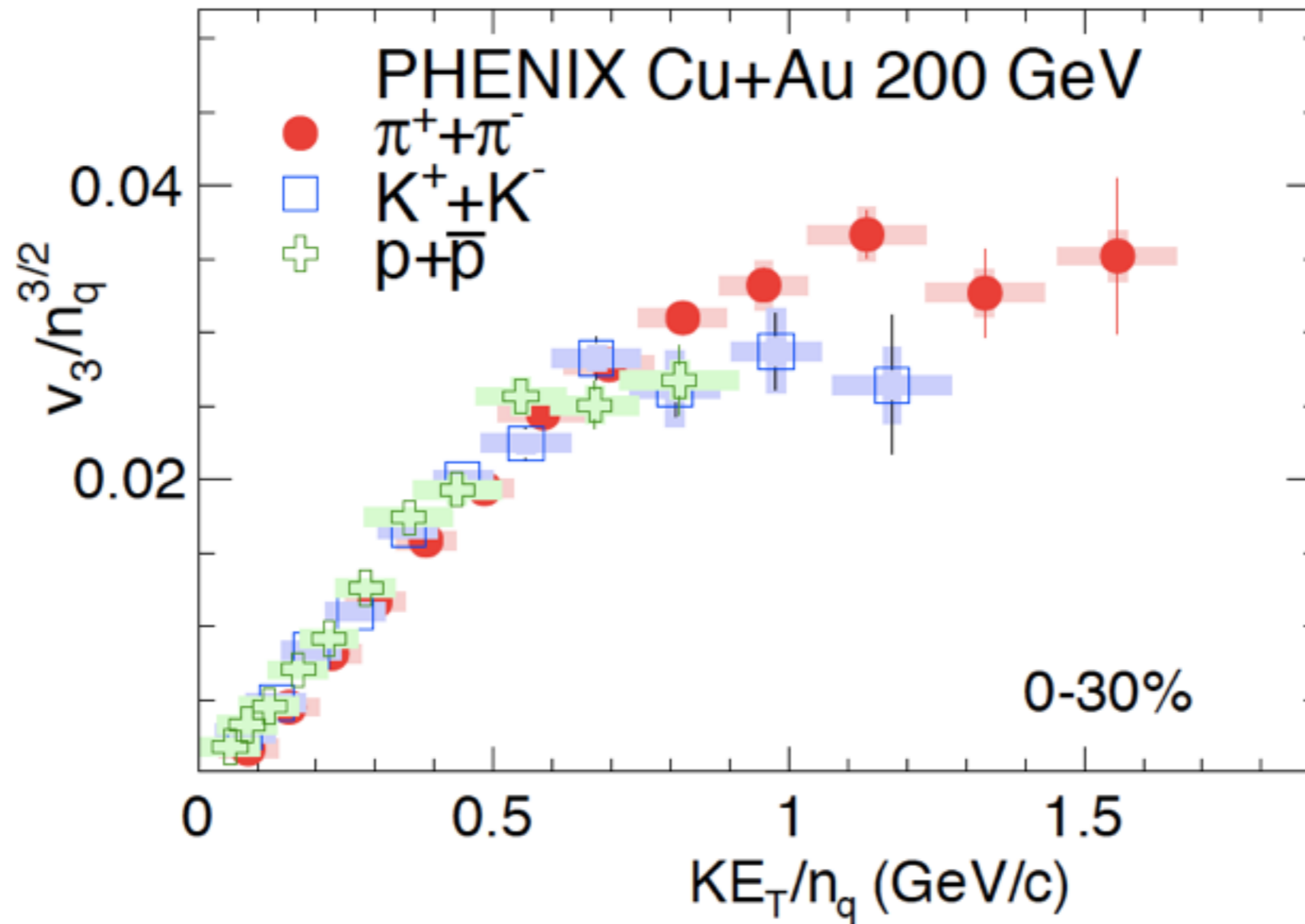
- Same particle dependence of v_3 is seen as seen in v_2
 Mass ordering is also seen for v_1
- At $1 < p_T < 2.5 \text{ GeV}$, Mass ordering is seen
 - At low and high p_T region, baryon $v_1 \sim$ meson v_1
 - Not same trend as seen in v_2, v_3

Quark Number Scaling of v_2



Quark Number Scaling works v_2 in CuAu

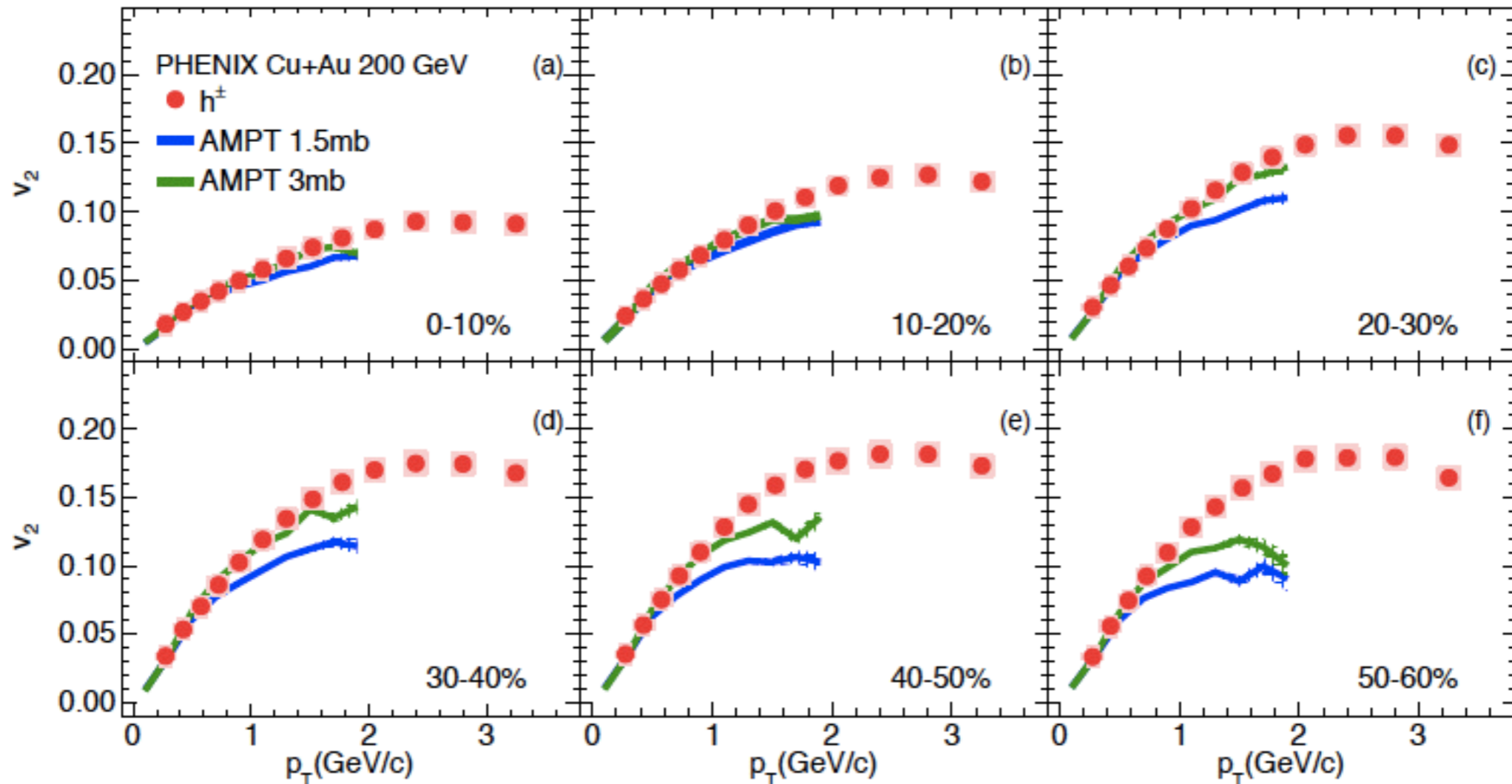
Quark Number Scaling for v_3



Quark Number Scaling work v_3 in CuAu

Comparison to AMPT v2

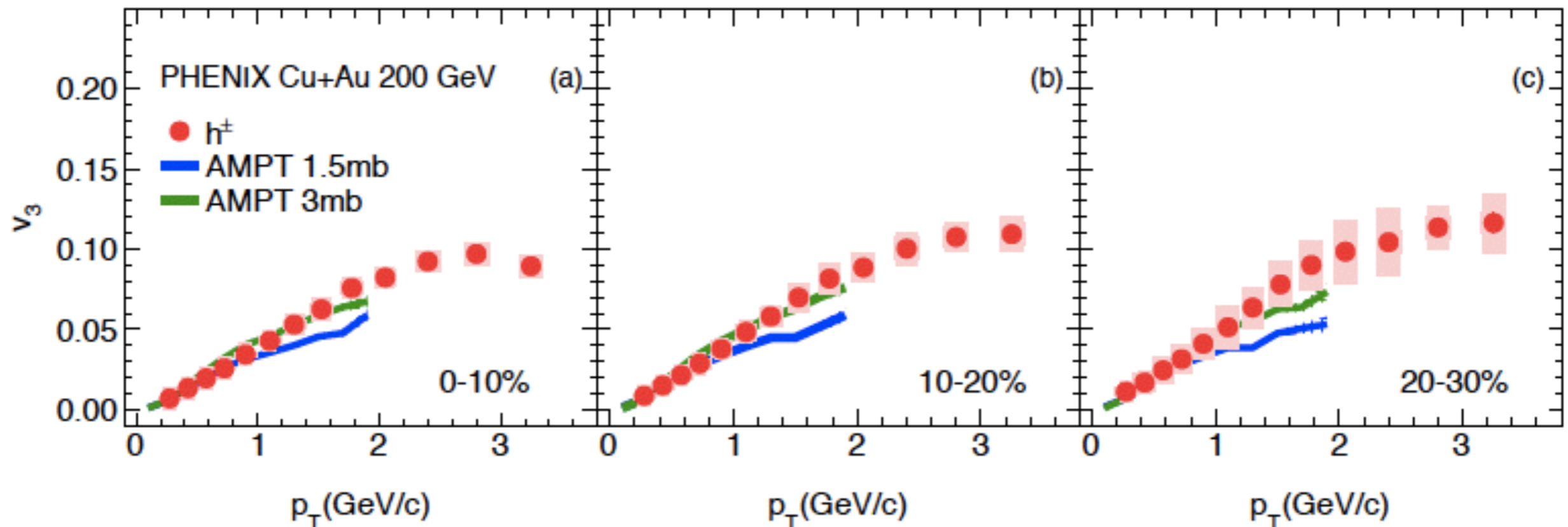
arxiv:1509.07784



AMPT with 3mb reproduce v_2
-In 0-30%, up to 2GeV
-In 30-60%, up to 1GeV

Comparison to AMPT v3

arxiv:1509.07784



**AMPT with 3mb reproduce v_3
-In 0-30%, up to 2GeV**

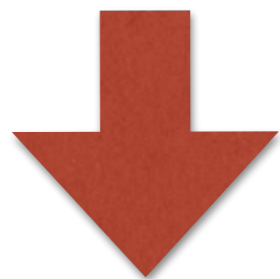
Azimuthal anisotropic flow

In relativistic heavy ion collisions, the azimuthal distribution of produced particles is anisotropic

Anisotropic initial overlap region(ϵ_n)

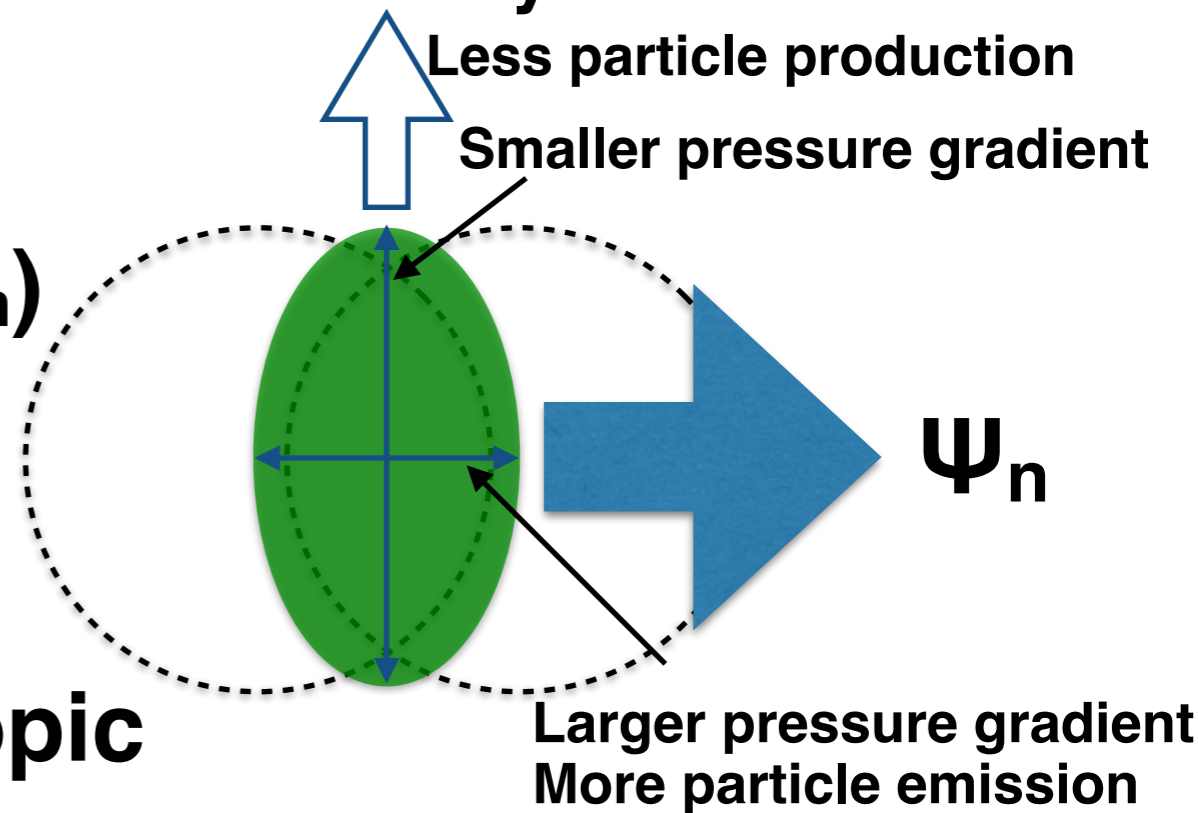
If $\lambda \ll R$, pressure gradient ΔP becomes anisotropic.

λ =Mean free path R =Size of the system



Anisotropic particle emission(v_n)

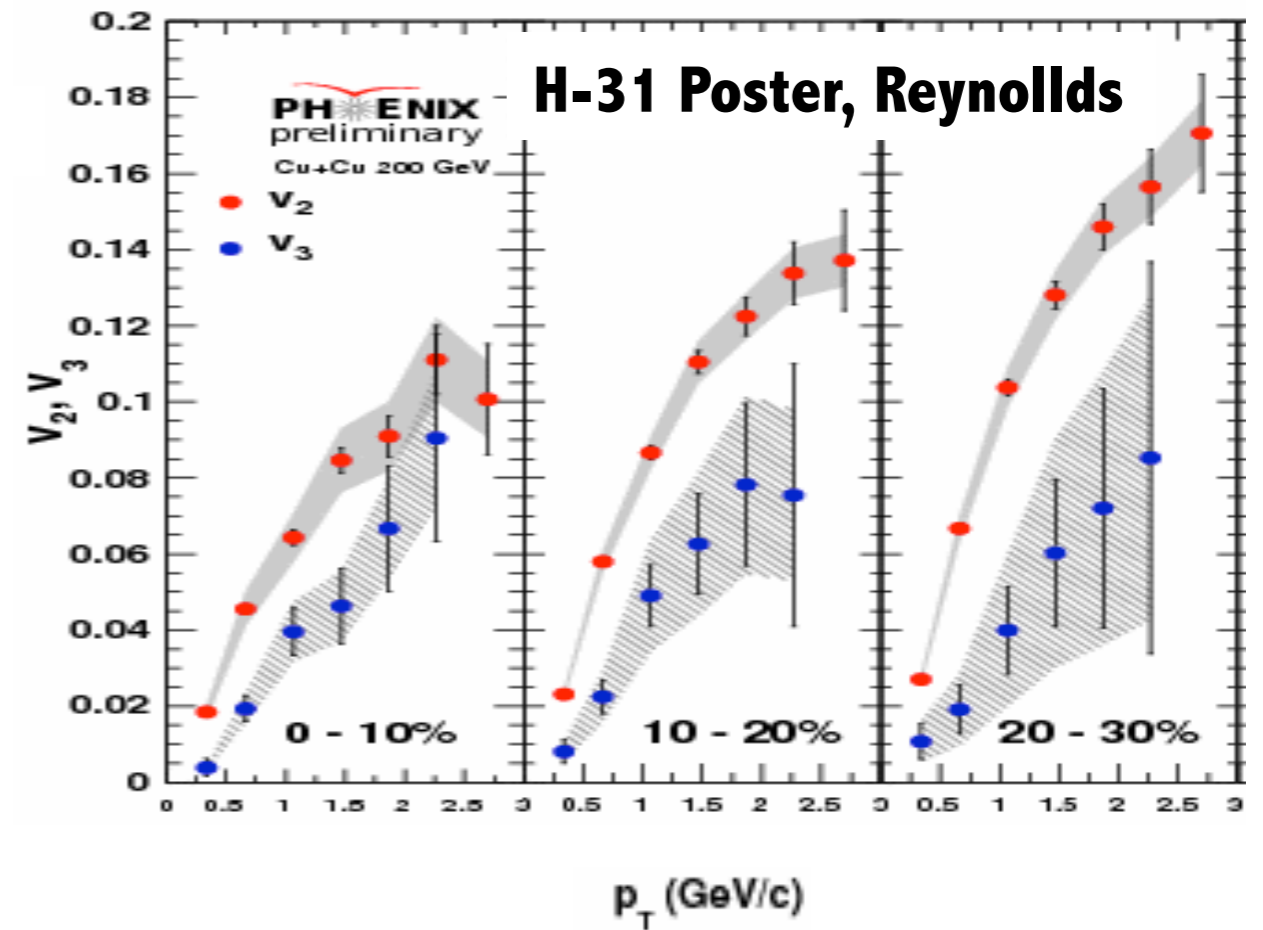
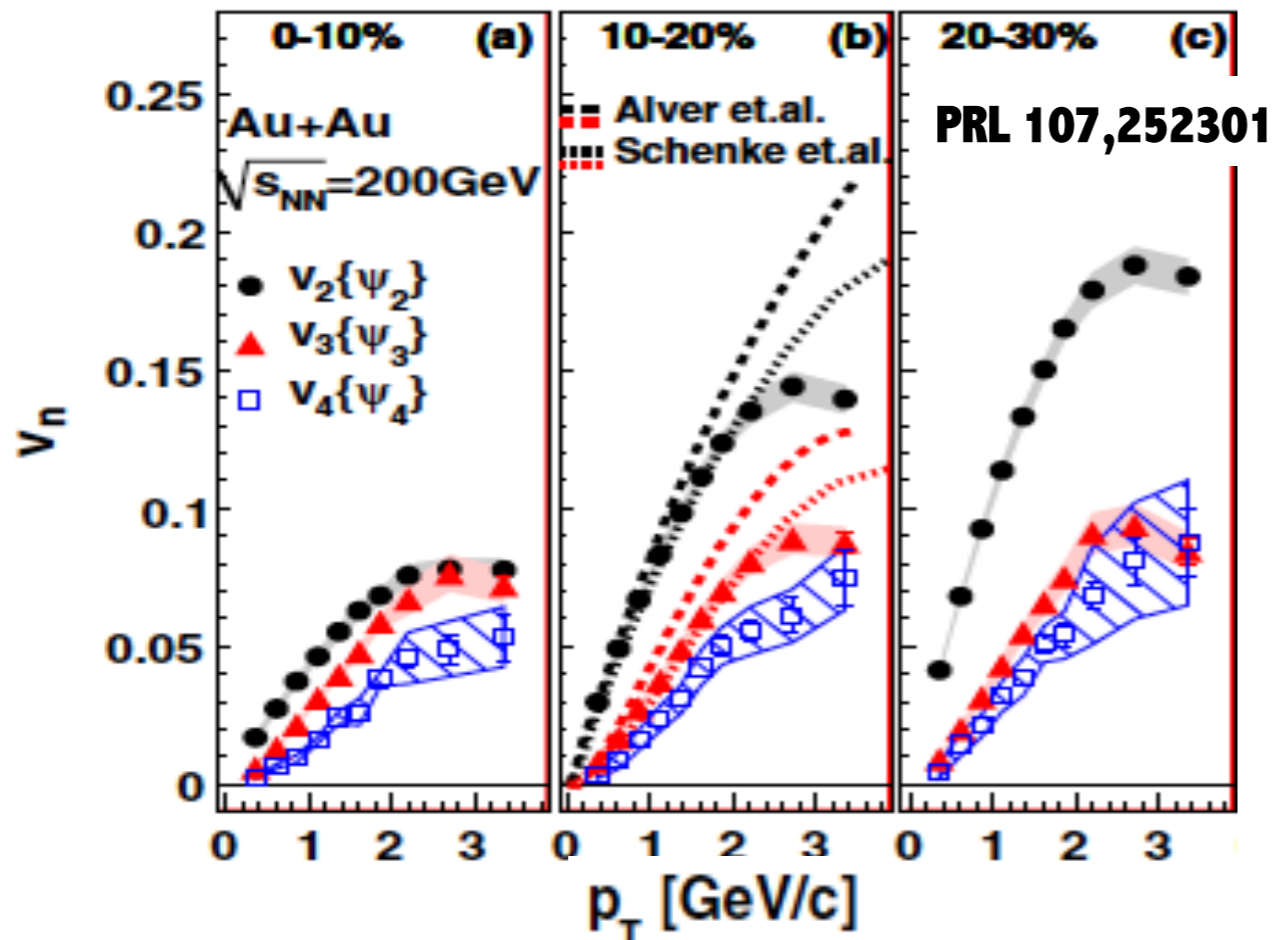
Expansion to short axis direction by anisotropic pressure gradient



Magnitude of azimuthal anisotropic particle emission is evaluated as

$$v_n = \langle \cos(n[\phi - \Psi_n]) \rangle \quad \text{ellipticity with respect to } \Psi_n$$

Flow in symmetric collisions system



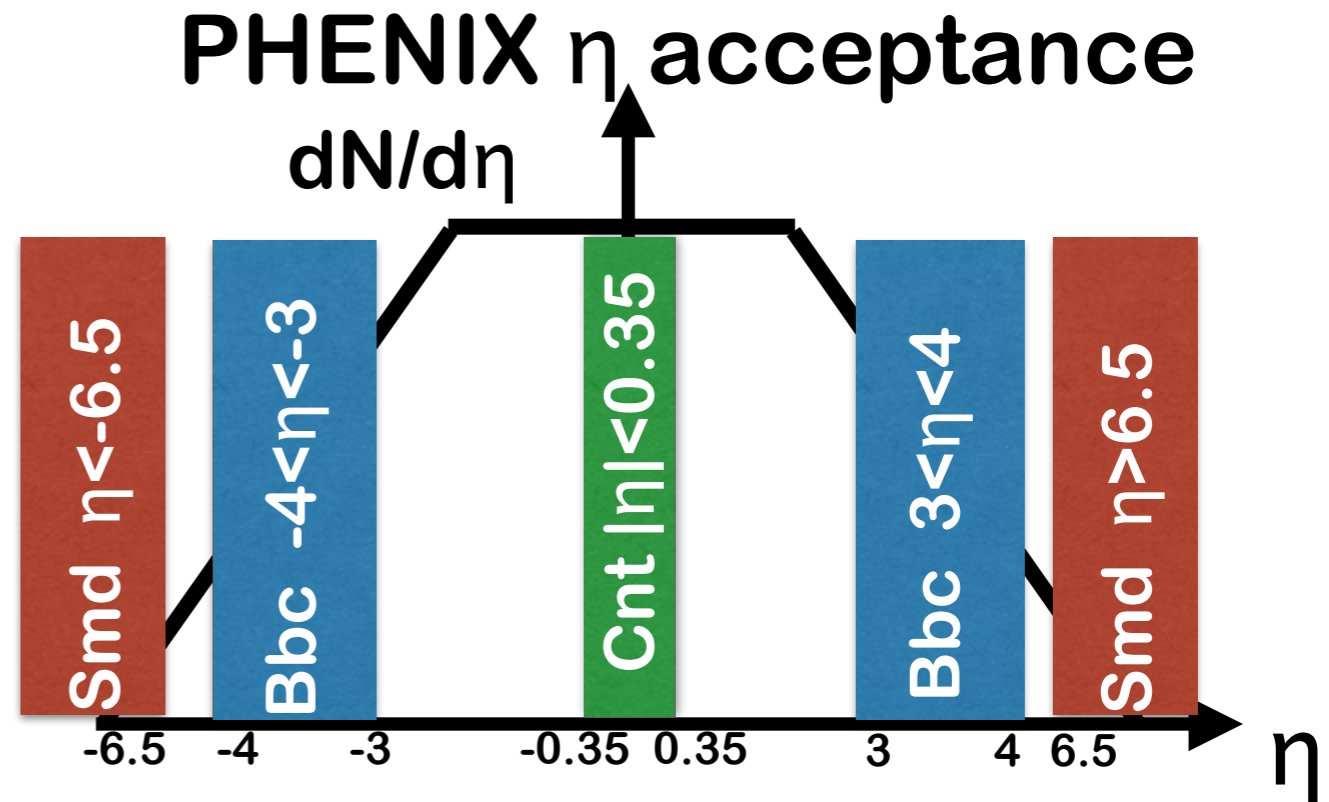
3sub method

Event Plane detectors

- 2nd, 3rd Event plane
- Bbc, Cnt
- 1st Event plane
- Bbc, Smd

Event Plane resolution

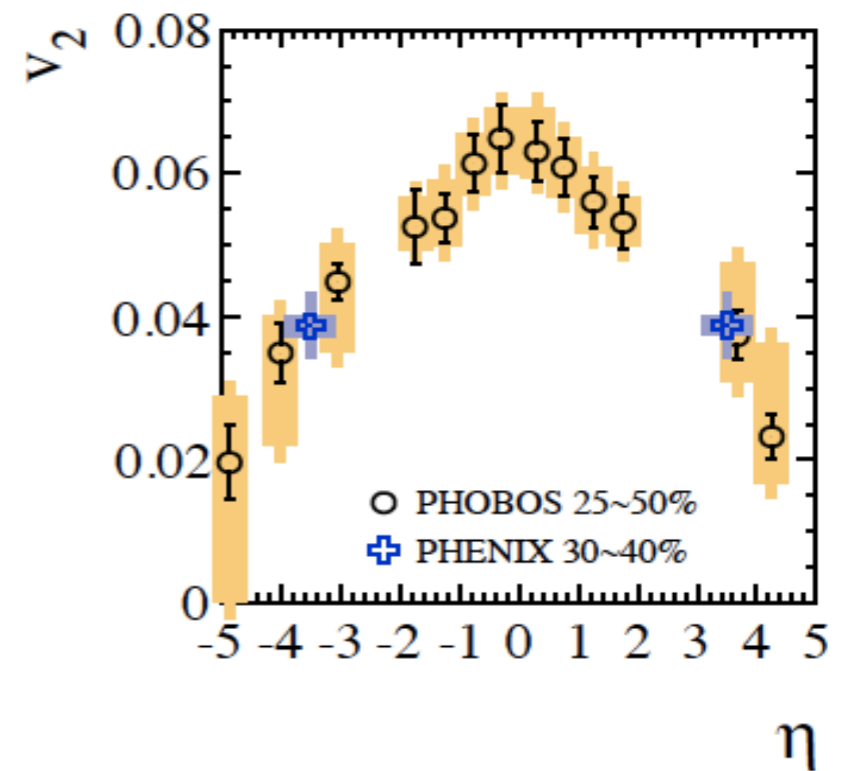
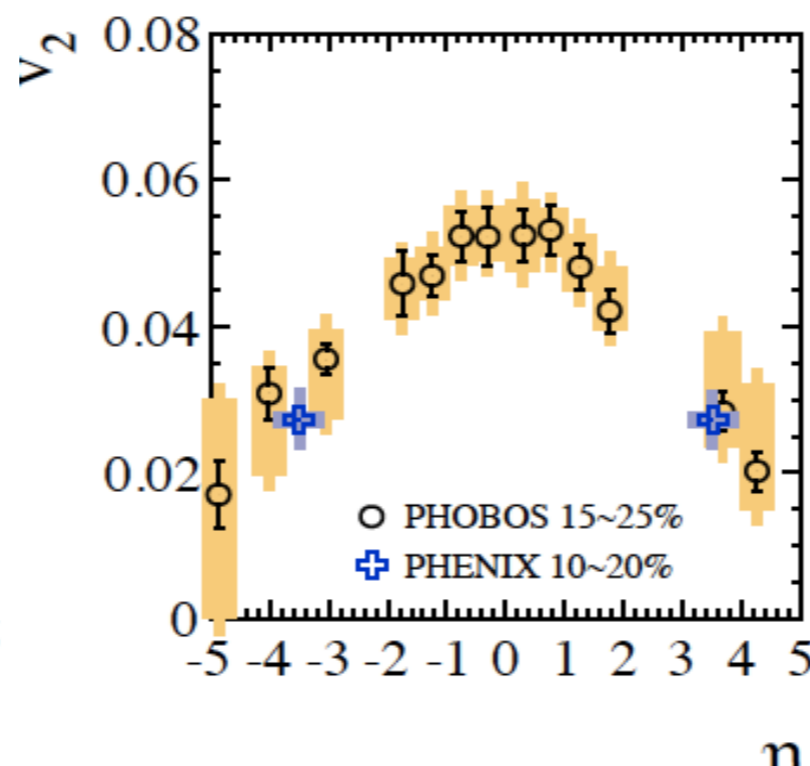
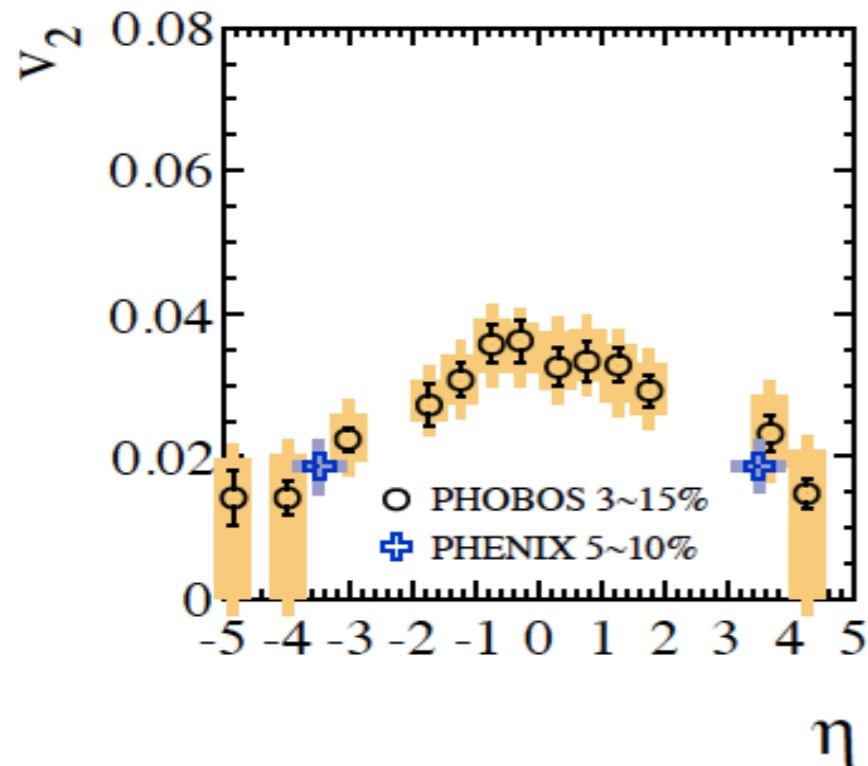
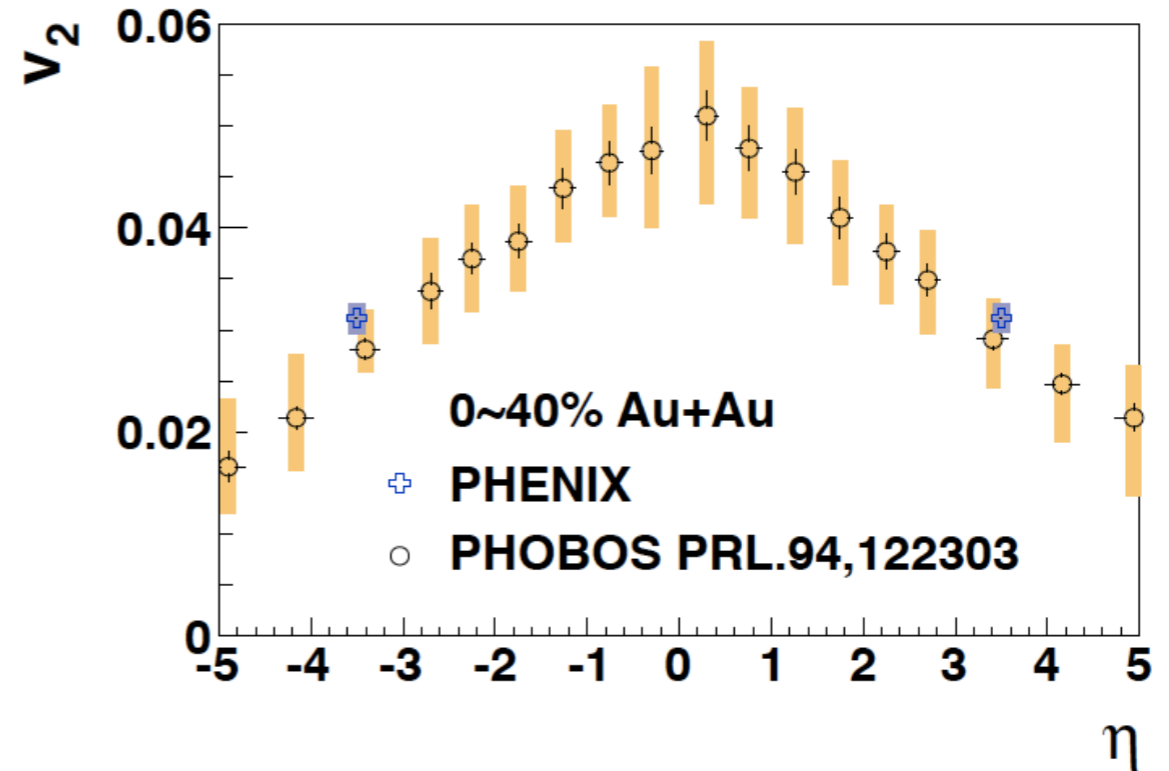
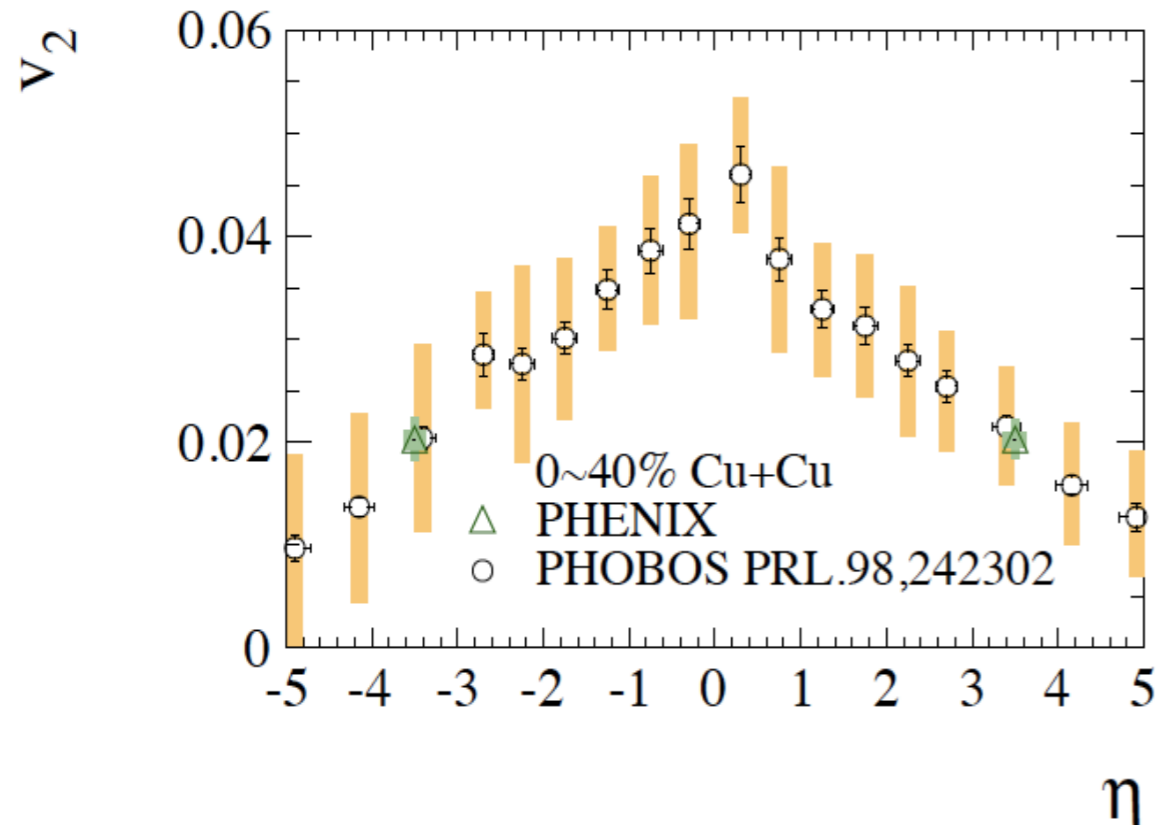
-Estimated from EP correlations(3sub method)



$$Res\{\Psi_{n,A}^{obs}\} = \sqrt{\frac{\langle \cos(n[\Psi_{n,A}^{obs} - \Psi_{n,B}^{obs}]) \rangle \langle \cos(n[\Psi_{n,A}^{obs} - \Psi_{n,C}^{obs}]) \rangle}{\langle \cos(n[\Psi_{n,B}^{obs} - \Psi_{n,C}^{obs}]) \rangle}}$$

$$\begin{aligned} \langle \cos(n[\Psi_{n,A}^{obs} - \Psi_{n,B}^{obs}]) \rangle &= \langle \cos(n[\Psi_{n,A}^{obs} - \Psi_n^{true} + \Psi_n^{true} - \Psi_{n,B}^{obs}]) \rangle \\ &= \langle \cos(n[\Psi_{n,A}^{obs} - \Psi_n^{true}]) \rangle \langle \cos(n[\Psi_n^{true} - \Psi_{n,B}^{obs}]) \rangle \\ &= Res\{\Psi_{n,A}\} Res\{\Psi_{n,B}\} \end{aligned}$$

Comparison to PHOBOS: v_2



My results are consistent with PHOBOS's results

$dN_{ch}/d\eta$ measurements at Bbc

Like v_n measurements, correction factors is estimated from single particle simulation

$$dN_{ch}/d\eta = R * Bbc \text{ Charge sum}(\text{real})$$

$$R = (2/3) / Bbc \text{ Charge sum}(\text{simulation})$$

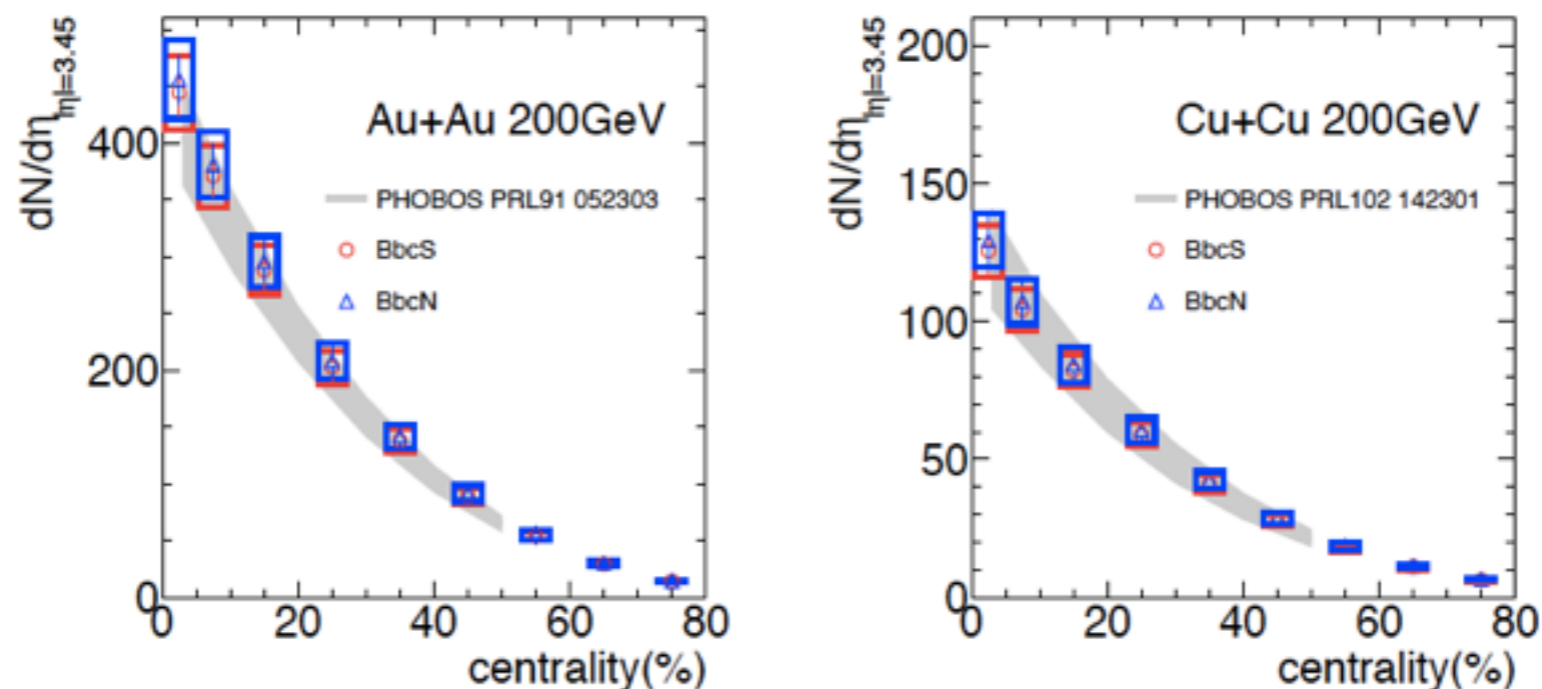
$$+ -\pi / (+ -\pi, \pi 0)$$



$$R \sim 0.5$$

Systematic source: Different η , p_T distributions

Comparison to PHOBOS



My results are consistent with PHOBOS's results

Average v_n at Mid-rapidity

How to integrate $v_n(p_T)$

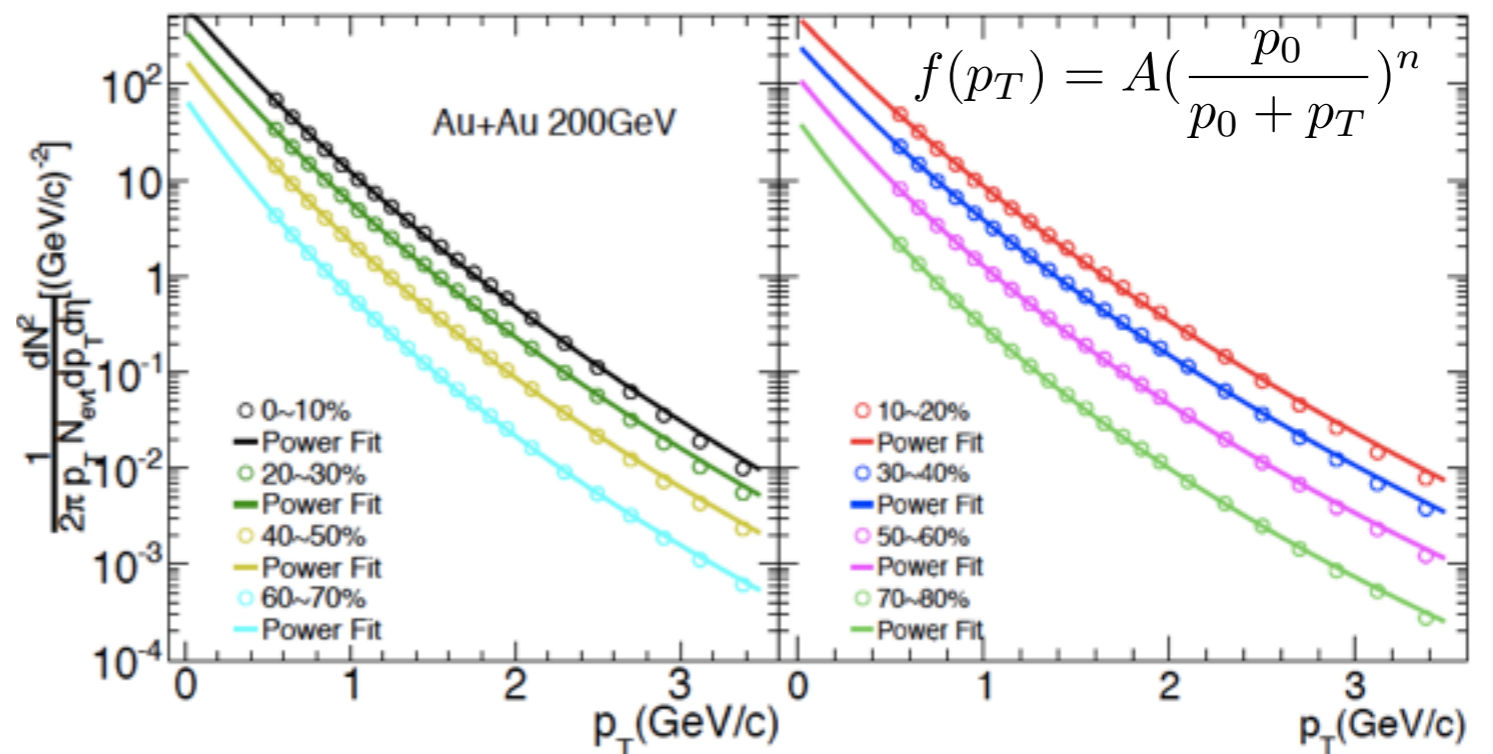
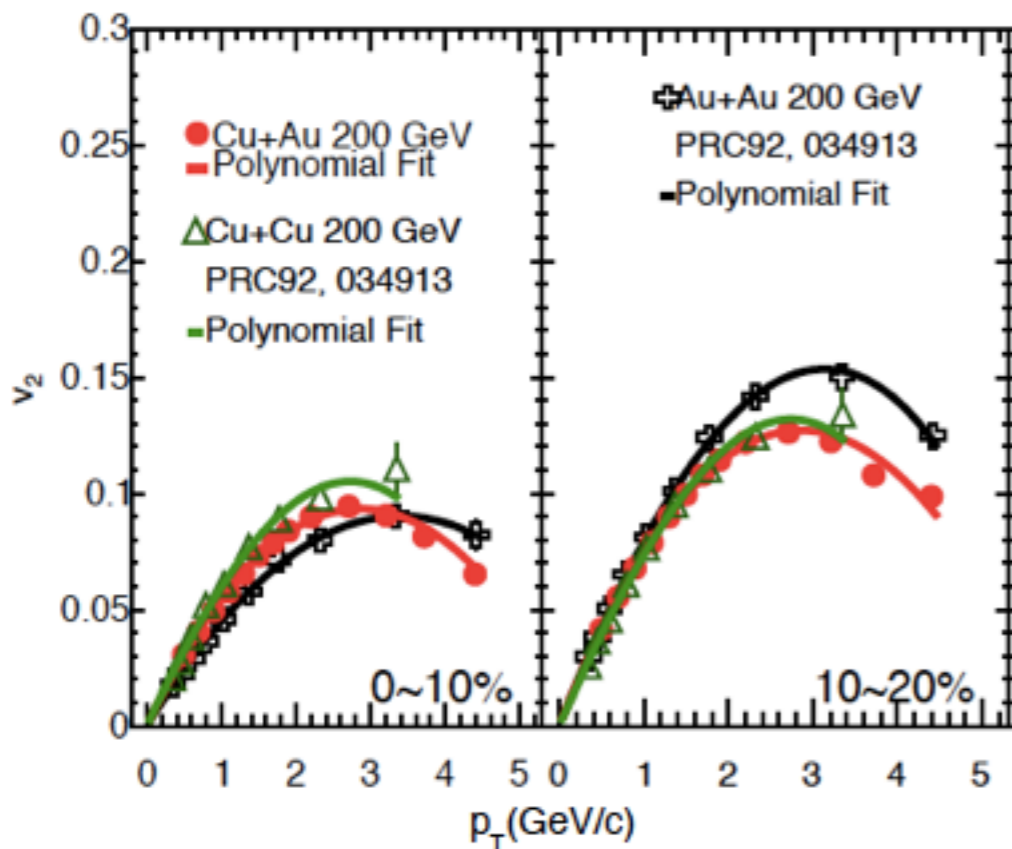
Weighted average using p_T spectra as weights

- p_T spectra: PHENIX AuAu (ppg023)

- v_n : PHENIX AuAu, CuAu, CuCu (ppg124, 132, 183)

$$\langle v_n \rangle = \frac{\sum_i \frac{dN}{dp_{T,i}} v_n(p_{T,i})}{\sum_i \frac{dN}{dp_{T,i}}}$$

- $v_n(p_{T,i})$ and $dN/dp_{T,i}$ values are obtained from fitting functions



Determination of pT spectra in Cu+Cu and Cu+Au

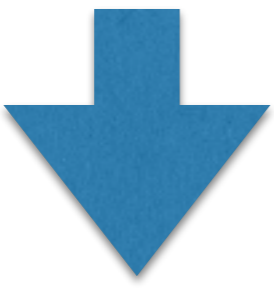
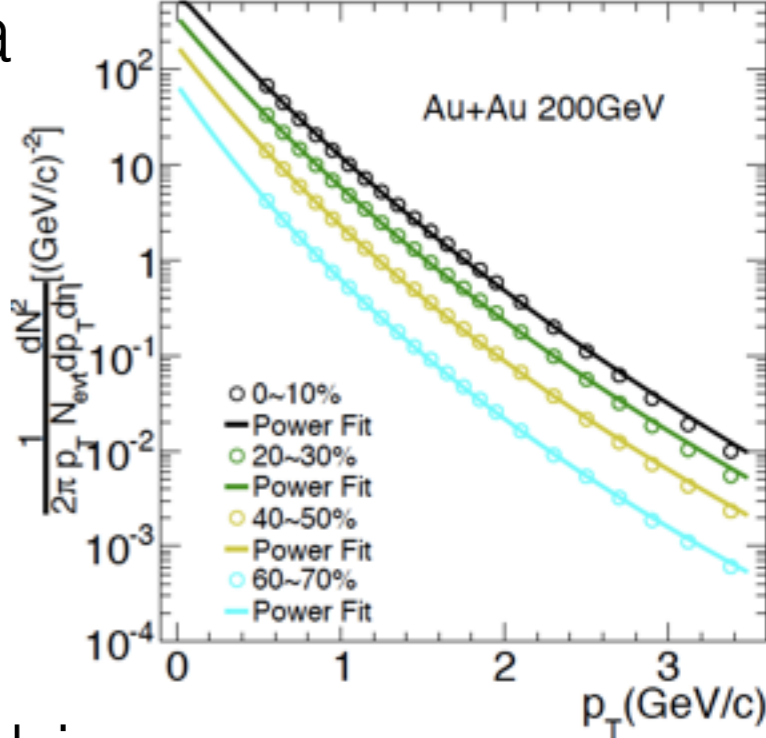
Cu+Cu and Cu+Au spectra are assumed using Au+Au spectra

-There no published Cu+Cu and Cu+Au spectra

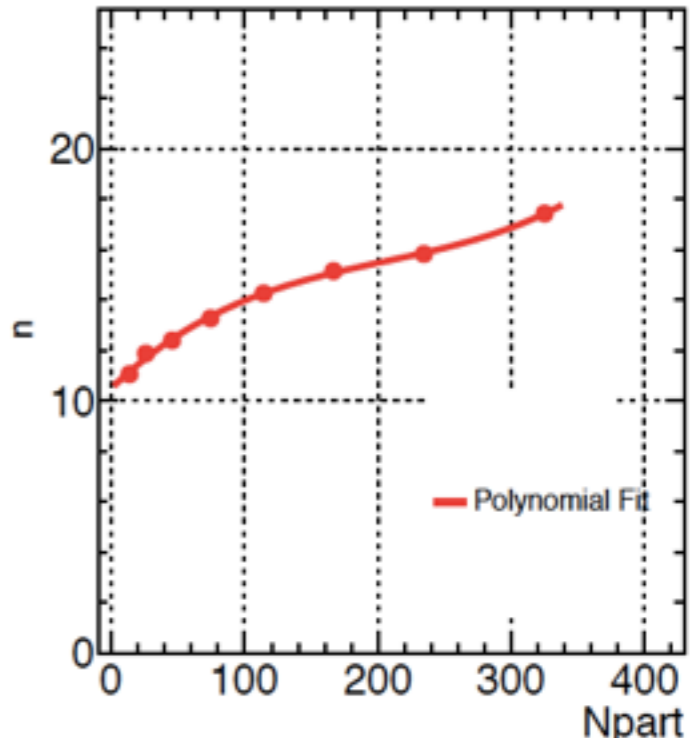
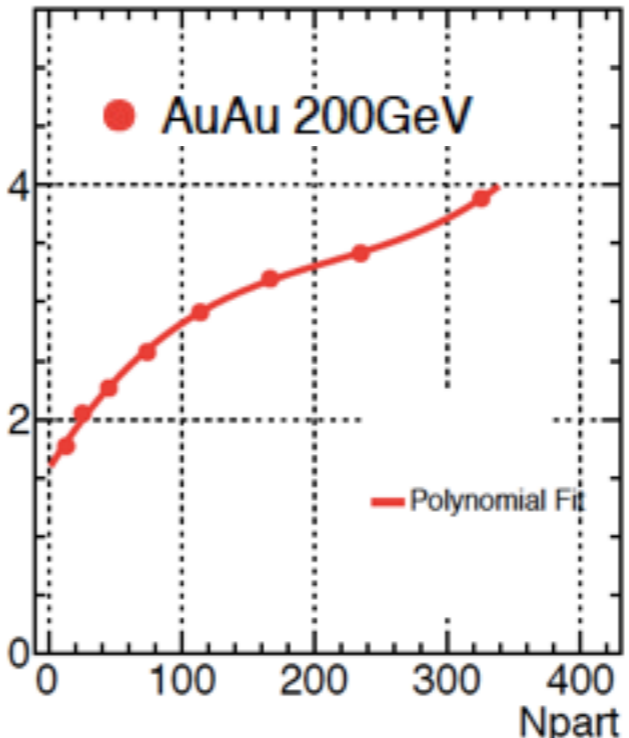
- $dN_{ch}/d\eta$ and $\langle p_T \rangle$ depends on N_{part}

Procedure

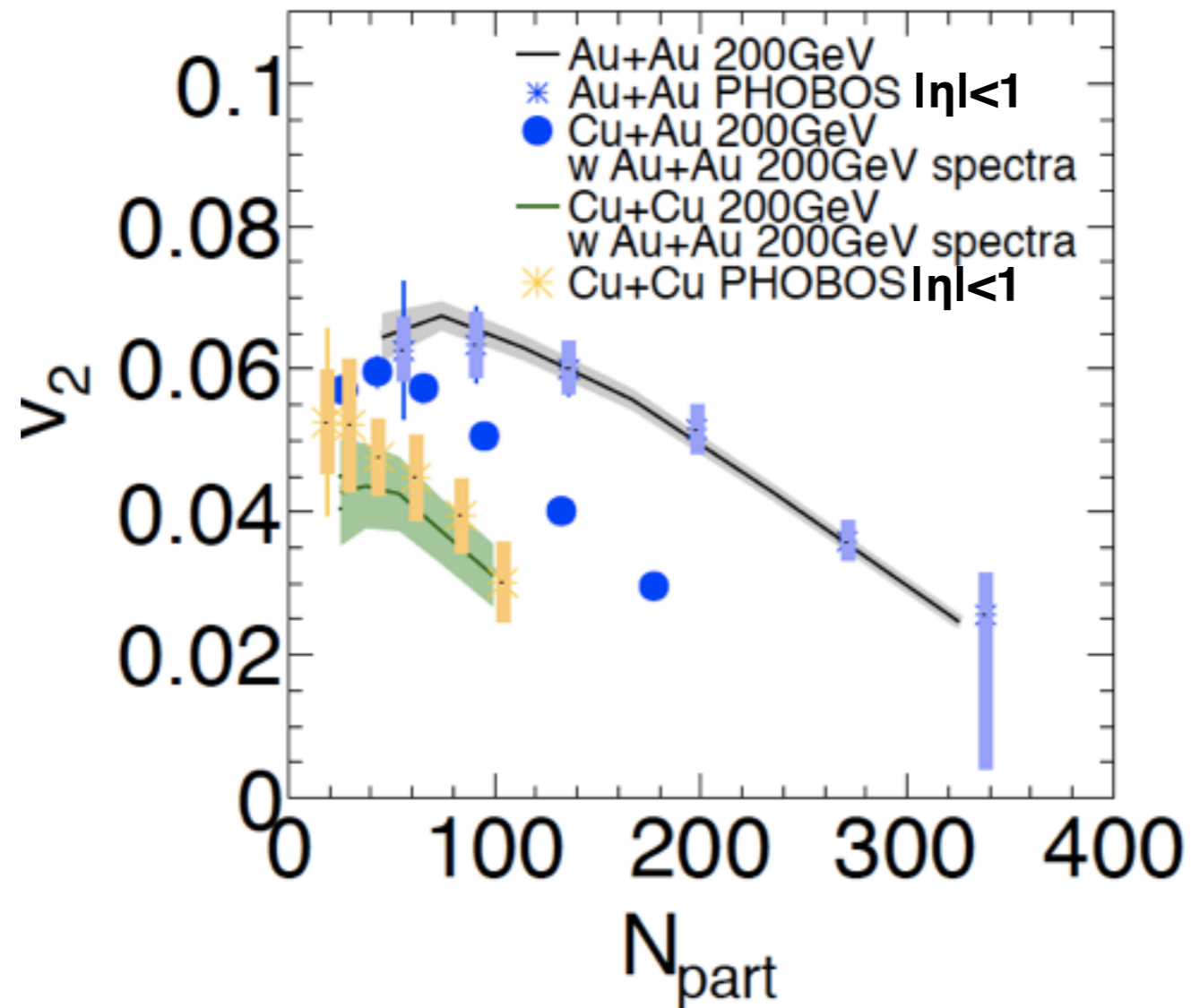
1. Fit Au+Au spectra with $f(p_T) = A \left(\frac{p_0}{p_0 + p_T} \right)^n$
 p_0 and n are free parameter
2. Obtain p_0 and n as a function of N_{part}
3. Make pT spectra for Cu+Cu and Cu+Au
 using $p_0(N_{part})$ and $n(N_{part})$ for corresponding N_{part} bins



$$f(p_T, N_{part}) = \left(\frac{p_0(N_{part})}{p_0(N_{part}) + p_T} \right)^{n(N_{part})}$$



Comparison to PHOBOS



My results are consistent with PHOBOS within the error
- η range is different, PHOBOS's results are obtained wider range
 p_T integration is successfully done